

V605 AQL AND ITS SURROUNDING PN A58

Michaela F. M. Lechner

Master thesis to obtain the degree of a 'Magistra der Naturwissenschaften' at the
Leopold-Franzens University of Innsbruck

Supervisor: A. Univ. Prof. Dr. Stefan Kimeswenger

September 10, 2003

Contents

1	Introduction	4
1.1	Planetary Nebulae PNe	4
1.2	The Born Again Phenomenon	6
1.3	V605 Aql (IRAS 19158+0141)	9
2	Reduction and Data Analysis	12
2.1	Geometry of the EMMI NTT CCD Chip	12
2.2	Bias	12
2.3	Flatfield	16
2.4	Findings of a closer CCD Chip Investigation	20
2.5	Wavelength Calibration	22
2.6	Hot Pixels and their Rows	23
2.7	Complete Reduction of the Spectra	24
2.8	Complete Reduction of the Images	25
3	The old PN Abell 58	26
3.1	Appearance and general Discussion	26
3.2	Distance Estimation out of Radio Observations	27
3.3	Extinction using the Balmer Decrement $H\alpha/H\beta$	29
3.4	Electron-Density n_e using the [SII] Doublet	30
3.5	Ratio R of the [OIII] and [NII] Lines and Temperature	31
3.6	Recombination Time-Scales in A58	32
3.7	Modelling the PN with CLOUDY	33
4	The Born Again Core V605 Aql	38
4.1	General Discussion and Appearance	38
4.2	Densities and Mass of the Dust Shell	39
4.3	The Hydrogen Content of V605 Aql	41
4.4	Identification of spectral Lines	43
4.5	Blueshifts	46
4.6	Close-up to the C_{IV} Wolf Rayet feature	46
4.7	High Resolution Spectra and Speculations	48
5	Conclusions and future Prospects	50
A	Midas Batches	58
A.1	Defragmenting the Images	58
A.2	Looking at the seven different Bias Sessions	59
A.3	Standard Approach to compute a correct Bias	59
A.4	Meanrow out of the different Bias Sessions	61
A.5	Reassambling the Flatfield Images	61
A.6	Subtracting the Reference Bias from the Flats	62
A.7	Splitting the Flats for the different Grisms	63
A.8	Proof of the Scattering in the upper left Corner	63
A.9	Influence of scattered Light on each Grism	63
A.10	Testing if ΔB is really zero	64
A.11	Statistically weighting the Flats for each Grism and Slit	65
A.12	Wavelength Calibration for Grism 2	66
A.13	Correct Bias Reduction for the Spectra	67
A.14	Reducing the Flatfield in the Spectra	67
A.15	Rebinning all Spectra and Reducing the Cosmics	68

A.16 Finding good Standard-Stars to correct the Extinction	69
A.17 Correction Functions for the Quantum Efficiency	70
A.18 Airmass Correction	71
A.19 Correcting the Quantum Efficiency in the Spectra	72
A.20 Splitting the Skyflats in the different Filters	72
A.21 Correct Bias Reduction for the Images	74
A.22 Correcting hot Pixels and Flatfield of the Images	74
A.23 Proof that the Rebinning was successful	75
A.24 Creation of Compound Spectra for each Grism	76
A.25 Correction of the Interstellar Extinction	78
A.26 Determining an Angel-Dependency	80
A.27 [SII] Clump Density at the outer Rim of A58	83
A.28 The Gauss-Fit of the C _{IV} Feature	84
A.29 The C _{IV} Feature in High Resolution	85
A.30 Spatial Resolution and different Velocities	87
B Acknowledgements	88

1. Introduction

1.1. Planetary Nebulae PNe

Planetary Nebulae (PNe) should not be confused with (proto-)planetary disks or even planets. Their name traces back to William Herschel's classification of nebulae (1784), who found that these objects looked like the greenish faint disk of Uranus which he himself discovered in 1781.

Billions of years from now our own sun - like other low-mass stars - will turn into a PN as a consequence of stellar evolution. A PN consists of two interacting parts:

1. a spherical cloud or shell of gas centered around and originating in
2. the central star (CS) - descending from a AGB antecessor - that once has expelled the gas shell during the late stages of its evolution.

The exposed, hot central star (30 000 to 300 000 K) has now only a small diameter and radiates mainly in the ultraviolet spectral region, exciting the expelled outer layers of gas by photons with energies of about 10 to 100 eV. The nebular component reradiates most of the energy through a number of emission lines. These strong lines are produced by recombination of ions or transitions of electrons from higher, collisionally excited levels to lower ones. Spectra and narrow-band images are used to investigate the gaseous nebula.

The ideal PN shows a specific signature in many regions of the spectrum, particularly the visible, the radio and infrared domains. It should also have a well-defined outline or morphology. In reality, a diversity of radiation patterns and morphological features far from spherical symmetry can be found at the individual objects. The morphology is affected by various processes, which are poorly understood: the ejection mechanism, momentum, energy mass input, the nebular mass and the interaction between the ejected gas shell and the interstellar medium (ISM). The nebular spectrum, on the other hand, is influenced by the radiation properties of the central star as well as by the physical properties of the circumstellar gas envelope itself and its chemical abundances.

The emission-line object is visible only for a few tens of thousands of years, expanding at a roughly constant velocity (typically 20–30 km s⁻¹ - although values up to 500 km s⁻¹ have been found). Its central star produces energy by the fusion of hydrogen or helium in a shell around the stellar core. As soon as the thermonuclear reactions cease, its energy output diminishes, the luminosity decreases and the star cools down. In the end, the star's photons cannot ionize or excite the nebula any more: the nebula itself will have expanded so far from the central star that its density is too low to emit detectable radiation. Thus the nebula dissolves into the ISM, losing up to one solar mass to it, and leaves its former central star behind as a slowly cooling white dwarf.

Since PNe reflect the chemical conditions of their central stars, they are used to make up a complete history of the galactic chemical evolution and for refining the models of stellar evolution. PNe also have other applications: Synced with other PNe of the same galaxy a PNe luminosity function can be built to determine the

distance of this galaxy from the solar system.

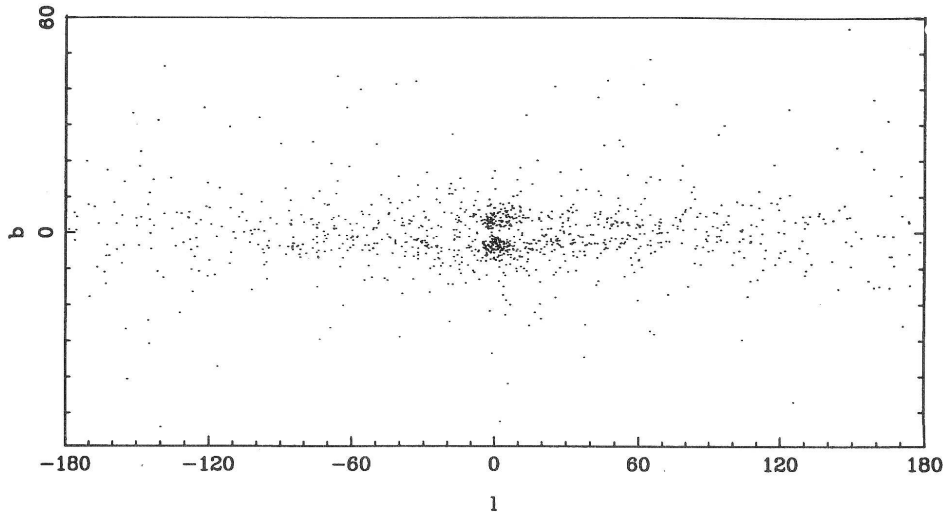


Figure 1.1: Galactic distribution of PNe.

The concentration towards the galactic plane and toward the bulge is obvious. The influence of interstellar extinction can be seen. Figure taken from [Strasbourg-ESO Catalogue of Galactic Planetary Nebulae (1992)]

The galactic distribution (see figure 1.1) of PNe affirms that PNe are probably part of the thick disk population and are concentrated towards the bulge. Some weaker non symmetric concentrations can be associated with spiral arms inside the disk.

The most successful attempt to reproduce the global properties of PNe is the 'interacting winds' model of [Kwok *et al* (1978)]: The fast radiatively driven wind ($> 2000 \text{ km s}^{-1}$) of the now exposed nucleus meets the slow ejecta (10 km s^{-1}) from the former AGB phase (the so called superwind) of the central star. The impact of this fast wind on the slow ejecta produces a 'two-shock' flow pattern and the ejecta are swept up into a shell and photoionized by the radiation field.

In the simplest model we have constant mass ejection rates and velocities, spherical symmetry and a constant Lyman continuum output from the central star. To explain the diversity of the morphology and get a deeper insight, it is necessary to improve this model and generalize it. Significant changes can occur if even relatively minor variations are introduced into the model. It is generally agreed that the density structure in the slow ejecta is one of the most important parameters. Many features can be explained by a density contrast between the polar and equatorial regions of the slow wind. The delay between the ending of the slow wind and the initiation of the fast one is another crucial variable, and we don't know much about this transition. Current evolutionary models produce further shells and Rayleigh-Taylor (R-T) instabilities. The clumps in the gas are not yet fully explained. Are they primordial or introduced by R-T instabilities and in which way do they influence the dynamics?

1.2. The Born Again Phenomenon

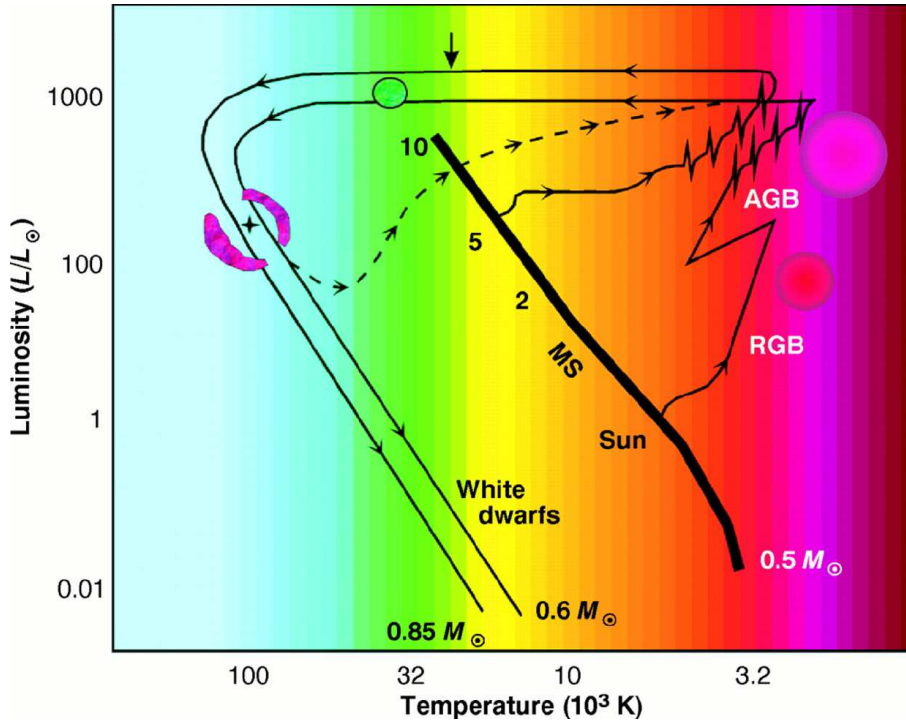


Figure 1.2: Figure and caption from [Weinberger & Kerber (1997)]: Hertzsprung-Russell (HR) diagram, which plots the surface temperature of a star versus its luminosity L (L_{\odot} is the luminosity of the sun). About 90 % of all stars in the Milky Way lie on a single narrow band running diagonally from hot, bright stars to faint, cool ones: This region is known as the main sequence (MS, numbers indicate star masses in units of M_{\odot}). Giants and supergiants are much more luminous at a given color, at the cool end of the diagram. Well below the main sequence are the white dwarfs. The position of a star in the HR diagram is mainly determined by two parameters, mass and age (by age, the stage of evolution is meant; different stars evolve at different rates and therefore reach similar stages of evolution with different ages in years). In recent years, the HR diagram and variations of it have mainly been used for comparison of sophisticated theoretical stellar models with observations. The two solid lines are evolutionary tracks (arrows show direction of evolution) of stars that leave the main sequence at 1 and 5 M_{\odot} and end as white dwarfs of 0.6 and 0.85 M_{\odot} , respectively. Between the thick vertical arrow that marks the onset of photo-ionization and the white dwarf regime, these stars are the central stars of their PNe. RGB means red giant branch, and AGB means asymptotic giant branch. Spikes in the diagram represent thermal pulses, and the dashed line represents a 'born-again' evolution.

A born again PN arises from the central star of a normal PN, which undergoes a very late helium flash before the final cooling of the white dwarf. As a result of this flash the star returns to the AGB. The evolution of this transition is amazing: the luminosity increases by around 4 mag, the effective temperature drops by many tens of thousands of Kelvin and the chemical composition of the stellar photosphere changes completely to heavier elements like He and C, and also N, O and s-process materials; and all this occurs in only a few years.

Because of the short timescale, only few born again objects are known. Late helium-flash objects are of fundamental importance for the understanding of processes during the late stages of stellar evolution. Those PNe are characterized by highly processed hydrogen-deficient nebular material and dust. At the moment there are actually only three objects, where we can observe more than the final H-deficient PN. This makes individual detailed studies of these objects of the utmost importance.

Calculations done in the early 1980's demonstrated that luminous central stars of PNe could be undergoing a final helium shell flash. It was reviewed by [Iben & Mac Donald (1994)] that the final helium shell flash brightens a white dwarf to AGB luminosity and results in a sudden change in abundances as the residual hydrogen envelope is consumed in the helium-burning convective shell. The authors performed the first calculations including a realistic treatment of combined H and He burning and time dependent mixing.

In newer models relevant to the investigation of the born-again stars, mass loss occurs at the stellar surface rather than further inside in the star.

Noted born again objects:

- Sakurai's Object (V4334 Sgr) is the proto-typical final helium shell flash object. It had its flash in 1996 (see [Clayton & de Marco (1997)]). The brightening began in late 1994 or early 1995. A significant decrease in temperature then took place within the last six years. The old PN of V4334 Sgr has been found and its spectrum reveals it to be an ordinary PN (see [Pollacco(1999)]). The composition of V4334 Sgr closely resembles that of the RCrB star V854 Cen ([Asplund *et al* (1998)]).
- FG Sge is the central star of the PN He 1-5 and had its flash in 1894. It has undergone born-again behavior for more than 120 years now and is still burning. Even though its visual brightness rose significantly, the bolometric magnitude remained almost constant. In 1992 the visual brightness faded by 5 magnitudes. IR observations suggest that this may be due to dust condensation in a new formed shell. The brightness fluctuations since then are similar to those of RCrB stars. Between the 1960's and the 1970's the abundances changed from approximately solar to strengthened rare earth elements. Its distance is 2.5 kpc, but Hipparcos measured only 200 pc.
- V605 Aql (see next section).
- A30 and A78 - H-deficient PNe with strong IR emission, they may be older born again objects, where the outer PN has already faded into the ISM. The hydrogen poor gas near the central stars has an extremely asymmetric distribution (see figure 1.3). A30 and A78 are similar to each other in kinematic age and morphology ([Kimeswenger *et al* (1998)], [Borkowski *et al* (1994)]).

[Blöker (2001)] has proposed that FG Sge is the result of a 'late thermal pulse' (LTP), not a 'very late thermal pulse' (VLTP), but the alternative theory is a double-loop evolution as claimed by [Lawlor & MacDonald (2003)]. A double-loop evolution means that the born again stars follow a double-loop path in the HRD: quickly back to the AGB for the first time, returning to the blue, and then evolving more slowly back to the AGB for a second time before the final cooling to a white dwarf (see figure 1.4). Actually there is only one VLTP, but it doesn't stabilize

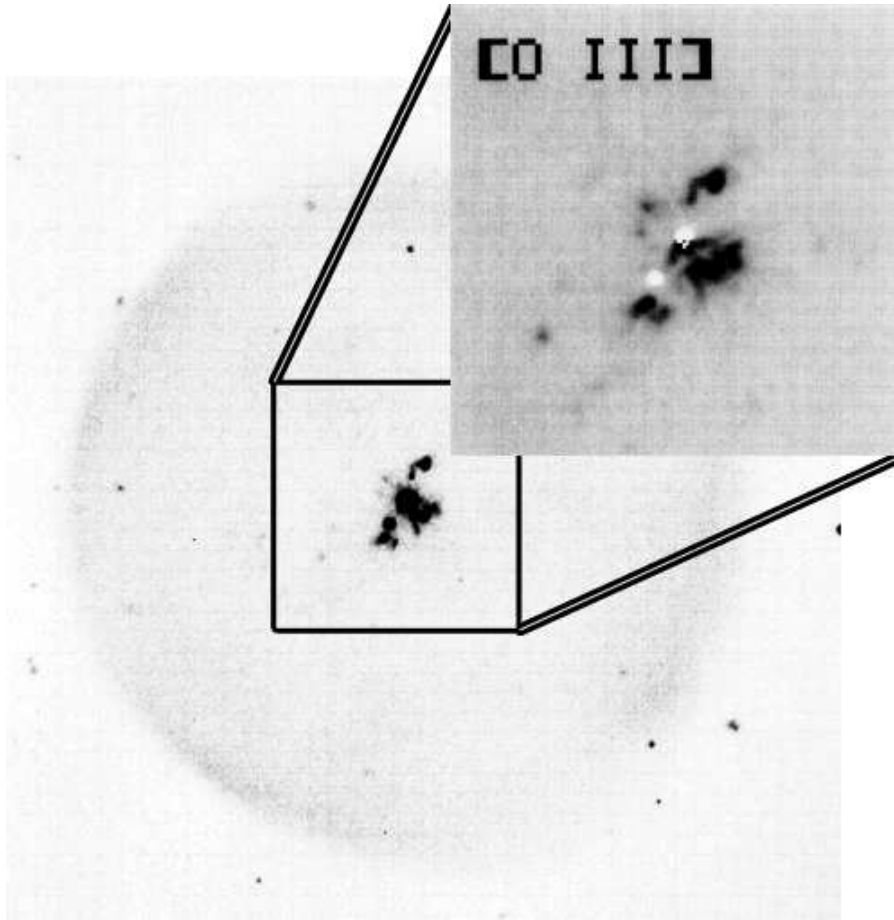


Figure 1.3: Inner Region of A30. Figure from [Borkowski *et al* (1994)].

at once and the increasing and decreasing helium burning causes the inner loop. They argue that FG Sge has been observed during its second return to the AGB, which should also explain the differing timescales between FG Sge and the faster born agains V4334 Sgr and V605 Aql. Furthermore they predict, not only as others before (see [Clayton & de Marco (1997)]) that V4334 Sgr will develop similar to V605 Aql, but also that V605 Aql will have a second flash like the one of FG Sge in about 50–70 years.

[Herwig (2001)] has shown that the evolutionary timescale of VLTP stars strongly depends on the value chosen for the convective mixing parameter. The theoretical model of [Lawlor & MacDonald (2003)] says that a VLTP occurs in 10–15% of post-AGB stars. Their convective mixing parameter is also very low at 10^{-4} , much lower than predicted by standard mixing-length theory and crucial for their double-loop model. The reasons for a low convective mixing efficiency could be magnetic fields, effects of molecular weight gradients or something completely different. In other cases of stellar evolution the convective mixing doesn't seem to be so decisive, and a relatively low convective mixing could be actually quite common.

There is not yet a consent about other crucial parameters either: Opacities at high ionization energies, the importance of convective overshoot and surface cooling by means of stellar wind are all disputed. They can significantly revise all hitherto results. [Asplund *et al* (1998)] found that the photospheric parameters derived for

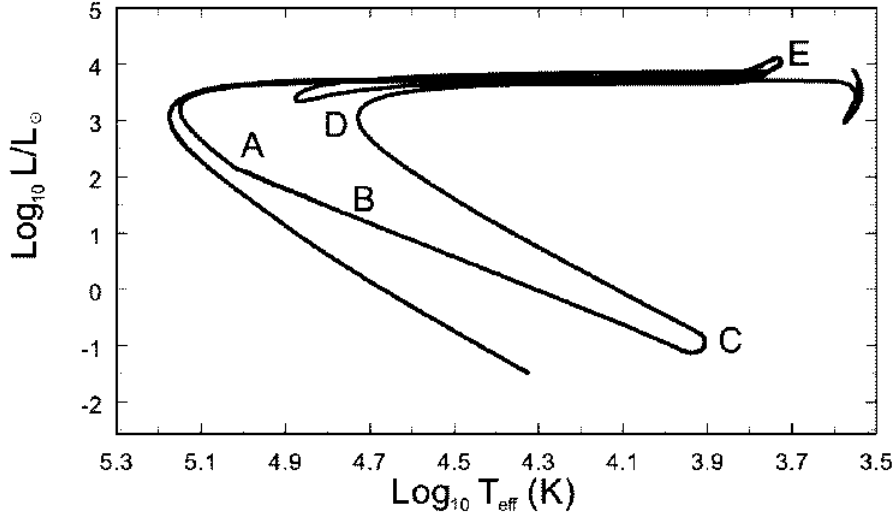


Figure 1.4: Figure taken from [Lawlor & MacDonald (2003)]. Double-loop scenario in the HRD.

V44334 Sgr from analysis of spectra obtained in 1996 May and October are not consistent with the constant luminosity deduced from photometry. Further investigation is needed to fix the important parameters.

1.3. V605 Aql (IRAS 19158+0141)

The surrounding old PN of V605 Aql is A58. V605 Aql was discovered in 1919 as 'Nova Aquilae No.4' and later renamed V605 Aql. Only in the 1980's was it recognized to be a final helium flash object. Thus it was observed less than Sakurai's object or FG Sge. It had its flash in 1917. V605 Aql is often referred to as the 'older twin of Sakurai's object' since many similarities exist, and it serves as pathfinder for future events in V4334 Sgr, which had its flash in 1996.

Coordinates:

- $\alpha = 19^{\text{h}}18^{\text{m}}20^{\text{s}}.42$ $\delta = +01^{\circ}47'01''.1$ from [Kimeswenger *et al* (2000)]
- Galactic coordinates: $l = 37.60$ $b = -5.16$

The photographic magnitude in 1917 was $m_{pg} = 15^{\text{m}}0$ ($m_{pg} = m_B - 0^{\text{m}}11$) corresponding to a blue luminosity of about $50 L_{\odot}$ for a distance of 3.5 kpc and $A_B = 2^{\text{m}}3$ (see later discussion). V605 Aql reached a maximum photographic magnitude of $m_{pg} = 10^{\text{m}}2$ in August 1919, a secondary maximum was reached in 1921. A spectrum of V605 Aql in 1921 was scanned by [Clayton & de Marco (1997)]. They found deep Swan bands of C_2 and violet bands of CN, a characteristic absence of Balmer lines, the G Band of CH and $^{12}C^{13}C$ bands, and described this spectrum as being typical of a cool RCrB star (T_{eff} about 5000 K). With an assumed distance of 3.5 kpc and an interstellar reddening of $A_B = 2^{\text{m}}3$, their estimation for the luminosity in 1919 is about $10^4 L_{\odot}$. In 1923 two more optical brightenings occurred (see [Seitter (1987)]).

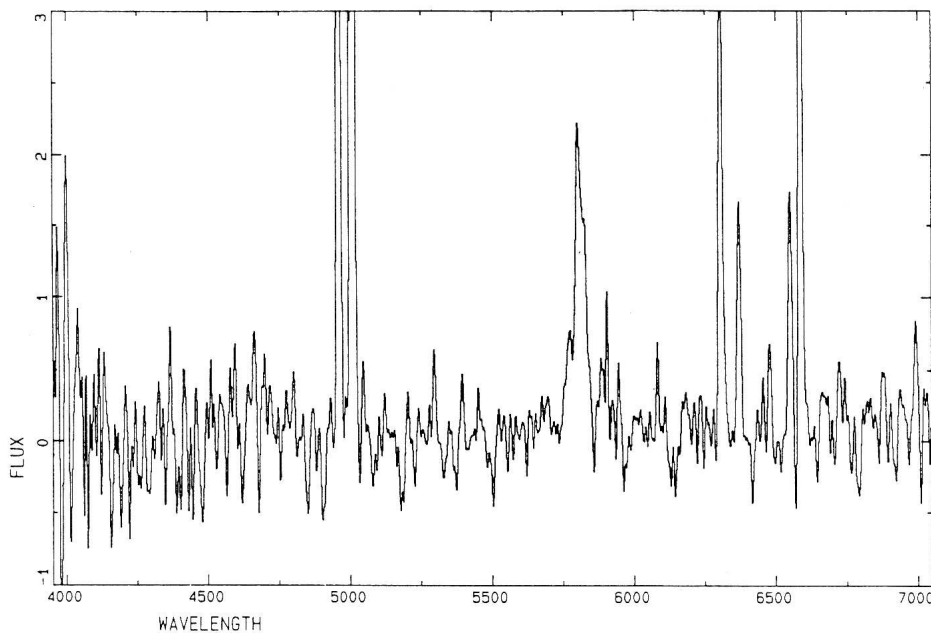


Figure 1.5: First spectrum of V605 Aql after recognizing it as a possible hydrogen poor object. Giving a first idea of the C_{IV} Wolf Rayet feature. Figure from [Seitter (1987)].

In 1971 a small knot of nebulosity of about $1''$ has been resolved in the center of Abell 58. But the first spectrum of V605 Aql after 1921 was not taken until [Seitter (1987)], after [Pottasch *et al* (1986)] has first suggested that it might be a hydrogen poor object. This spectrum (see figure 1.5) had a high noise-level, as the faint, central spot ($m_v \approx 21^m$) needs a series of long exposures for more reliable data. However, she still gave a first estimation for the physical conditions of the inner and outer nebula, such as the severe hydrogen and ^{13}C deficiency. She specially looked at the [OIII] and [NII] lines and found also that V605 Aql shows the presence of a broad C_{IV} emission, which is a characteristic feature of a Wolf Rayet star. The C_{IV} emission was confirmed by [Guerrero & Manachado (1996)]. [Clayton & de Marco (1997)] estimate that V605 Aql has currently an effective temperature in excess of 50 000 K, if this C_{IV} emission dominates the stellar spectrum. [Seitter (1987)] claims furthermore a radial expansion-velocity of 60 km s^{-1} for the central knot. Because of her poor signal, the data of [Pollacco(1999)] who derives a v_{exp} of 100 km s^{-1} might be more reliable.

The born-again PNe V605 Aql and V4344 Sgr (Sakurai's object) give us the rare chance to follow shell formation and building of the winds in 'real-time'. The high carbon abundance, and thus the high dust formation rate, enhances these mechanisms. Therefore the timescales are shortened, and maybe we can already see an evolution from the spectra of [Guerrero & Manachado (1996)]. The velocity shift and line shape of some emission lines are surprising (also in Sakurai's Object). One possible explanation of these lines is that the final flash objects have a circumstellar shell with a complex geometry. Near infrared photometry of V605 Aql was obtained in 1992 by [Harrison (1996)]. His analysis of this data and the IRAS fluxes indicated that V605 Aql is surrounded by a dusty shell that obscures a hot central source. Although he also misidentified the object (see [Kimeswenger *et al* (2000)]), it is likely that V605 Aql, which returned already to its pre-outburst brightness changed its luminosity only little, but is now obscured by a thick cloud of dust.

The coexistence of a hot wind and a cool dust shell is quite interesting. A gas-dust combination model has been presented by [Koller & Kimeswenger (2001)]. In addition, [Hinkle *et al* (2002)] pointed out that V605 Aql seems to consist of a dense inner core and a second clump separated from this region by about $0.8''$.

2. Reduction and Data Analysis

2.1. Geometry of the EMMI NTT CCD Chip

Observations were taken with the EMMI Instrument on the New Technology Telescope (NTT) in the European Southern Observatory situated in LaSilla. Information about the characteristics of the detector can be found in the New RED CCD Commissioning report under:

<http://www.lis.eso.org/lasilla/Telescopes/NEWNTT/emmi/newRed/newRed.html>

The current valid version of the Commissioning report is the update of May, 18th of 2002.

"The new EMMI Red detector is a 2x1 mosaic of 2kx4k MIT/LL, thinned CCDs, known as CCID20-14-5-3, nicknamed "Michelle" and "Zeus". The new detector system is basically a copy of the FORS2 upgrade. The 15micron pixel (0.1665") match well the resolution of the EMMI-Red optics (0.21"). The mosaic is controlled by FIERA which, together with the ATM connection between the CCD controller and the instrument workstation, ensure a very small overhead.

The two chips are mounted side by side. Each chip uses two independent amplifiers. The resulting frame therefore contains 4 independent sub images (which are stored as extensions in the FITS frame). Refer to the Astrometry section for the accurate relative positioning of the chips."

2.2. Bias

The logfiles of the observation-data from Sun Aug 4 2002 to Tue Aug 6 2002 were scanned for the biasfiles. The EMMI group has written an own programm to re-assemble the 4 different amplifiers to one image. So the first thing to do was to convert the biases, which was done with the aid of a batch. For all data reduction the MIDAS Version 02FEB has been used. All important batches are collected in the appendix. The whole code for the reassembling is printed in A.1. Two lines out of it as an example:

```
@@ inemmi ONTT.2002-08-03T21:23:47.347.fits b1001
@@ inemmi ONTT.2002-08-03T21:24:04.444.fits b1002
```

Looking at the bias images with another batch (listed in A.2) and concentrating on the third amplifier, where the spectra were placed on, a structure on each bias can be detected as shown in figure 2.1, admittedly only on a small scale. This brick-like structure's wandering is relatively fast, so it can be found shifted on all the biases of one session. Therefore the overall effect for each of the seven different bias sessions is already smaller. In the end this brick-like structure fixes the standard deviation of the readout noise. Another batch (listed in A.3) computed the mean values for the seven bias sessions. Now the readout noise can be calculated.



Figure 2.1: Bias structure of a single image

`load b2004 cuts=290,315`

This single brick-like structure is not constant over time, but is wandering. All the more this effect predefines the standard deviation of the readout noise.

Exemplarily here for the seventh session:

```
do i = 1 9
  COMPUT/IMAG tmp = b7{i} - bmean007
  stat/ima tmp [@1050,@20:@1550,2050]
enddo
```

This results in a readout noise of about 4.5. There is no particular change in y-direction of the picture, as easily shown via overplotting different rows of one bias. Thus this dimension can be economized by taking the average of all rows to improve the further reduction. This row can again be blown up to a whole image.

With a further batch listed in A.4 the average rows for the different bias sessions and out of these a mean row were computed and plotted as shown in figure 2.2. The spread between the bias sessions can be seen clearly. This feature is a real bias offset of about 9 pixel that has to be corrected. The spreads of amplifier 3 and 4 are by far worse than those of the first ones. I tried to correct this real bias offset with the help of amplifier 1, because it is barely exposed in all observational data. This correction is allowed, if there is no multiplicative effect on the chip. To test the multiplicative effect it is enough to divide the most deviating bias-session with the mean row.

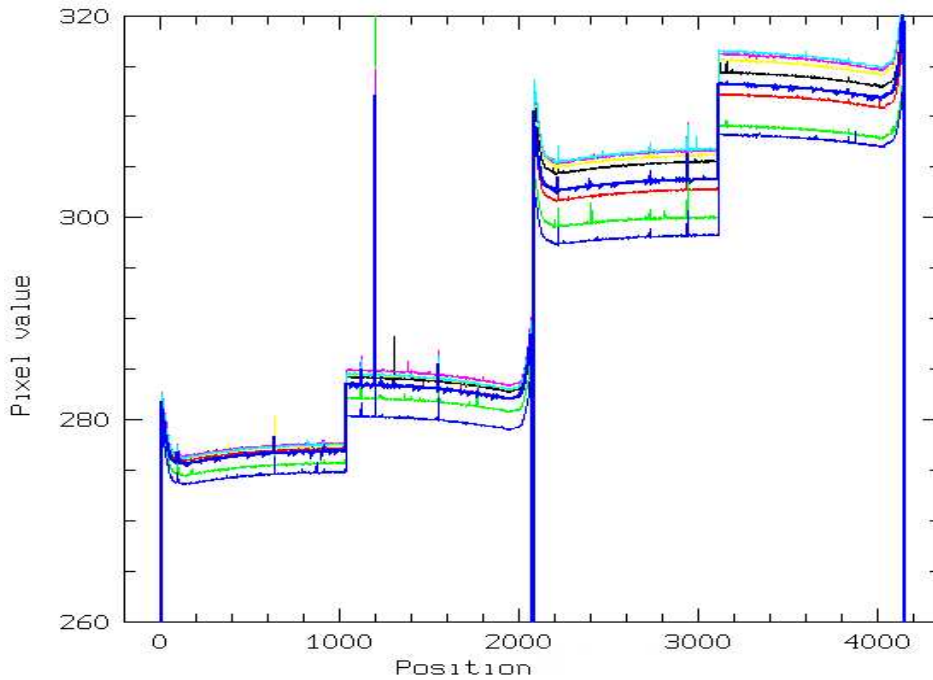


Figure 2.2: Graph created by the batch listed in A.4. The gaps between the seven thin lines are obvious on all four amplifiers. The thick line is the mean row of them, building a reference line for further calculations.

```
COMPUT/IMAG tmp = meanrow.bdf / bmean004row.bdf
plot tmp
```

With these two lines the figure 2.3 is produced. Again it can be seen that amplifier 3 clearly has been the worst choice to put the spectra on. The chip would have been much better if turned upside down. In fact, the multiplicative factor to the reference row is almost 2 percent, this means 6 pixel.

To deduce the bias offset of amplifier 3 ($\Delta B3$) from the one of amplifier 1 ($\Delta B1$), the reference row was subtracted from each session row and the mean value of the area of amplifier 1 was plotted against the mean value of the area of amplifier 3, as shown in figure 2.4. This correction has still an error of 0.76 pixel-values, but this is obviously much smaller than 9 and even smaller than the read out noise. Hence the total error is:

$$\sigma_{bias} = \sqrt{\sigma_{read}^2 + \sigma_{corr}^2} \approx \sigma_{read}.$$

For the further data reduction of the objects firstly the reference bias computed by

```
grow/imag refbias = meanrow.bdf 1,2,2055
```

has been subtracted. Then in this reduced image $\Delta B1$ has been identified and $\Delta B3$ obtained using the correlation function between $\Delta B1$ and $\Delta B3$. In the end $\Delta B3$ has been added to the reduced image.

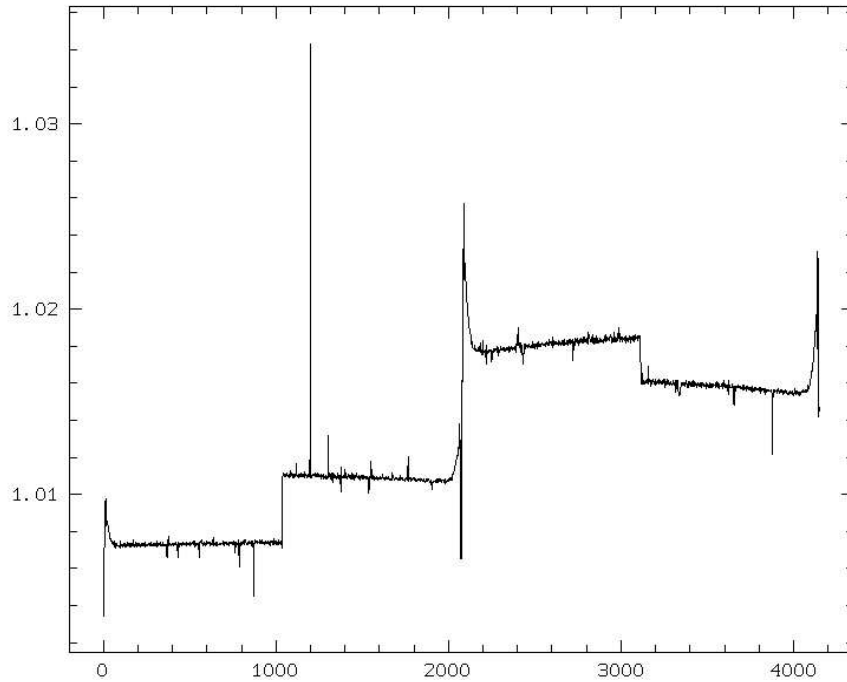


Figure 2.3: Multiplicative factor
`COMPUT/IMAG tmp = meanrow.bdf / bmean004row.bdf`
`plot tmp`

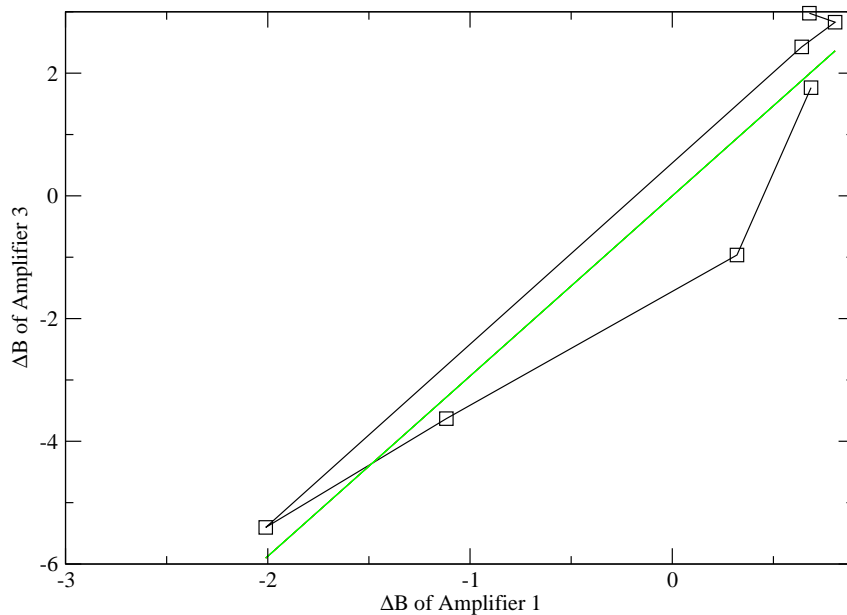


Figure 2.4: Correlation between $\Delta B1$ and $\Delta B3$ created with the help of the batch listed in A.4. The seven sessions are marked with squares. The straight linear fit goes through zero. The ascending slope is 2.9369. The correlation coefficient is 0.822 and the RMS error is 0.76 pixel-values.

2.3. Flatfield

At first again the logs of the observations from Sun Aug 4 2002 to Tue Aug 6 2002 were scanned for the flat files. I had to notice that no flats were done in the second night. The four amplifiers of the images were reassembled with a batch (listed in A.5). Then the correct bias could be subtracted from the flat fields using another batch listed in A.6.

It is useful to arrange the flats in order of their grisms. The commands in A.7 write out the used grism at the time the flat was created, as well as the exposure time. During the observation only three different grisms were used, namely grisms 2, 3 and 6. For every grism I tested the complete removal of the bias. The concept of this test is quite clear, considering that every flat image is composed of the bias (that should be the same for every flat) plus the part that is proportional to the exposure time. So the division of two bias corrected flats is approximately the ratio of their exposure times.

A problem was that several files seemed to have some scattered light. You might see it in figure 2.5. This effect can be seen in all grism 2 files, whereas grisms 3 and 6 look fine. The lower 700 pixels in all grism 2 files cannot be used.

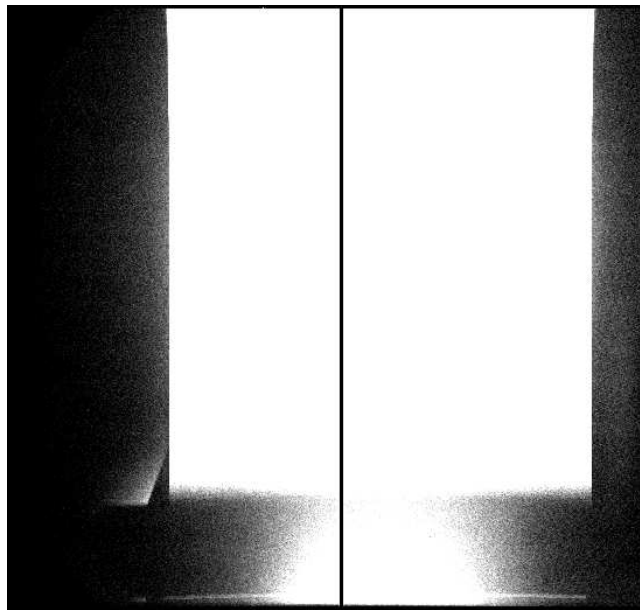


Figure 2.5: Flatfield with Grism 2. Obviously we have got red light of first order at the lower side of the picture. The grism is shorter than the chip.
load F1bnight0001 scale=-4

The fact that probably the bias is different on each picture was the next problem. Moreover this chip is of so high quality that this cannot be due to a dark. If we look at a similar picture as 2.5, only different in exposure time, we see that we have got a lot of scattered light. In figure 2.6 the same cuts as in 2.5 are used, so this arises as being obvious. In the same figure the cross section of these two flats near the upper left corner is shown.

To proof that the bias changes, I looked especially at my flats. Assume that, after

subtracting the bias, the intensity I_1 of a little area in the left upper corner (look at figure 2.9 that will be explained later, to locate the meant area) of the flat field is

$$I_1 = \delta B + \xi(I_{up} - \delta B),$$

where δB is the Bias offset, I_{up} the intensity of an upper exposed area and ξ the importance of the scattered light. Then, if ξ is low enough, δB can be neglected inside the braces, and thus:

$$\delta B = I_1 - \xi I_{up}. \quad (1)$$

To get ξ , a batch (listed in A.9) has been written that produces a table of the two intensities of the respectively used flats for the different grisms. With them the graph in figure 2.7 has been drawn with I_1 on the x-axis and I_{up} on the y-axis. The slope is the ratio I_{up}/I_1 . Dividing equation (1) we get

$$I_1/I_{up} = \delta B/I_{up} + \xi.$$

Again neglecting the term with δB , the importance of the scattered light ξ can be identified with the reciprocal of the slope (I_{up}/I_1) which has been measured for all three different grisms with figure 2.7.

Now the equation can be solved for δB . Doing this by means of the batch in A.10, the finding is that δB is approximately zero. That means that apart from the little one mentioned in section 2.2, there is no real bias offset, as expected on such a good chip, but only scattered light everywhere on the flat, and there is nothing that can be done about this.

In the final treatment the flats were only reduced by the reference bias and then weighted statistically for each grism and each of the two slits with the batch given in A.11. In the resulting images the columns, where the spectra lie in the object images, were averaged:

```
AVERAG/COLU fcolugr2s11 = flatbgr2s11.bdf @1148,@1170
AVERAG/COLU fcolugr2s15 = flatbgr2s15.bdf @1148,@1170
AVERAG/COLU fcolugr3s11 = flatbgr3s11.bdf @1148,@1170
AVERAG/COLU fcolugr3s15 = flatbgr3s15.bdf @1148,@1170
AVERAG/COLU fcolugr6s11 = flatbgr6s11.bdf @1148,@1170
AVERAG/COLU fcolugr6s15 = flatbgr6s15.bdf @1148,@1170
```

Then the flat images were divided by the grown continuum of these averaged columns to get the normalized flat images for the spectra:

```
MODIFY/GCUR fcolugr2s15.bdf tmp
CONTIN/SPEC tmp contis15 ? ALL 2 3
grow/imag conts15full = contis15 1,2,2076 ? C
COMPUT/IMAG fbngr2s15 = flatbgr2s15.bdf / conts15full.bdf
load fbngr2s15.bdf scale=-4 cuts=0.5,1.1
```

The continuum and the average column are shown in figure 2.8.

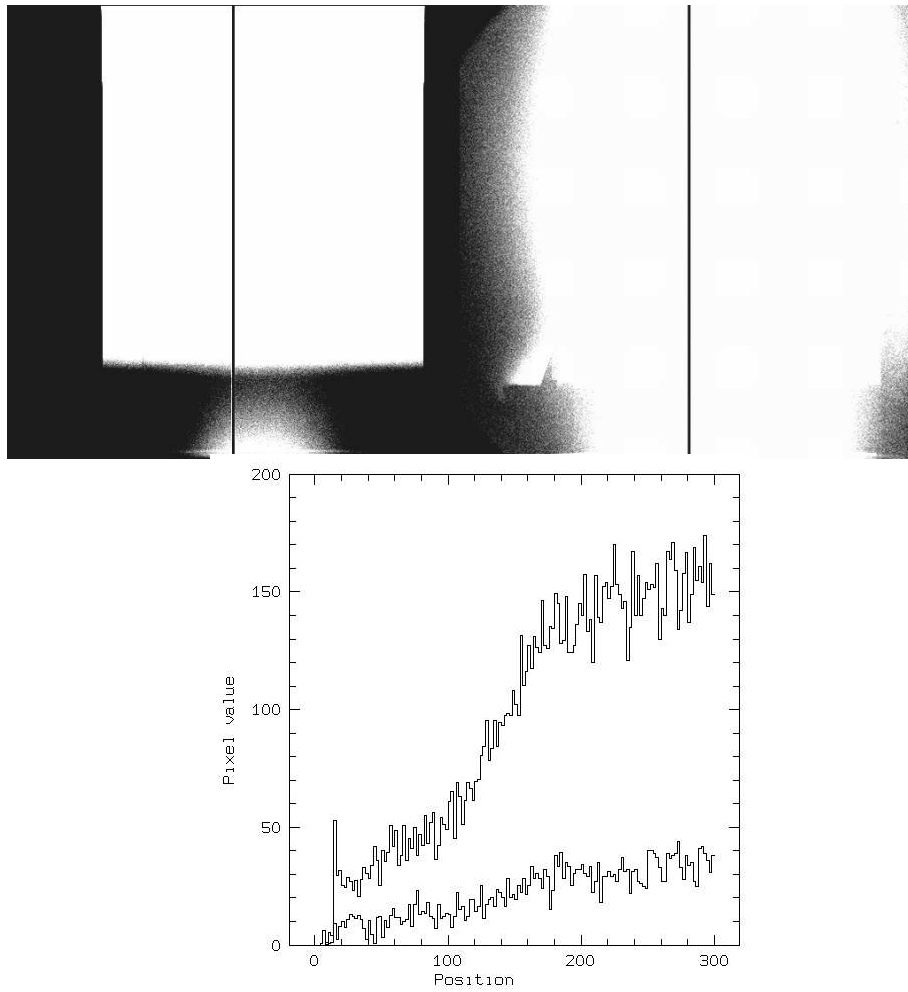


Figure 2.6: The comparison between two default bias corrected flat fields, both with grism 2, shown here with the same cuts. The only difference are the exposure times: the left one has 2.2206 seconds, the right one 9.7189 seconds.

```
load F1bnight0001 scale=-4 cuts=130,230
```

```
load F1bnight0002 scale=-4 cuts=130,230
```

Cross section near the upper left corner of these two flats produced with the batch listed in the appendix A.8.

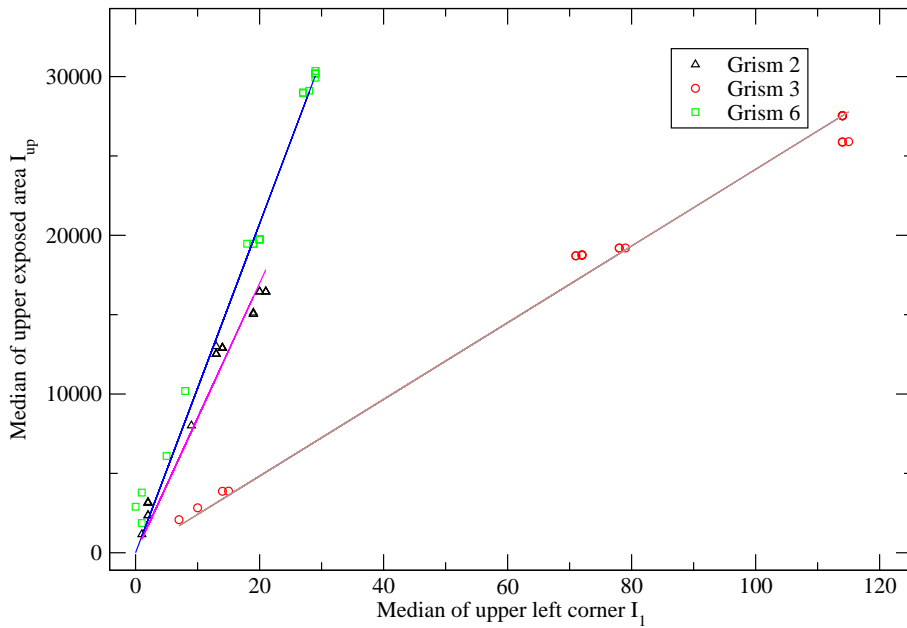


Figure 2.7: Specifying the different proportions of scattered light for each grism. The calculated values for the slopes I_{up}/I_1 are: 900 for grism 6, 700 for grism 2, 235 for grism 3. The RMS percent error is less than 0.3.

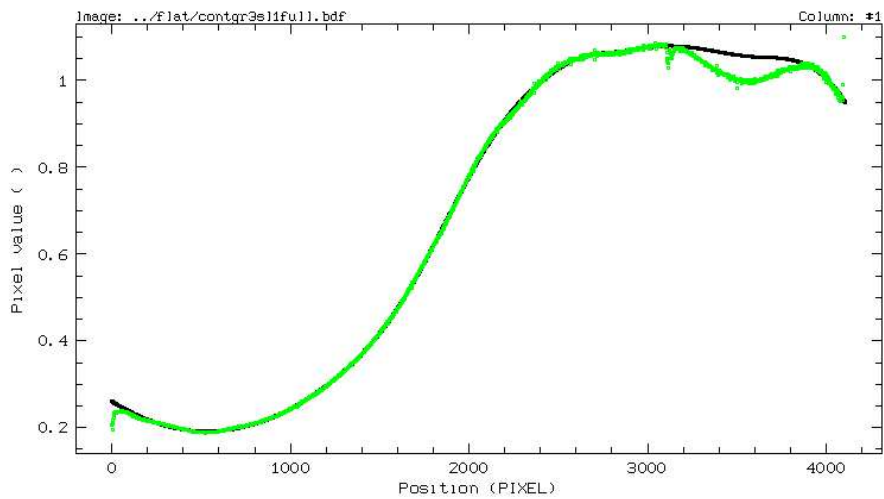


Figure 2.8: Average column of the flat used for grism 3 and slit 1 and the fitted continuum.

2.4. Findings of a closer CCD Chip Investigation

The previous complications together with the rather poor documentation in the commissioning report (see section 2.1) suggested to find out more about the EMMI CCD chip. All images (direct images, spectra, biases and flats) have been taken, to look at the action between amplifier 1 and amplifier 3. The first target was to define the areas where it can be definitely said that only bias is measured. I plotted a lot of graphs to determine the end of the trailing edge and the transition to a constant value. There were few areas fulfilling this obligation and they were different for direct images and spectra. Spectra with grism 5, which seemed to have a special problem, were excluded, but since the observational data is mainly focused on grisms 2, 3 and 6, this was not much of a restriction. Furthermore only images have been taken with $bin = 2$ in x- and y-direction.

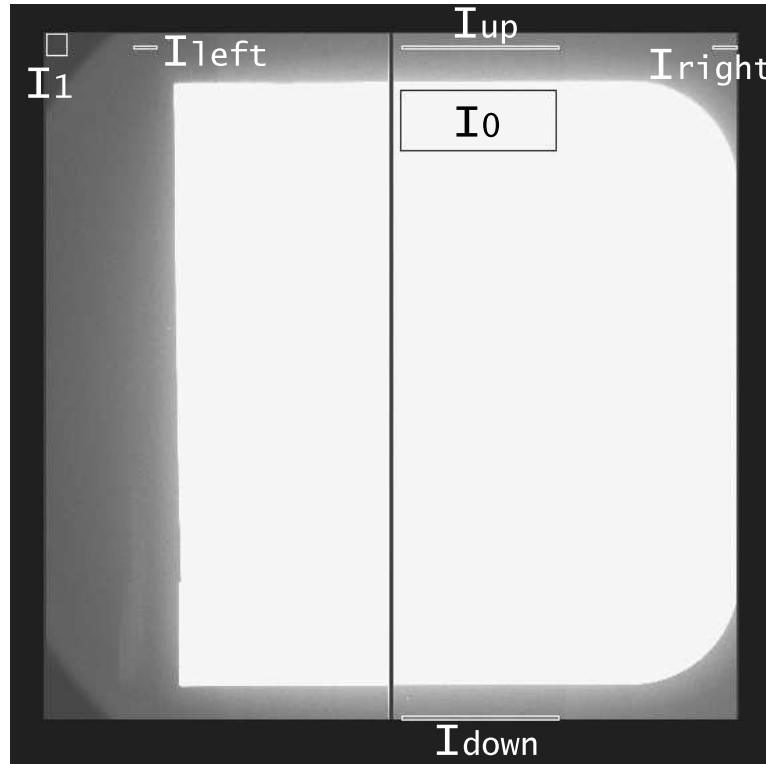


Figure 2.9: Defined areas used for the reduction

The first conclusion was that the offset between amplifier 1 and 4 is stable, concerning both the spectra and the direct images, apart from the fact that the right side is more affected from the scattered light. The upper edges seemed to be more resistant to the scattering. For testing the offset between amplifier 1 and 3, only the direct images could be used, since only there a rather unexposed part at the upper and lower part of amplifier 3 was found.

$$I_{up} - I_1 = O_{13} + I_0 \times \xi$$

is the describing equation; if the offset O_{13} between amplifier 1 and 3 is constant, no more terms are missing. Now it is assumed that the intensity I_1 at the upper left edge on amplifier 1 mirrors the true bias (which is surely the case if not for the flats), I_{up} is again the intensity at the upper non exposed area of the picture as shown in figure 2.9, and I_1 is the intensity of the exposed area. As above ξ is the

fraction of scattered light. The values $I_{up} - I_1$ and I_0 can be measured. Plotting it, a clear correlation with no splitting up should be seen. However, doing this at first glance there is only a big cloud of values, but when splitting up for the different filters of the direct images, the correlation is clear and obvious, as seen in figure 2.10. This clear correlation is the justification for the use of amplifier 1 to adjust the bias on amplifier 3.

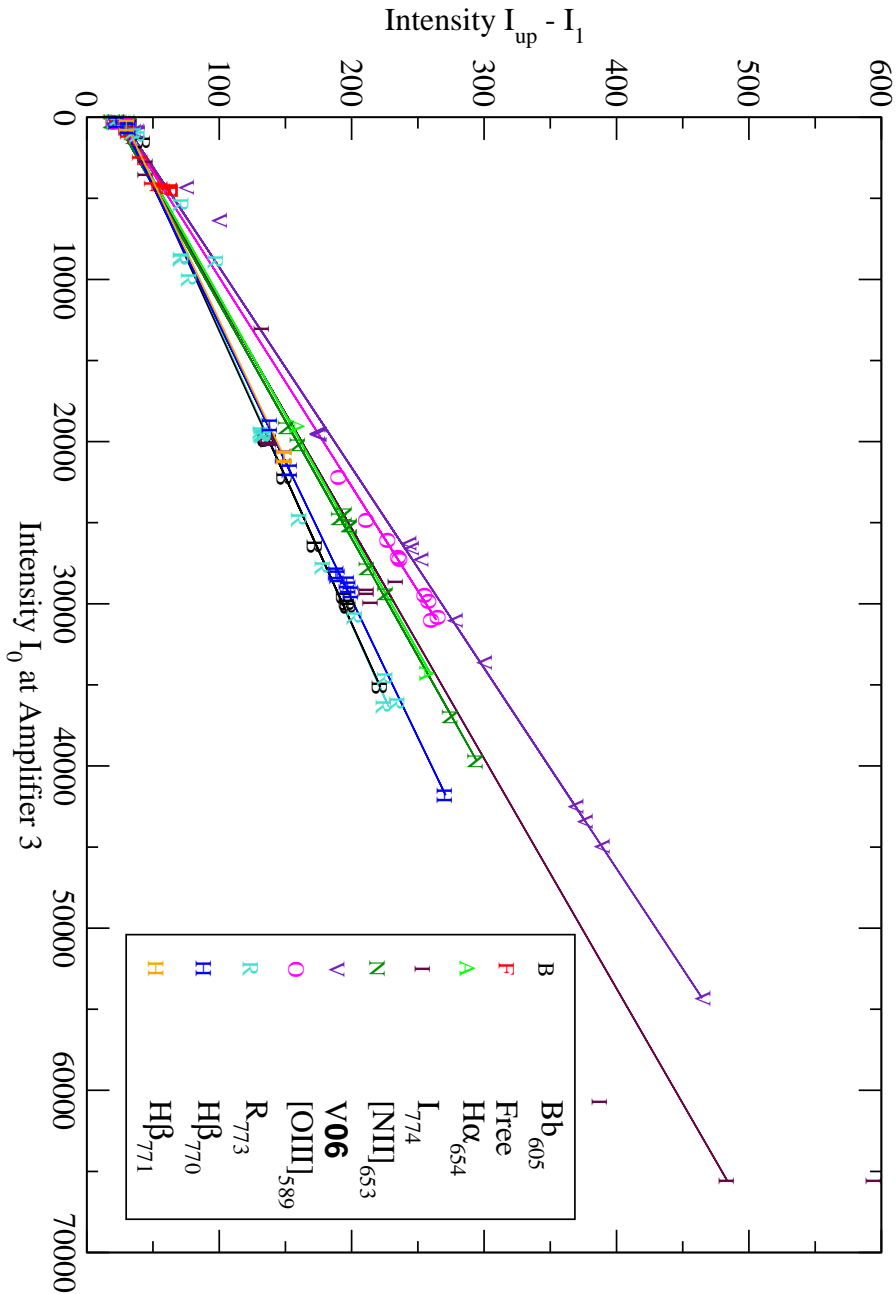


Figure 2.10: Proof that the offset between amplifier 1 and 3 is stable.

2.5. Wavelength Calibration

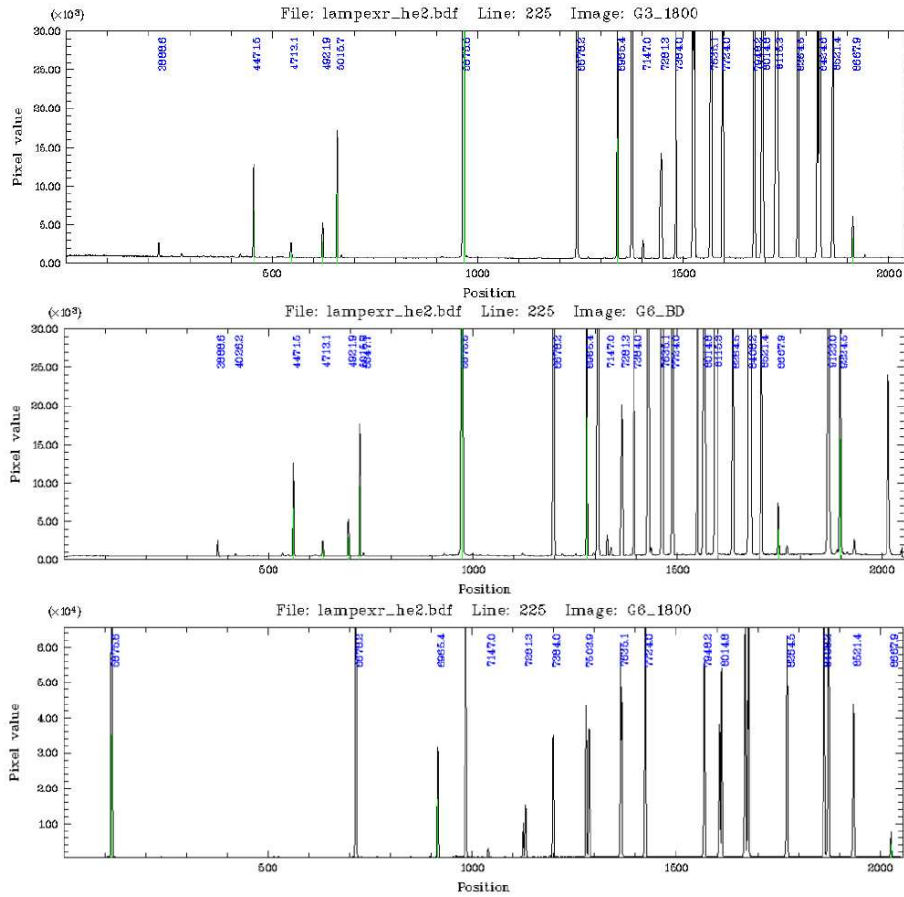


Figure 2.11: Wavelength calibration for gratings 2,3 and 6.

Grism 2: stepsize=3.535, begin=2785, end=9788

Grism 3: stepsize=2.863, begin=3353, end=9085

Grism 6: stepsize=1.478, begin=5730, end=8712

The helium-argon wavelength calibration table delivered with MIDAS at `/midas/calib/data/spec/line/hear.tbl` and the commands of the context LONG have been used. I couldn't fall back on the ESTIMATE/DISPERSION function, since it is not yet implemented for two-dimensional calibration. Nevertheless the two-dimensional calibration was needed, since the wavelength lines were slightly bent, hence it was necessary to identify the lines manually.

Another problem was a kind of overflow with the most prominent line on each lamp spectrum, which caused that all lines above 2^{16} were reduced by that specific amount. Thus the very strong line looked like two. Before really being able to run the wavelength calibration, the gap of the curved(!) line had to be refilled.

For the actual wavelength calibration the spectra were rotated and their binning factors set to 1.0. At the same time the relevant part on amplifier 3 was extracted from the whole image. Then ignoring some wrong information concerning the wavelength calibration on the EMMI homepage (see section 2.1) and using common sense, pretty clean results as seen in figure 2.11 have been achieved. This was done for grism 2 with the batch given in A.12 and analogically for the gratings 3 and 6.

Furthermore I controlled with the batch given in the appendix A.23, if the flection of the objects is the same as for the lamps. In the resulting figure 2.12 you can see that the straightening is well done.

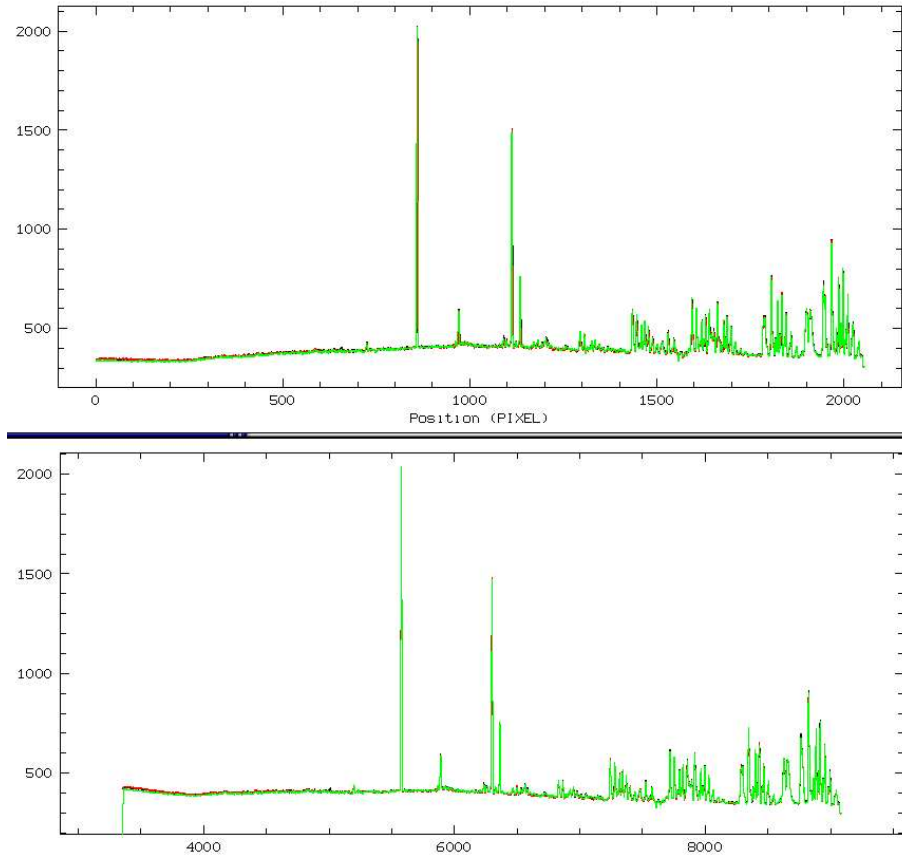


Figure 2.12: Three different rows of a spectral object before and after the rebinning process. The flection of the second dimension has been straightened.

2.6. Hot Pixels and their Rows

In all pictures were two hot pixels located in the area of amplifier 3. The problem about those always overexposed pixels was that they influenced and adulterated all the other pixels of their row in read out direction. The attempt to find an underlying law for the alteration, taking into account their neighboring pixels, the exposure time, etc., was not successful. Therefore I just ensured that the affected rows are not really important in the spectra, and left it at that. Regarding the images, the mean of the two neighboring rows was computed for the mentioned sectors.

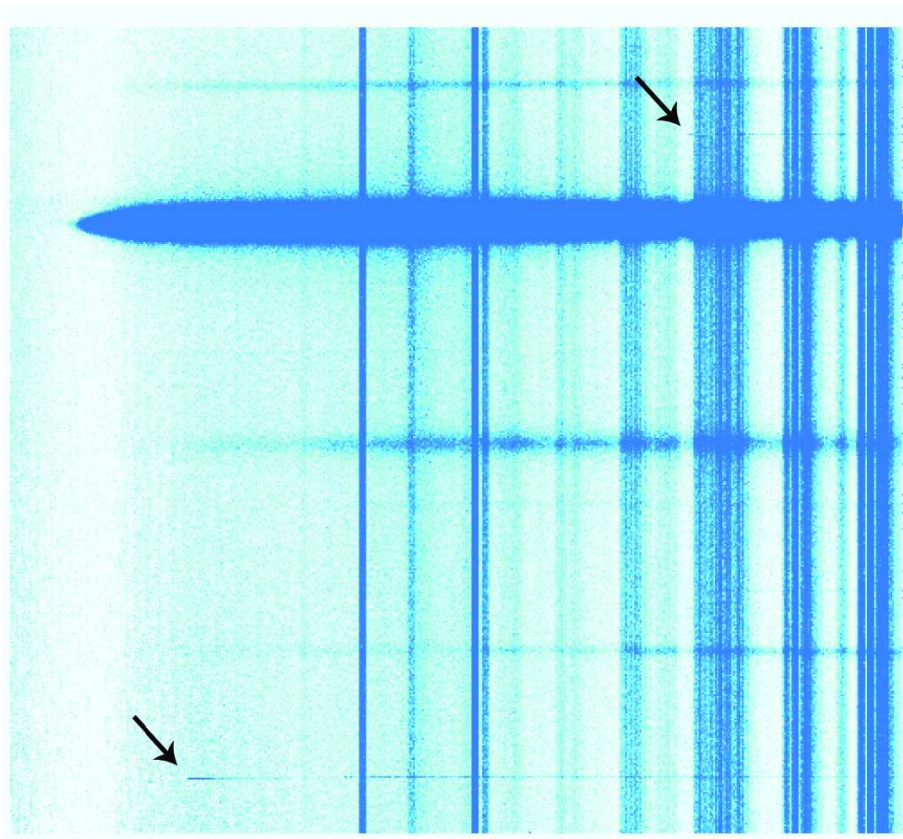


Figure 2.13: Two hot pixels affecting the rest of their rows in read out direction, seen here on the grism 3 spectrum of the standard star LTT6248. As seen above, the rebinning procedure seemed to have made a systematic error on the upper row.

2.7. Complete Reduction of the Spectra

(For the sake of readability, the A.xx numbers in braces are references to the batch-listings in the appendix.)

At first the bias has been reduced (A.13), as described in section 2.2. Then the flat has been reduced, amplifier 3 cut out, and the spectra have been rotated (A.14). They were all rebinned and reduced of the cosmics (A.15). After picking out the standards and looking for the best for each grism (A.16), the correction functions for the quantum efficiency were computed (A.17). There was a problem with some of the standards of the third night, where the extinction seemed to be color dependent. A possible explanation are condensation trails from airplanes. These standards were neglected. Apart from this - consulting meteo data - the third night was in the majority of cases by far the best night.

Then the spectra were normalized to one second and airmass 1.0 (A.18). At last the quantum efficiency was rectified (A.19). I also compared the combined correction functions with the combined functions for throughput and quantum efficiency as declared in the tables of the commissioning report (see section 2.1). The general tendencies agreed with each other within the error bars. Nevertheless the tables have not enough accuracy to feel secure about the response-functions of the grisms

(see figure 2.14). Specially in the blue there is an obvious tendency to overestimate the final spectrum.

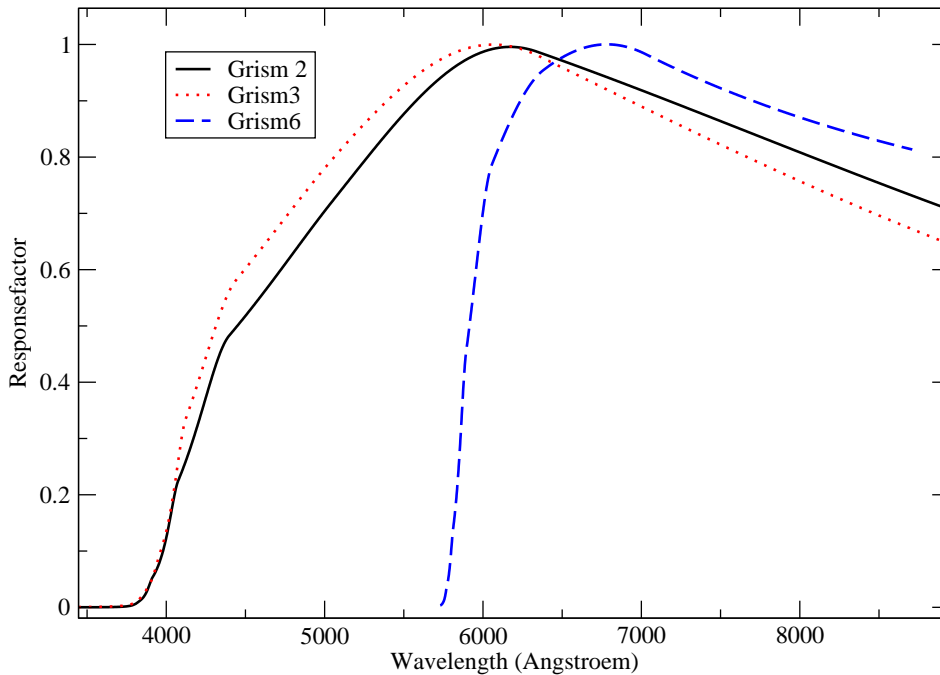


Figure 2.14: Response-curves of the three gratings, where the black solid line represents grism 2, the red dotted line grism 3 and the blue dashed line grism 6. It can be seen that smooth tendencies are missing in the blue part, so that mistakes can be easily done here.

2.8. Complete Reduction of the Images

(Again, the A.xx numbers in braces are references to the batch-listings in the appendix.)

For the reduction of the images the skyflats were subtracted by the reference bias. The skyflats were separated by filter and weighted statistically (A.20). Skyflats with stars on them were neglected or corrected for achieving a good skyflat for each filter.

The bias of the images has been reduced (A.21) as described in section 2.2.

According to the filter, the flat reduction was accomplished with the batch in A.22, which also paid attention to the hot pixels and their rows, as mentioned in section 2.6.

3. The old PN Abell 58

3.1. Appearance and general Discussion

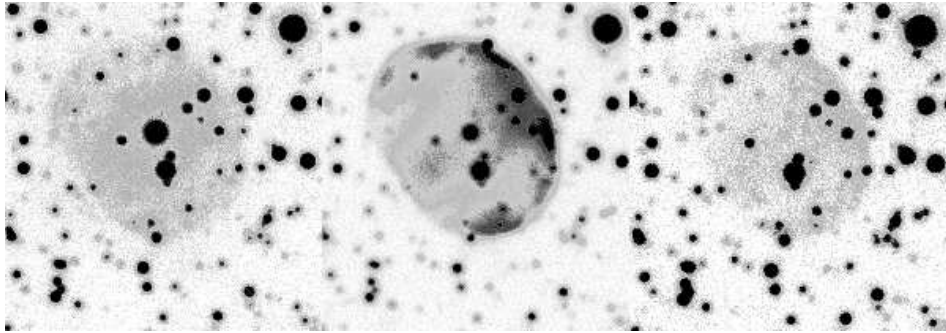


Figure 3.1: Three narrowband images of PN A58. [OIII] is on the left side, [NII] in the middle and $H\beta$ on the right. The position angle to the normal nord-east orientation (compare figure 3.2) is 132.381. The pictures are not rotated to prevent information loss. Note that in the $H\beta$ image no central knot is visible. The edge enhancement in [NII] that appears even in $H\beta$ provides an indication of nebular interaction with the ISM.

According to the manual the EMMI CCD chip has a resolution of $0.''333$ per pixel, but the seeing was not sufficient to derive the size of the V605 Aql knot as done by [Hinkle *et al* (2001)]. The shape of PN A58 seems to depend strongly on the excitation as seen in figure 3.1. The [OIII] image of the PN looks rather roundish, whereas in $H\beta$ and in [NII] a western rim is clearly visible. In all three images the nebula seems to consist of three parts; an inner central part and two 'polar caps' drifting away from it, which is most obvious in the [OIII] image.

In figure 3.2 it is shown, which slit-positions have been used for the spectra.

On the basis of the CCD images my estimation for the size of the old PN A58 is $50''$ for the longitudinal axis and $38''$ for the secondary axis.

Assuming a distance of 3.5 kpc as recommended by [Clayton & de Marco (1997)], this gives with the easy $\tan(\theta)$ -law a mean diameter of 0.75 pc. [Pollacco *et al* (1992)] argued the opposite way around, that 1.2 pc would be a nice diameter for an old PN like A58, and derived a distance of 6 kpc for A58. This is till now the highest distance assumption. Other previous distance estimates have been done by [Abell (1966)], [Ford (1971)], [Cahn & Kaler (1971)] and [Maciel (1984)]. [Van der Veen *et al* (1989)] favored higher distances like 5 kpc to explain the integrated infrared luminosity of V605 Aql, but they misidentified the target ([Kimeswenger *et al* (2000)]).

Because of the edge enhancement due to the ISM interaction I strived to determine the physical properties of the old nebula Abell 58 out of the inner part, near to V605 Aql.

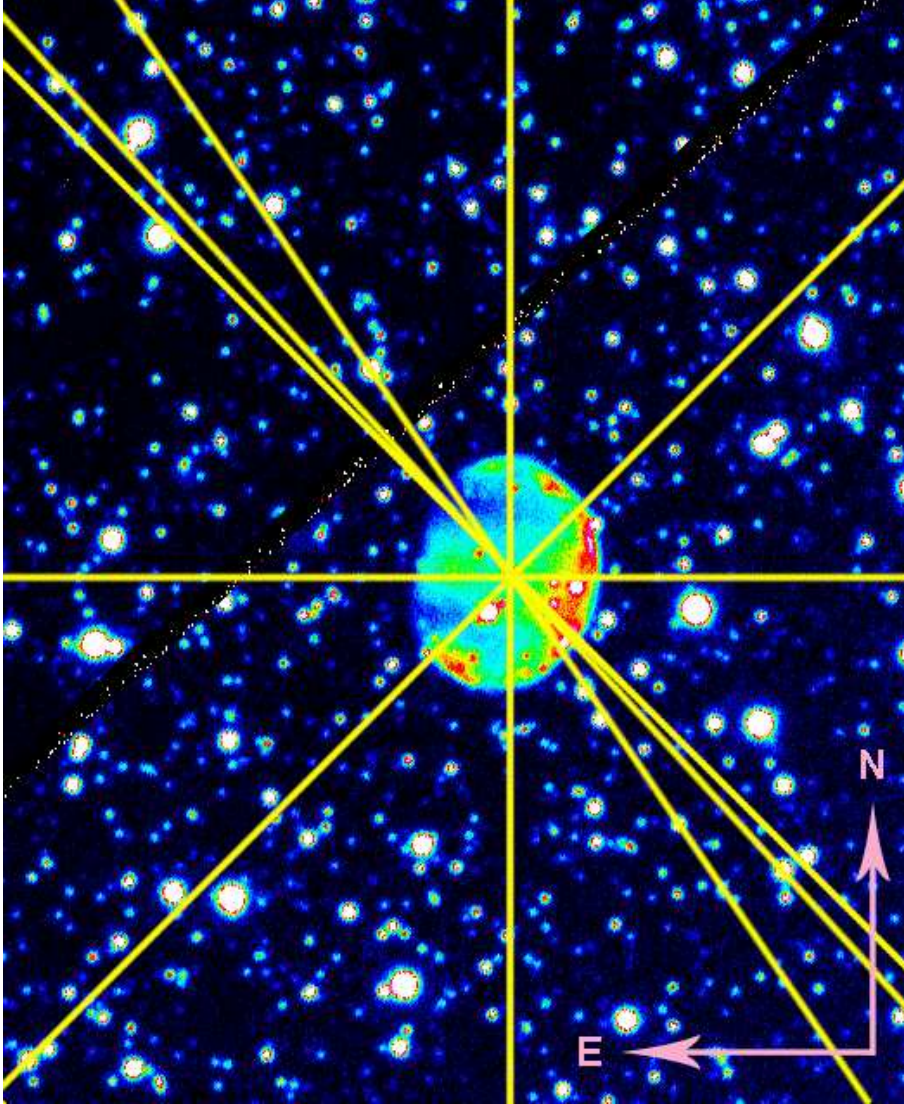


Figure 3.2: Narrowband [NII] CCD image of the old PN A58 with indicated slit positions. The black band from the east to the north is the CCD gap.

3.2. Distance Estimation out of Radio Observations

The VLA Sky Survey by [Condon & Kaplan (1998)] gives a $S = 2.7$ mJy flux-density peak at 1.4 GHz (according to a wavelength of 21 cm), with an 0.8 mJy RMS uncertainty for PN A58. Usually distances are calculated by the 6 cm radio fluxes (according to a frequency of 4885 MHz), but with the theory of free-free radiation that claims that

$$I = I_0 \nu^{-0.1}$$

we can easily translate this value in the usually wanted S_{6cm} and find

$$S_{6cm} = 2.4 \pm 0.7 \text{ mJy} .$$

Now the method by [Cahn *et al* (1992)] can be applied. The optical thickness parameter τ , given by

$$\tau = \log \left(\frac{4\theta^2}{S_{6cm}} \right),$$

where S_{6cm} is inserted in Jansky and θ is the angular radius of the PN in arcseconds (a mean value of $22''$ has been used), is fixed to the value 5.91 ± 0.12 . For $\tau > 3.13$ the ionized mass μ of the PN can be described with

$$\log(\mu) = -0.87.$$

Using these equations, the Radius R and the distance D of the PN can be determined from the ionized mass by

$$\log(R) = \frac{\log(\mu)}{2.5} - 1.306 + \frac{\tau}{5} = -1.654 + \frac{\tau}{5}$$

and

$$D = 206.265 \frac{R}{\theta}.$$

So the solutions using [Condon & Kaplan (1998)] and [Cahn *et al* (1992)] are

$$R = 0.34 \pm 0.02 \text{ pc}$$

and

$$D = 3.15 \pm_{0.15}^{0.23} \text{ kpc}.$$

The radio continuum brightness temperature T_b is given by

$$T_b = \frac{c^2}{2\pi k\nu^2} \frac{S_{6cm}}{\theta^2} =_{\nu=4885 \text{ MHz}} 18.4 \frac{S_{6cm}}{\theta^2},$$

now with S_{6cm} in mJy. The calculated value is 9.05×10^{-2} . From this temperature, which is a measure for the brightness of the nebula at radio frequencies, together with their fitted linear regression line through a sample of bulge PN also [van de Steene & Zijlstra (1995)] specify a radius R :

$$\log(R) = -0.35(\pm 0.02) \log(T_b) - 0.51(\pm 0.05)$$

leading to $R = 0.71 \text{ pc}$ and $D = 6.6 \text{ kpc}$. This approximation is generally a factor of 2 too big.

Normally the best and most faithful results (see [Schmeja & Kimeswenger (2002)]) are derived by the method of [Schneider & Buckley (1996)]. Their equation is:

$$\log(D) = -\log(\theta) - 0.0261 \log^2(I) - 0.299 \log(I) + 1.198,$$

where the surface brightness $I = S_{6cm}/(\theta^2\pi)$ is measured in mJy arcsec⁻². This leads to $D = 3.08 \pm_{0.12}^{0.17} \text{ kpc}$.

For all further calculations I will therefore assume a distance of $D = 3.1 \text{ kpc}$. This means that the radius R of the PN A58 equals 0.33 pc .

3.3. Extinction using the Balmer Decrement $H\alpha/H\beta$

On the way from the object to the observer there is always extinction, as the radiation from the object is absorbed by the interstellar medium (ISM) consisting of gas and dust, and usually re-emitted at another wavelength (causing a reddening). The interstellar extinction is mostly due to the dust. Since the degree of extinction is not only proportional to the quantity of material along the line of sight, but also depending on the wavelength, the ratio of observed spectral lines is changed by the interstellar extinction, too. The extinction constant is defined as:

$$c(H\beta) = \log (F(H\beta)^{th} / F(H\beta)^{obs}) .$$

The theoretical value for $F(H\alpha)/F(H\beta)$ is 2.85. Therefore:

$$c(H\beta) = \frac{1}{0.325} \log \left(\frac{(F(H\alpha)/F(H\beta))^{obs}}{(F(H\alpha)/F(H\beta))^{th}} \right) .$$

I measured the ratios of the two Balmer lines in the old PN A58 with the batch listed in A.24 and received an extinction constant of $c(H\beta) = 0.67 \pm 0.07$.

For comparison reasons we convert this value into the color excess E_{B-V} . I used the equation

$$E_{B-V} = c(H\beta)/1.536 .$$

[Clayton & de Marco (1997)] postulated the extinction values $A_B \approx 2^m3$ and $A_V \approx 1^m7$ for a distance of 3.5 kpc. As

$$E_{B-V} = A_B - A_V ,$$

this gives a color excess of $E_{B-V} = 0^m6$. Rescaling to a distance of 3.1 kpc (see previous section) leads to $E_{B-V} = 0^m6 \times \frac{3.1}{3.5} = 0^m53$. My value of $c(H\beta)$ yields $E_{B-V} = 0^m45 \pm 1^m0$. For further calculations I used the value $E_{B-V} = 0^m5$.

With the aid of the batch listed in A.25 a correction function for the interstellar extinction was computed, using the context LONG in MIDAS and the command EXTINCTION/SPECTRUM. The correction function (see figure 3.3) emphasizes the blue end of the spectra.

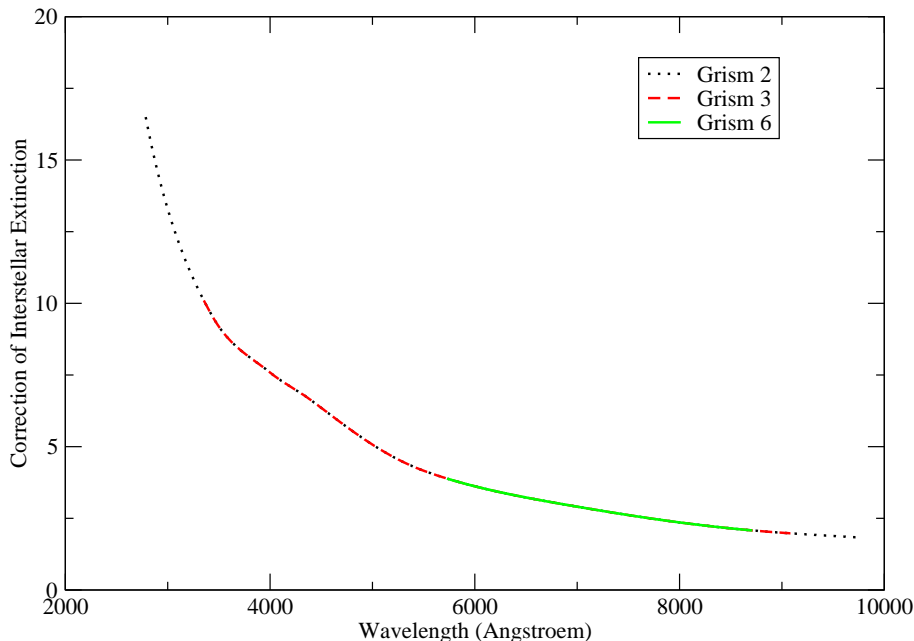


Figure 3.3: Correction of the interstellar extinction. The correction function is the same for all grisms, but only grism 2 (dotted line) needs the whole field. Grism 6 (solid line) needs only a small band and grism 3 (dashed line) lies in between.

3.4. Electron-Density n_e using the [SII] Doublet

[Osterbrock (1974)] has shown that for optically thin nebulae the red emission line doublet $[\text{SII}]_{6716+6731}$ is very sensitive to the electron density n_e . It is a safe assumption that we have an optically thin nebula.

Typical densities for PNe are $10^5 \text{ e}^- \text{cm}^{-3}$ for young compact nebulae down to $1 \text{ e}^- \text{cm}^{-3}$ for very old extended nebulae. The measured ratio of $[\text{SII}]_{6716}/[\text{SII}]_{6731}$ for the whole nebula was at 1.34 ± 0.04 , which gives an electron density of A58 of $80\text{--}100 \text{ e}^- \text{cm}^{-3}$. Actually at 1.34 the ratio is already beginning to converge, a ratio of 1.4 means $40 \text{ e}^- \text{cm}^{-3}$.

The compound spectrum of the PN was generated with the batch given in A.24. Comparing this compound spectrum to the single spectra with the different slit-positions there is no difference in densities detectable. The error-bars on the single spectra (produced with the commands in A.26) are higher, but the electron-density is everywhere surely less than $300 \text{ e}^- \text{cm}^{-3}$.

With another batch (given in A.27) I specially focused on the rim area in the south-west. In the rim the intensities of the lines were higher, but the derived ratio of this region is about the same (1.32 ± 0.04).

Generally [SII] provides higher density results, since there are always little blobs in a thinner gas, and [SII] gives the density of these blobs and not their dispersion in the surrounding gas, the so called filling factor.

For further calculations a value of $100 \text{ e}^- \text{cm}^{-3}$ has been used.

3.5. Ratio R of the [OIII] and [NII] Lines and Temperature

$$R = (I_{5007} + I_{4959})/I_{4363} = 7.73 \exp(3.2910^4/T)(1/K)$$

with $K = 1 + 4.510^{-4}d/T^{1/2}$. This ratio of the [OIII] lines results from computations of collision strengths and transition probabilities and was published by [Osterbrock (1974)]. The intensity I_{4363} is theoretically a factor 2.9 smaller than I_{5007} . We can give an approximation neglecting the density d , to directly determine the electronic temperature T out of R . This approximation is:

$$T = 3.2910^4 / \ln(R/7.73)$$

Nevertheless this relation is not used much. The reason might be, that the S/N in the blue is in the majority of cases too small and the third relatively weak line at 4363 Å is a problem. In my case this is also due to the high insecurity of the response-functions of the grisms. The spectra were produced with the batch given in A.24. My interstellar extinction corrected solution for grism 2, where I've got a good signal, is 18 000 Kelvin. In grism 3 it is only a guesswork (the solution would be about 16 000 Kelvin). Furthermore we have to take into account the overestimation of the blue end, which shifts the solution to higher temperatures. It is difficult to state an error derived from the inaccuracy of the response-functions.

Qualitatively the same calculation can be done with the [NII] lines, where the problems with the response curve should not be so overdominating:

$$R = (I_{6548} + I_{6583})/I_{5755} = 6.91 \exp(2.5010^4/T)(1/K)$$

with $K = 1 + 2.510^{-3}d/T^{1/2}$. The intensity I_{6548} is here theoretically a factor 2.99 smaller than I_{6583} . Using the same approximation as with the [OIII] lines, the solution for grism 2 is 10.100 K, for grism 3 with less signal 9 600 K. Most people before assumed an electron temperature of 10 000 K, which seems to be quite justified.

Generally it can be said that the intensities of [NII] and [OIII] in the individual grisms differed more often from each other than comparable lines, which all had about the same intensities in all three grisms. This fact may be due to a slight temperature dependency over the whole nebula.

3.6. Recombination Time-Scales in A58

There is definitely HeII₄₆₈₅ in the spectrum of A58 produced with the batch listed in A.24 (compare to figure 4.8 in section 4.4). This fact provides together with the knowledge of recombination timescales an estimation for the time between the ending of the UV radiation of the central star and the nova burst.

Using the same dielectric recombination coefficients α as [Pollacco(1999)] we can calculate a table for the recombination time-scales given by $\tau_r = \frac{1}{n_e \alpha}$. This table was computed for electron densities n_e of 100 and 200 e⁻cm⁻³ (see table 3.6).

Table 3.1: Recombination time-scale for atomic states at $T_e = 10.000$ K for electron densities n_e of 100 and 200 e⁻cm⁻³. The terms 'r' and 'd' refer to the radiative and dielectronic components in the total recombination coefficient 't'.

State	$\tau_r(n_e = 100)$	$\tau_r(n_e = 200)$
H ⁰	760	380
He ⁰	1500	750
He ⁺	206	103
O ²⁺ (r)	31	16
O ²⁺ (d)	28	14
O ²⁺ (t)	19	9
O ⁺ (r)	155	78
O ⁺ (d)	190	95
O ⁺ (t)	85	43
N ⁺ (r)	139	70
N ⁺ (d)	155	78
N ⁺ (t)	73	37

It can be seen that the recombination times for [OIII] are relatively low, but this table is only valid for single atomic systems. We have to take into account the Bowen resonance-fluorescence mechanism within in the PN. Due to their high density some of the HeII Lyman α photons are absorbed and excite the $3d^3P_2^0$ level of [OIII] and prevent so the premature recombination of [OIII]. Thus this mechanism slightly decreases the HeII recombination times but enlarges the [OIII] recombination time-scales. (For a more detailed study refer to [Osterbrock (1974)].)

The derived time-scales have an upper limit of a few hundred years only. The favored values lay around one hundred years or even lower.

3.7. Modelling the PN with CLOUDY

On the basis of the line fluxes presented in table 3.2 the old PN was modelled with Cloudy ([Ferland (1996)]). The final goal was not to reproduce the ionization and thermal equilibria within the nebula in detail but to qualify the stellar continuum before the helium flash pulse. The PN sees still its old central star at the time of the helium flash. Thus a large grid of photoionizing models was calculated, giving us the position of V605 Aql in the HRD during its hidden past.

Table 3.2: Dereddened line fluxes for the PN A58 relative to $H\beta$.

Line ID	λ	Intensity
HII	4686	27
$H\beta$	4861	100
OIII	4959	286
OIII	5007	804
NII	5755	4.5 ± 1.0
HI	5876	18
NII	6548	92
$H\alpha$	6563	286
NII	6584	280 ± 20.0
SII	6716	42
SII	6731	31
ArIII	7136	13

Usually blackbody radiation is used for such calculations of other objects (e.g. [van de Steene (1995)], [van Hoof & van de Steene (1999)], [Kerber *et al* (1999)], [Nürnberg *et al* (2001)], [Cuisinier *et al* (2002)]). [Armsdorfer *et al* (2002)] and [Armsdorfer & Kimeswenger (2001)] showed that the use of real stellar atmospheres changes especially the helium lines. Here I thus used NLTE central star models of Rauch ([Rauch (1997)], [Rauch (2003)]). The same grid of model atmospheres was used also by [Pollacco(1999)] for the twin object V4334 Sgr.

The temperature of the central star of the PN (CSPN), its luminosity, the gas density and the filling factor of the gas were varied (see figures 3.6 and 3.7). While the range for the filling factor was selected to fit to the typical findings for evolved nebulae (see [Armsdorfer *et al* (2002)]), the gas density range of 100 to 300 $e^- \text{cm}^{-3}$ was taken from the sulphur lines (see Section 3.4). The distance of 3.1 kpc was adopted from Section 3.2, leading with the average angular radius of 22'' to the linear radius of the shell.

The strength of the helium lines is nearly independent from the CSPN luminosity. Thus this fixes the abundance of this element clearly. The variations of the parameters were chosen to get a optimized intersection of the solutions for the HeI_{5876} , the $[\text{OIII}]_{4948+5007}$ and the $[\text{NII}]_{6548+6583}$ lines at the level of $I_{\text{observed}}/I_{\text{model}} = 1.0$. These solutions are not completely independent from the chosen abundance. The $[\text{NII}]_{5755}$ line then should intersect, if the resulting electron temperature is suited, there as well. This fixes the nitrogen abundance and thus the whole solution. The best fit model is shown in figure 3.4.

The placement of the derived CSPN luminosity and temperature together with the theory of stellar post-AGB evolution by [Blöcker (1995)] yields the mass of the final

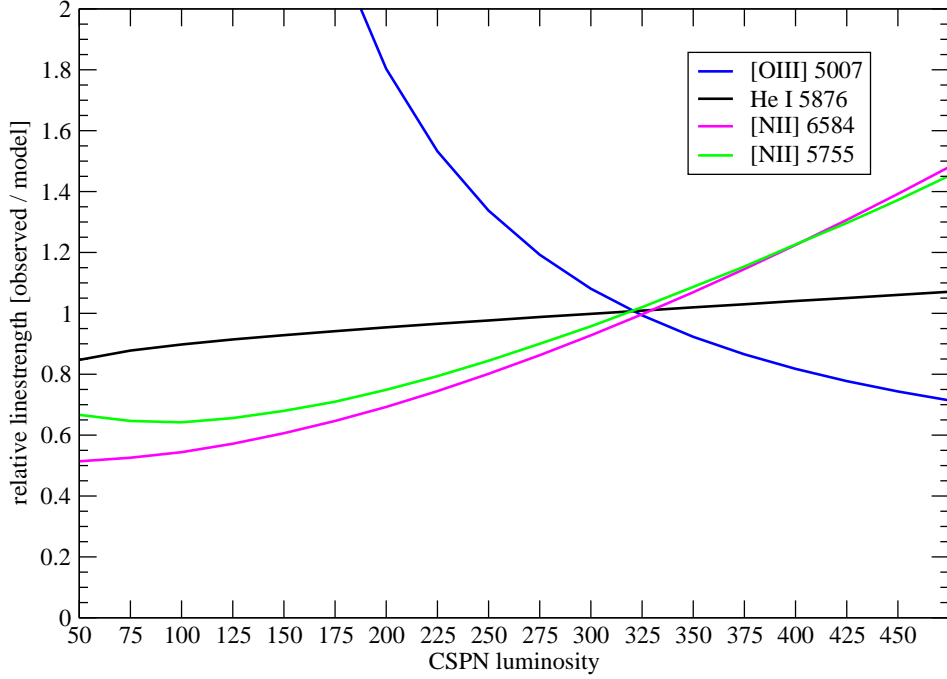


Figure 3.4: The best fit model shows a good intersection of the solutions for the Helium, Oxygen, the Nitrogen lines at the level $I_{\text{observed}}/I_{\text{model}} = 1.0$. The resulting model is given in Tab. 3.3.

white dwarf and the transition time t . The position of the CSPN in the HRD is shown in figure 3.5. The age zero of the CS evolution corresponds to the point where the mass-loss rate has decreased enough to be described by a rather simple law, the so called Reimer's rate. In other evolution theories there is a clear cut between the final strong AGB mass loss rates and the low or even none mass loss afterwards. [Blöcker (1995)] prefers a non-abrupt decrease of mass-loss rates, as suggested by dust-shell calculations, and decreases the AGB mass-loss rate proportional to the pulsational period P_0 starting at $P_0 = 100$ d. Age zero is reached at $P_0 = 50$ d. At a certain point depending on T_{eff} he switches to the radiation driven wind theory. The solutions are consistent with the initial-final relation and isochrones of observational data. Other models before favored higher transition times and couldn't describe correctly the fading time scales of higher mass cores. [Blöcker (1995)] found that the degeneracy in the interior of the star increases during the AGB evolution. The more degenerate a model leaves the AGB, the more compact and cooler is the interior, since a higher fraction of potential energy is used to raise the Fermi energy of the electrons, being no longer available for the thermal heating. Thus the longer the evolution on the AGB the faster is the fading.

The resulting model (see table 3.3) is completely self consistent. In addition it is also supported by the velocity measurements by [Pollacco *et al* (1992)], who derived for the expansion velocity of A58 $v_{\text{exp}} = 31 \pm 4 \text{ km s}^{-1}$, giving with the dynamical age of 8200 years a dynamical radius of PN A58 of

$$R = 0.26 \pm_{0.05}^{0.04} \text{ km s}^{-1},$$

which matches well our radius of $R = 0.33$ as derived in section 3.2. This is an especially good conjunction, if we take into account that the dynamical solution is usually a factor of 2 or 3 off target.

Table 3.3: Parameters of the best fit model.

Parameter	Value
distance	3.1 kpc (see Section 3.2)
<i>CSPN:</i>	
luminosity	$L = 325 \pm 100 L_{\odot}$
effective temperature	$T_{\text{eff}} = 121.5 \pm 6 \text{ kK}$
age from post-AGB	$t = 8300^{+1500}_{-500} \text{ years}$
white dwarf mass	$M = 0.605 \pm 0.02 M_{\odot}$
<i>PN gas shell:</i>	
average radius	angular $22''$ linear $r = 1.02 \cdot 10^{16} \text{ m}$
thickness	$\Delta_r/r = 0.2$
filling factor	$\epsilon = 0.05$ (adopted)
electron density	$n_e = 200 \pm 100 \text{ e}^{-}\text{cm}^{-3}$
abundances:	
helium	$[\text{He}] = -0.83$
nitrogen	$[\text{N}] = -4.00$
oxygen	$[\text{O}] = -3.40$

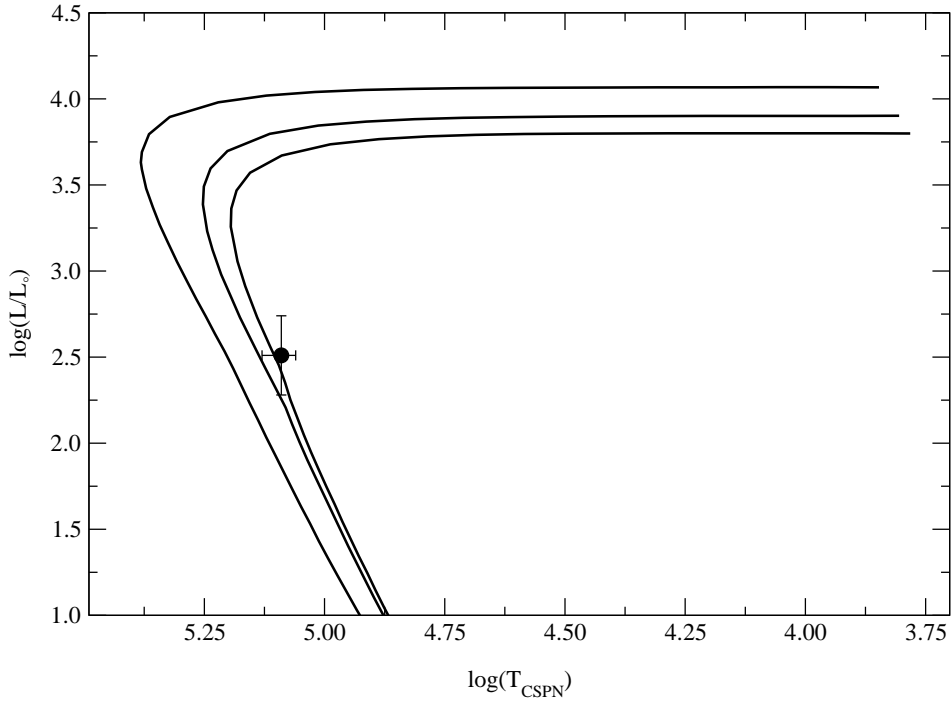


Figure 3.5: The position of the CSPN in the HRD at the moment of the helium flash. The evolutionary tracks for the post-AGB evolution for a 0.605, 0.625 and 0.696 M_{\odot} white dwarf from [Blöcker (1995)] are plotted.

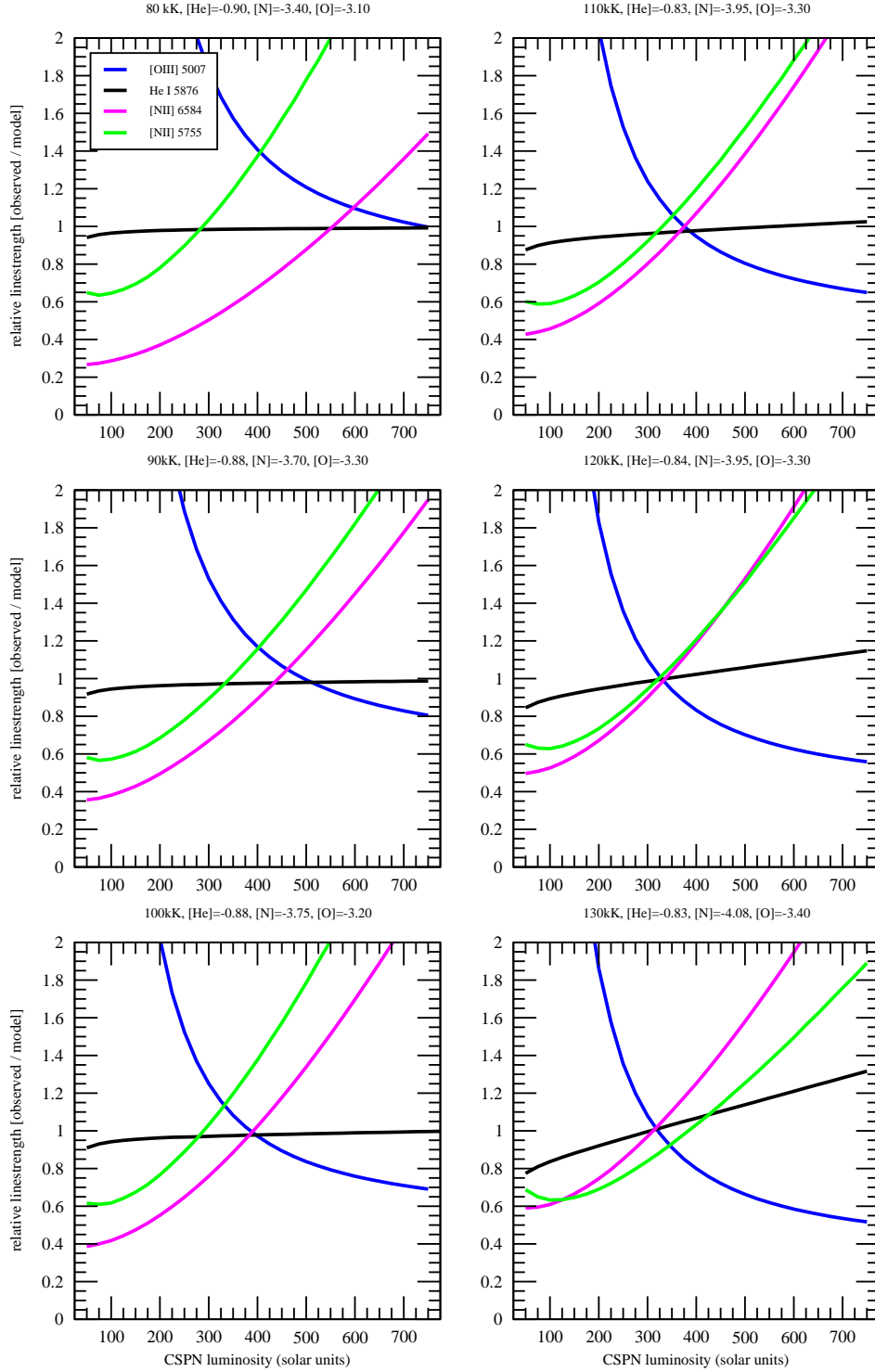


Figure 3.6: The influence of the CSPN temperature on the line ratios. The HeI_{5876} , the $[\text{OIII}]_{4948+5007}$ and the $[\text{NII}]_{6548+6583}$ lines were used to derive a solution for the abundances. While a model below 90 kK gives no common solution at all, there is always, using strange abundances a solution for $100 \text{ kK} \leq T_{\text{eff}} \leq 130 \text{ kK}$. Although the $[\text{NII}]_{5755}$ fixes (via the electron temperature in the gas) the solution towards 120 kK.

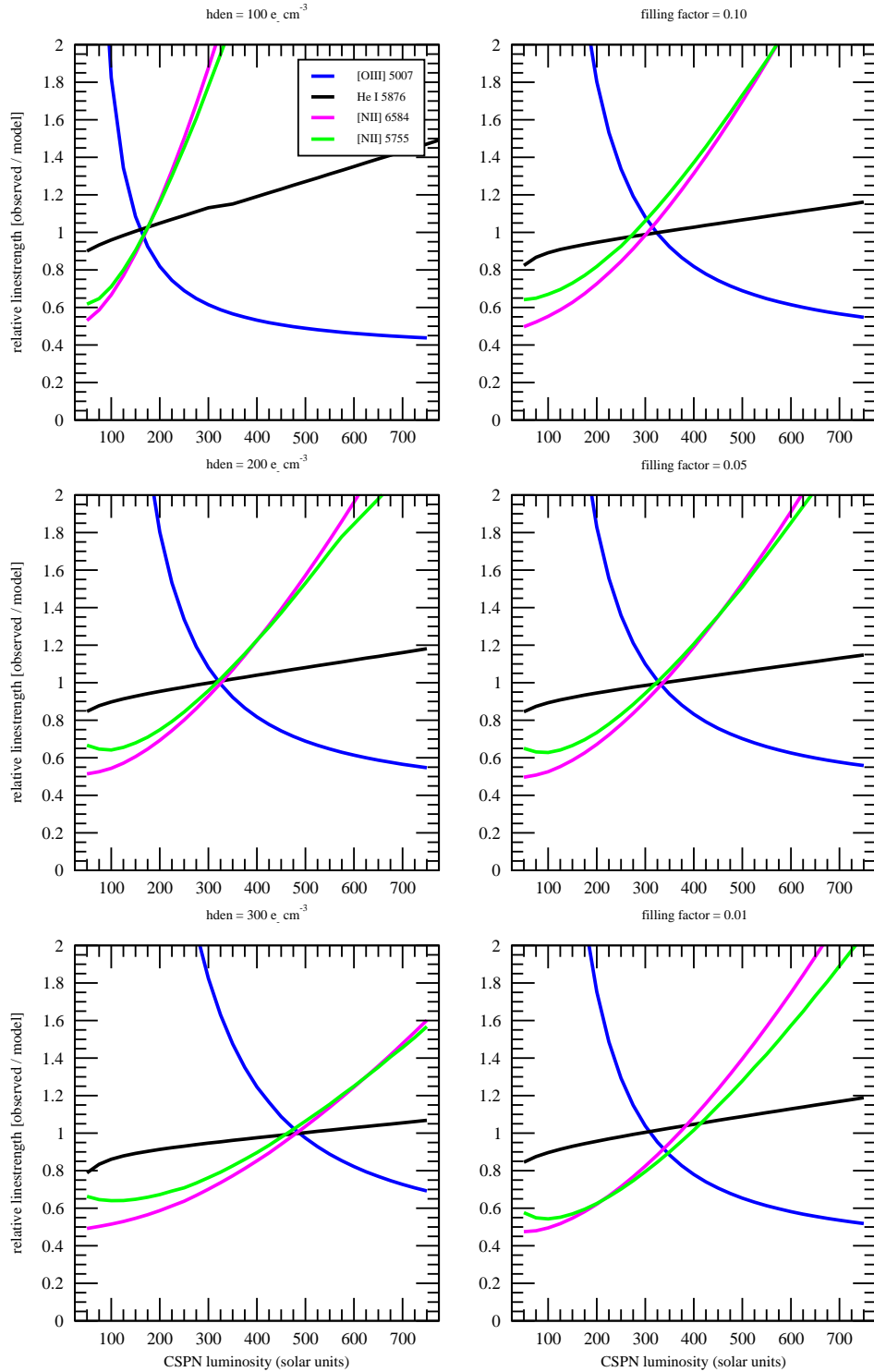


Figure 3.7: The influences of the gas density (left side) and of the filling factor (right side). While the filling factor does not influence the solution over a range of even one order of magnitude, the gas density shifts the solution along the stellar luminosity. T_{eff} and the abundances are not influenced at all.

4. The Born Again Core V605 Aql

4.1. General Discussion and Appearance

[Hinkle *et al* (2002)] were so nice to place a preview of their HST images at my disposal. The diameter of the the central knot of V605 Aql is about $1.2''$, as seen in the figures 4.1 and 4.2. In addition we can also see a structure, specially in the [OIII] image.

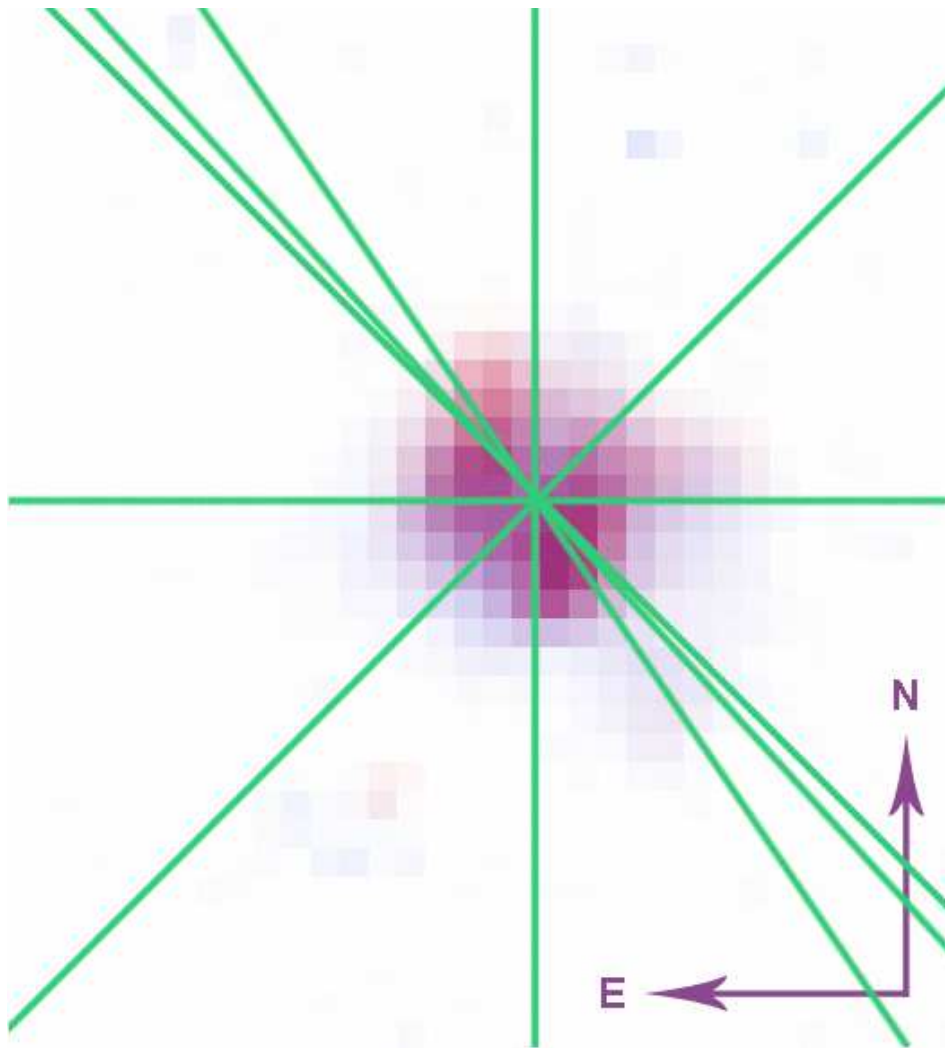


Figure 4.1: Indicated slit-positions of our spectra over HST images by [Hinkle *et al* (2002)]. Keep in mind that the used slit-width was $1''$, so that nearly the whole central knot was in the spectra. The background is a compound of [NII] (blue) and [OIII] (red).

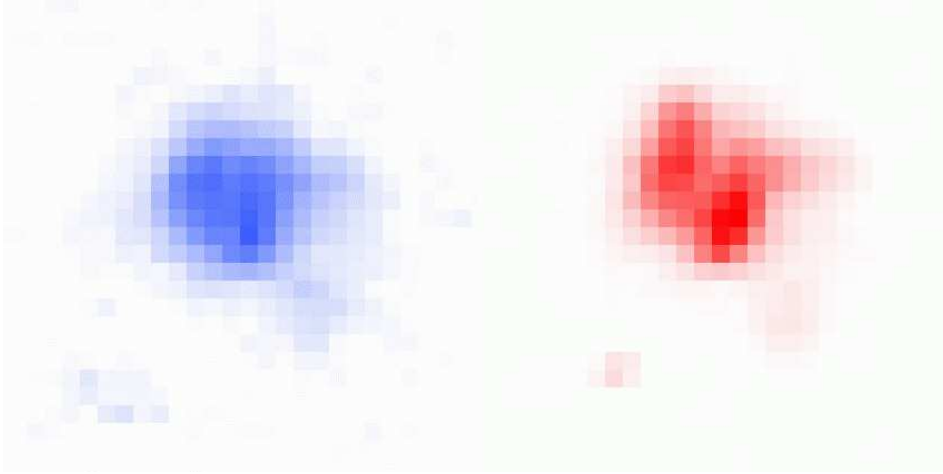


Figure 4.2: HST-Images of V605 Aql, split into [NII] (left side) and [OIII] (right side). North is up, east is left. The pixels in the southeast of V605 Aql are only intractable cosms. A structure can be clearly seen: a big luminous knot splitting into two parts and a smaller one in the southwest.

4.2. Densities and Mass of the Dust Shell

As in section 3.4 the ratio of the [SII]-doublet $[\text{SII}]_{6716+6731}$ was used again to derive the electron density. The measured ratio of $[\text{SII}]_{6716}/[\text{SII}]_{6731}$ for the central knot of V605 Aql was at 0.75 ± 0.01 , which gives an electron density for V605 Aql of $1800 \pm 100 \text{ e}^- \text{cm}^{-3}$. We can suppose that this density is the density of the thin outer shell of V605 Aql. Because of the high visual extinction, there should be a higher density in the whole shell.

With an outer diameter of $1.2''$ (see previous section) and a distance of 3.1 kpc, we get an outer radius of the dust shell of

$$r_{out} = 3100 \tan(0.6'') = 9 \times 10^{-3} \text{ pc} = 2.78 \times 10^{14} \text{ m}.$$

Using the result of the free distance parameter by [Kimeswenger & Koller (2002)], and letting

$$(r_{out} - r_{in})/r_{out} = const = 0.167,$$

we get the inner radius of the dust shell, where the temperature is too hot for dust

$$r_{in} = 2.31 \times 10^{14} \text{ m}.$$

For a single shell the dust mass of a wind shell where the density $\rho(r) = \Sigma \frac{1}{r^2}$ can be written as:

$$M_{dust} = 4\pi\Sigma(r_{out} - r_{in}),$$

where we adopt the density from [Koller (2000)]:

$$M_{dust} = 1.6 \times 10^{-16} (r_{out} - r_{in}) M_{\odot},$$

which gives

$$M_{dust} = 7.4 \times 10^{-3} M_{\odot}.$$

The real density $\rho(r)$ at the outer shell radius

$$\rho(r_{out})_{dust} = \Sigma \frac{1}{r_{out}^2} = 3.3 \times 10^{-16} \text{ kg m}^{-3}.$$

A gas-to-dust ratio lower than the typical values of 100–200 in the ISM has to be expected, since the the carbon richness enhances the dust formation, and values of about 100 would lead to a tremendously thick dust-shell. Assuming a reasonable gas-to-dust ratio of 10 as also implicitly given by [Koller & Kimeswenger (2001)], we obtain

$$M_{gas} = 7.4 \times 10^{-2} M_{\odot}$$

and

$$\rho(r_{out})_{gas+dust} = \Sigma \frac{1}{r_{out}^2} = 3.6 \times 10^{-15} \text{ kg m}^{-3}.$$

Let's now go back to the electron densities and make a rough estimation for the gas-mass. Normally we have 1.4 atomic units for one electron on average, assuming simple ionization. But in this central knot we have not the common hydrogen helium mix but a compound of 40% He and 60% CNO like in PG1159 stars (see [Werner *et al* (1997)]). One electron is now attached to a value of 8.8 atomic units. Therefore an electron-density of

$$1800 \text{ e}^{-}\text{cm}^{-3} = 1800 \cdot 8.8 \cdot 1.6605 \times 10^{-27} \cdot 10^6 \text{ kg m}^{-3} = 2.63 \times 10^{-17} \text{ kg m}^{-3}.$$

If we fill the whole volume with such a density (this means setting the filling factor of the [SII] blobs to 1 to get the upper limit), we get out of the [SII] electron densities:

$$M_{gas} = \frac{4\pi}{3} (r_{out}^3 - r_{in}^3) \cdot 2.63 \times 10^{-17} \text{ kg m}^{-3} = 10^{27} \text{ kg} = 5 \times 10^{-3} M_{\odot}.$$

If we compare now these two derived gas-masses, it is obvious that the emission lines on the spectra of V605 Aql are only from the thinner outer shell and not from the core body of the shell. However the density function alone is not sufficient to explain the whole discrepancy of about 2 orders of magnitudes. As [Guerrero & Manachado (1996)] indicate, the outflow can also be bipolar of which we only see the blueshifted side. Such a bipolar outflow can significantly reduce the required dust mass. Thus non-spherical shell models are needed. Also the images by [Hinkle *et al* (2002)] as shown in section 4.1 indicate clearly that the central knot of V605 Aql doesn't show a symmetric sphere.

4.3. The Hydrogen Content of V605 Aql

The finding of [Guerrero & Manachado (1996)] of an $H\alpha$ line as strong as 30% of $[NII]_{6548}$ is not supported by my observations. It may originate from an inaccurate subtraction of the line from the old nebula. Also in my spectra (see figure 4.3) there is a small hump in the region of $H\alpha$, but it has rather 10% of $[NII]_{6548}$. Furthermore it is not sure, if this is really $H\alpha$. If it is, then it has not the same blueshift as the neighboring $[NII]$ lines, but is by 40 km s^{-1} faster, which gives 160 km s^{-1} , adopting the value of 120 km s^{-1} for the $[NII]$ lines by [Pollacco *et al* (1992)] and their high resolution spectrum (see figure 4.4). On the other hand this hump may also be a compound of $HeII_{6560}$ and $H\alpha_{6563}$. It may even be that it is $HeII_{6560}$ alone (the total blueshift would then reach only 70 km s^{-1}), but that seems rather improbable, even though [Pollacco *et al* (1992)] give a blueshift of only 85 km s^{-1} for $[OIII]$. The S/N in their spectrum (see figure 4.4) was too low to find a $H\alpha$ line as given here.

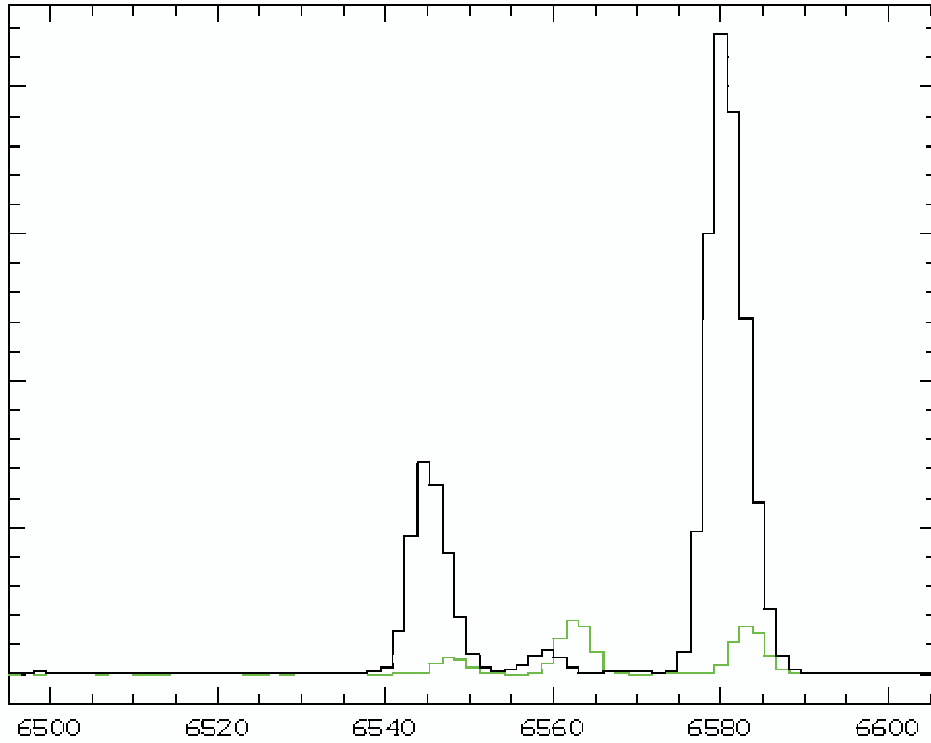


Figure 4.3: This spectral image of the $H\alpha$ region of V605 Aql was obtained with grism 6. The pale line is the interstellar extinction corrected spectrum of the surrounding PN which has been subtracted.

The same problem occurs with $H\beta_{4861}$ where we have also a neighboring helium line at $HeII_{4859}$. On all images of grism 2, there is clearly no $H\beta$ detectable. Only two images of grism 3 give the impression that there might be something at the wavelength of $H\beta$. But after subtracting the stellar continuum of the neighborhood, a confirmation of a $H\beta$ line is not justifiable. Figure 4.5 shows $H\beta$ and the corresponding offband, obtained to remove stellar components and continuum radiation. Those images show the same flux of V605 Aql in the hydrogen line and of the adjacent continuum. The flux thus comes from the continuum.

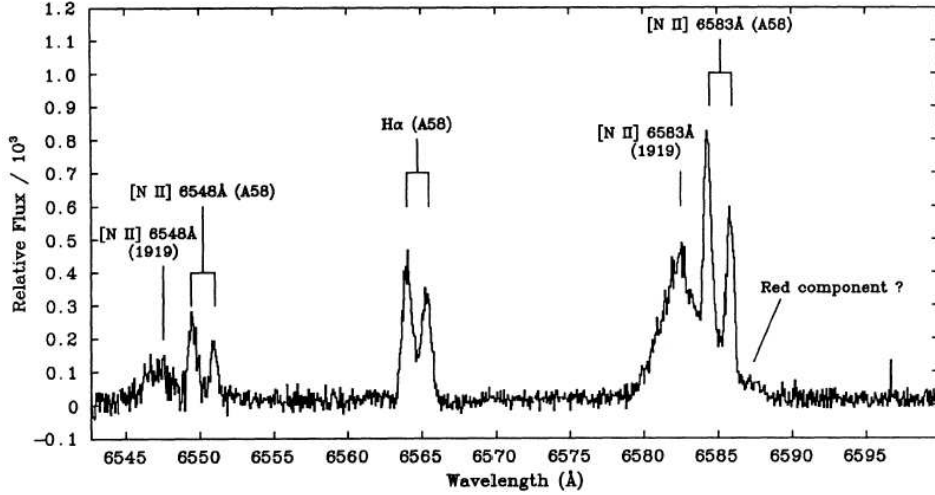


Figure 4.4: This high resolution spectrum was taken by [Pollacco *et al* (1992)]. The face and reverse sides of the PN shell are clearly resolved. For V605 Aql we see only the component moving to us, the red component cannot be seen because of the the optically thick dusty shell.

The conclusion is, that this object is much more hydrogen underabundant as given in [Guerrero & Manachado (1996)]. If the reduction of [Guerrero & Manachado (1996)] is reliable, this may be due to a temporal evolution.

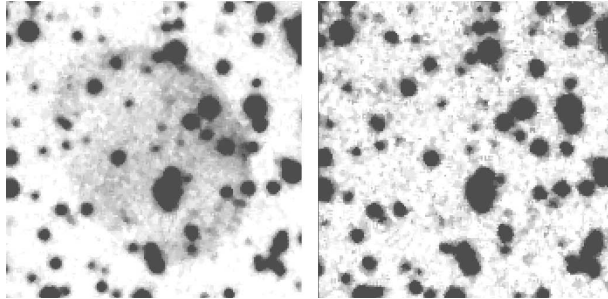


Figure 4.5: Narrowband image of $H\beta$ and the corresponding offband. The hydrogen line has about the same flux in V605 Aql as in the continuum, the central object is not detectable in $H\beta$.

The really faint $H\alpha$ and the quasi non existent $H\beta$ give an extreme $H\alpha/H\beta$ ratio. The physical explanation behind this fact could be that $H\beta$ vanishes completely in the internal extinction, this means that the emission lines of the spectra though they come not from the inner core of the dust shell (see section 4.2) are still originating in a region where dust plays a role in extinction, namely the outer region of the dust shell.

4.4. Identification of spectral Lines

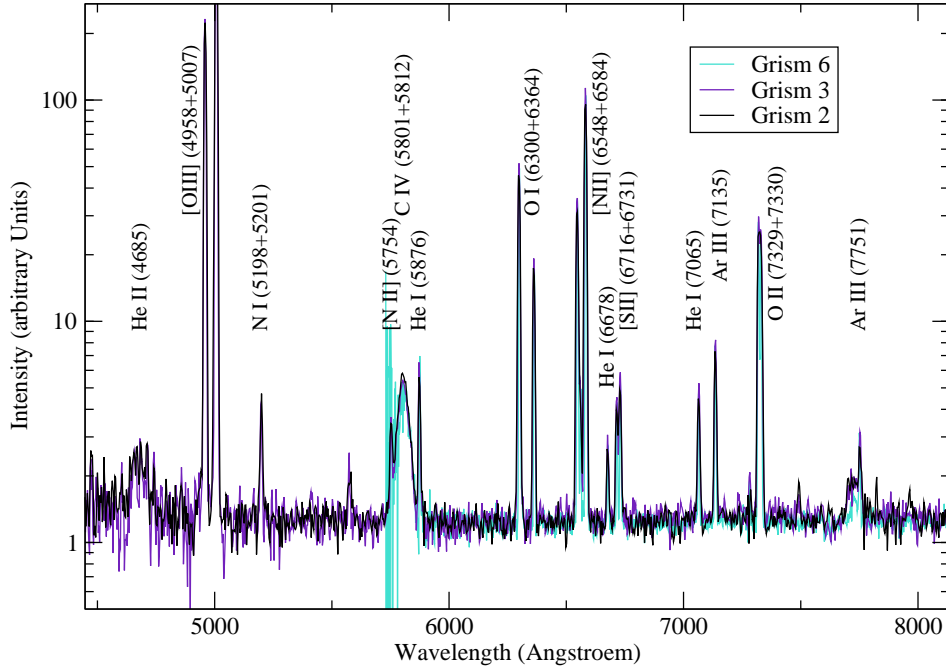


Figure 4.6: The logarithmic scale in this overview spectrum of V605 Aql was chosen to emphasize the fainter structures. The $C_{IV5802+5812}$ feature lies on the blue end of the response function for grism 6.

The whole spectrum is shown in figure 4.6. Lines over 8000 \AA were not identified because of the significant quantity of skylines in this region. High resolution spectroscopy is needed to filter out real lines in this maze, everything else can only be guesswork. The resolution is as well too low to see a dependency between line-profile and ionization degree in the PN or V606 Aql spectra.

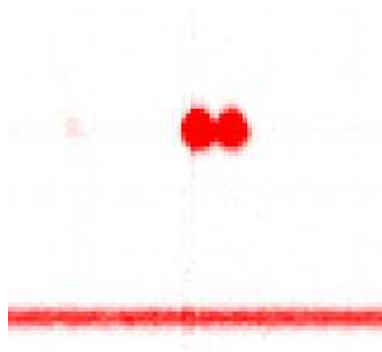


Figure 4.7: This grism 6 image of the $OII_{7330+7331}$ lines in V605 Aql was subtracted by the surrounding PN and the skylines and corrected of interstellar extinction. The splitting into the two lines can be seen clearly.
`load qamns3.bdf center=7330,340 cuts=0.1,4`

Significant parts like the $\text{OII}_{7330+7331}$ lines (see figure 4.7), the area around HeII_{4685} (see figures 4.9 and 4.8) and the feature around 7751 \AA (see figure 4.10) were zoomed out. The spectra were produced with the commands listed in the appendices A.26 and A.25.

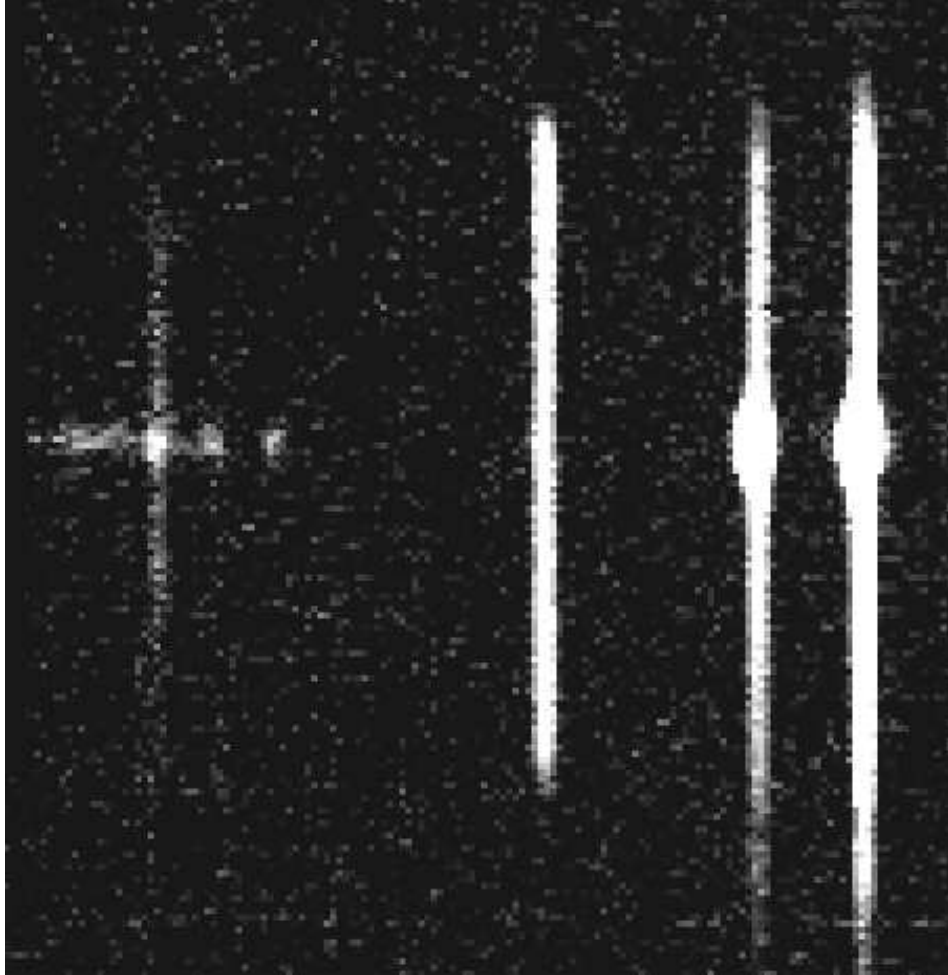


Figure 4.8: Spectral image with the PN lines of HeII_{4685} , $\text{H}\beta$ and $[\text{OIII}]_{4959+5007}$. A knotty structure of V605 Aql in the environment of HeII_{4685} can be seen. HeII_{4685} is a knot itself. This feature is seen in all images. The knots are identified in figure 4.9.

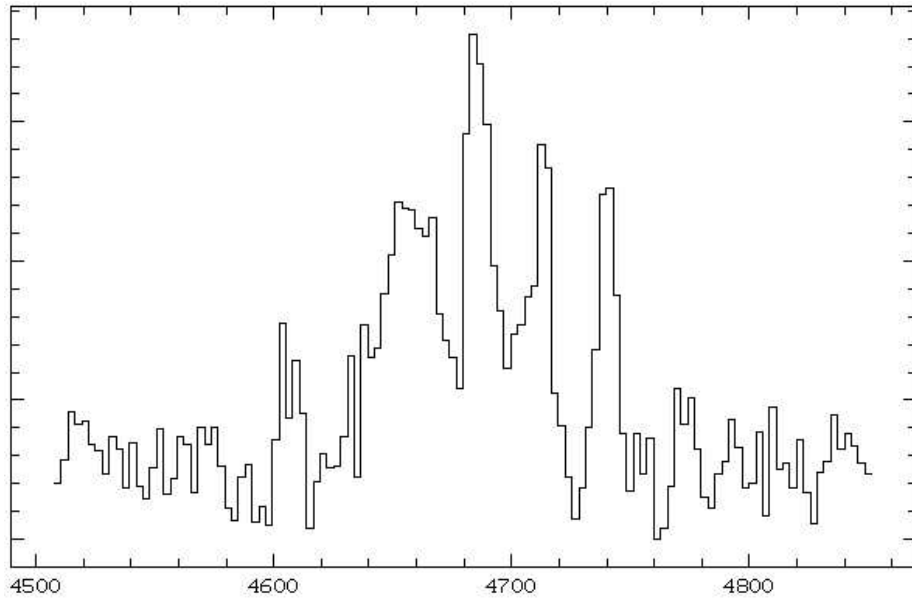


Figure 4.9: The broad component around 4650 is assumed to be $C_{III} 4647+4650+4651$, then comes $HeII_{4685}$, followed by a blended feature of $Ar_{IV} 4711$ together with HeI_{4713} . At 4740 there is another Ar_{IV} line.

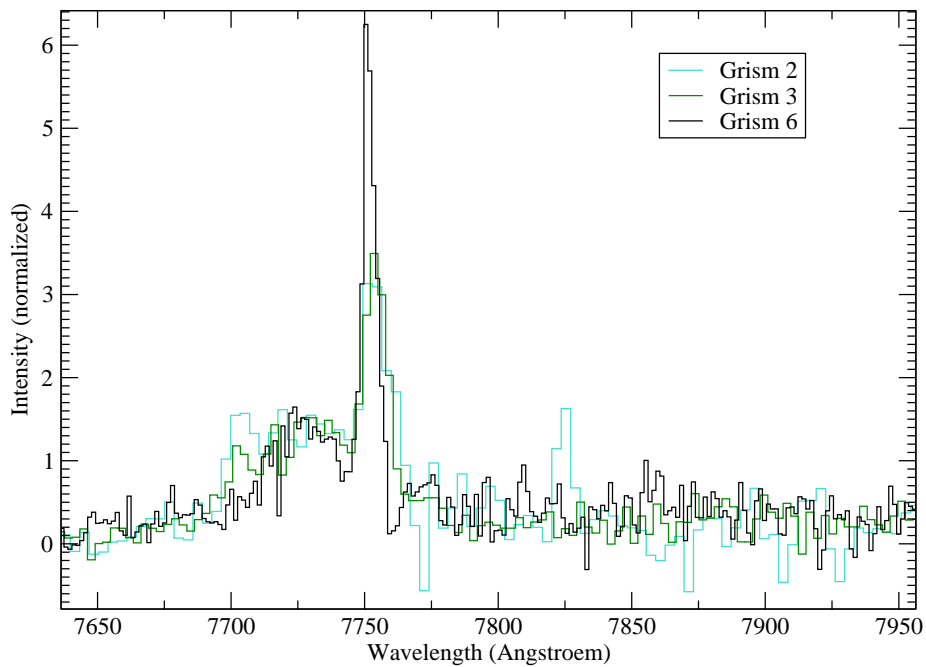


Figure 4.10: This interstellar extinction corrected close up of the V605 Aql spectrum after the subtraction of the PN and the skylines shows an interesting feature. I identified it as Ar_{III}_{7751} and another broad C_{IV} line at 7726 \AA .

4.5. Blueshifts

The correction of the night-sky lines has been controlled optically: the sky was averaged, blown up again to a whole image and then subtracted. The eye is a really sensitive instrument for recognizing a successful or rather bad correction. The seen continuum of V605 Aql after all reductions is scattered light from the CS. The correct subtraction of the sky is relevant for the blueshift, since an unfavorable rest or negative skyline at a certain position can also shift the gaussian center of a line.

The non-relativistic formula

$$v = c \frac{\Delta\lambda}{\lambda_0}$$

was applied to derive the relative blueshift between the PN and V605 Aql.

The Midas command CENTER/GAUSS GCURSOR was used to determine the position of the lines in the spectra produced by the batches listed in A.25 and A.26. Only a few lines are visible both in the PN and V605 Aql and therefore qualified for blueshift determinations. The used lines to measure the blueshift are listed in table 4.1. H α wasn't incorporated (see section 4.3).

Table 4.1: Measured blueshifts with the aid of grism 6

λ	Blueshift(km s ⁻¹)
6548.05	128
6583.45	123
6716.44	129
6730.82	129
7135.79	125

The effective resolution in grism 2 was too low to define a blueshift, the errorbars were over 40 km s⁻¹ in each direction. The general blueshift in grism 3 is $v = 120 \pm 16$ km s⁻¹. In grism 6, the grism with the highest resolution, the general blueshift is at $v = 127.0 \pm 2.5$ km s⁻¹. The [OIII]₄₉₅₉₊₅₀₀₇ lines were not in the range of grism 6.

Comparing the same slit-position taken one time with grism 3 and one time with grism 6, the results looked very consistent with each other within the errorbars. All the same the errorbars for the blueshifts of one single grism 3 spectrum are too high to make a definitive statement. The same is valid when comparing three different slit-positions with grism 3. No obvious tendency for an angle-dependency or special blueshifts for special lines can be seen, but the errorbars are again too high. Higher resolution spectroscopy is needed to obtain better founded correlations.

4.6. Close-up to the C_{IV} Wolf Rayet feature

Let's now look especially at the Wolf Rayet Carbon type wind line. Each of the two C_{IV}₅₈₀₂₊₅₈₁₂ (excitation 39 eV) lines is best fitted with a wide component and a narrow component, where the narrow component has the same width and blueshift as the neighboring HeI and [NII]. The wide component of each line has a FWHM of 2600 km s⁻¹ and is centered at the systemic velocity. This difference in blueshift

implies a model with an optically thick dusty shell covering only a very small outer section expanding with $\approx 125 \text{ km s}^{-1}$ and a wide optically thin hot bubble. The resolution is too low to define an angel-dependency of the C_{IV} feature.

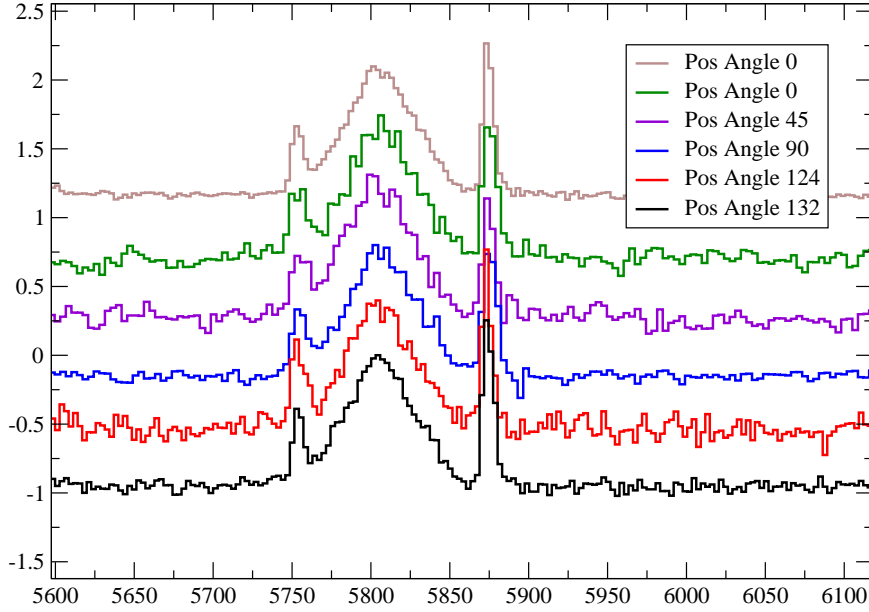


Figure 4.11: The C_{IV} line in all slit-positions, all normalized to 1.0. It is clearly steeper, than a gauss would be alone indicating two components for the individual C_{IV}₅₈₀₂₊₅₈₁₂ lines. No special angel-dependency can be seen with the applied resolutions. The single spectra were produced with the batch listed in A.26.

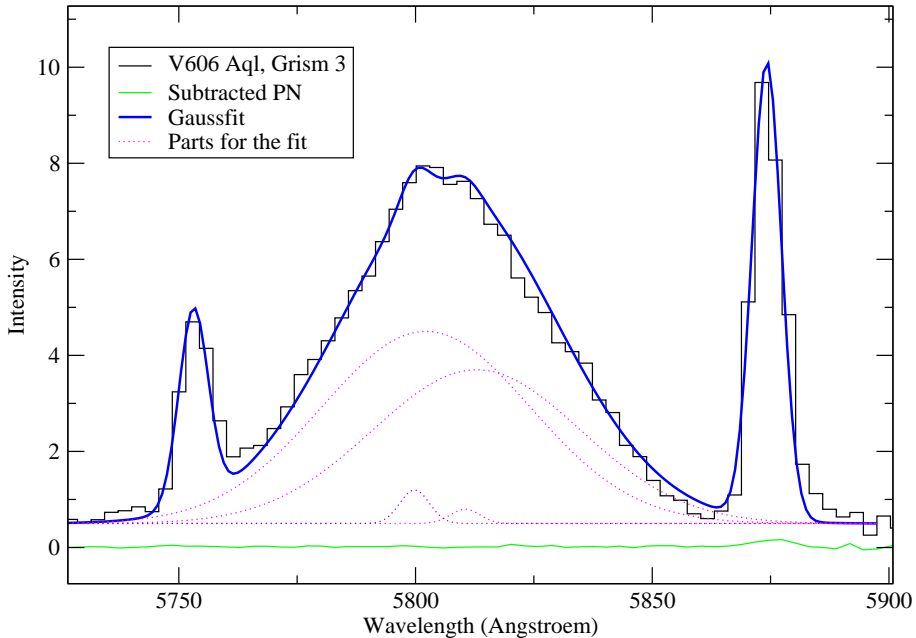


Figure 4.12: Best fit to the C_{IV}₅₈₀₂₊₅₈₁₂ lines. This completely reduced spectrum is a compound of the two grism 3 spectra with the best S/N. The seen continuum is scattered light from the CS. This figure was produced with the aid of the batches listed in A.25 and A.28.

4.7. High Resolution Spectra and Speculations

New data was obtained in July 2003 with the higher resolution mode EMMI REMD at the NTT with grating 6 (housing D). Information about the characteristics of the detector can be found under:

<http://www.ls.eso.org/lasilla/Telescopes/NEWNTT/emmi/emmiRemdBldm.html>

The resolution with a readout binning of 2 was at $0.2 \text{ \AA} / \text{pixel}$. The wavelength range of the REMD is rather small, and really high exposure times were needed to get any signal. Note that the medium-dispersion slit of the REMD is oriented North-South, when EMMI is at a position-angle of 0 degree. In figure 4.13 the spectrum around the C_{IV} line can be seen. Leaving out the base reductions I tried to get some preliminary results. The shape of the C_{IV} line (produced with the commands of the batch listed in A.29) indicated a slightly different form for different position angles. The slit-position was calibrated at the HeI_{5876} and $[NII]_{5755}$ lines. A difference in the spatial resolution for different position-angles would mean that also the velocities vary for this slit-positions. The result (produced with the batch listed in A.30 is shown in figure 4.14). Keep in mind that without the final data reduction this is only a speculation.

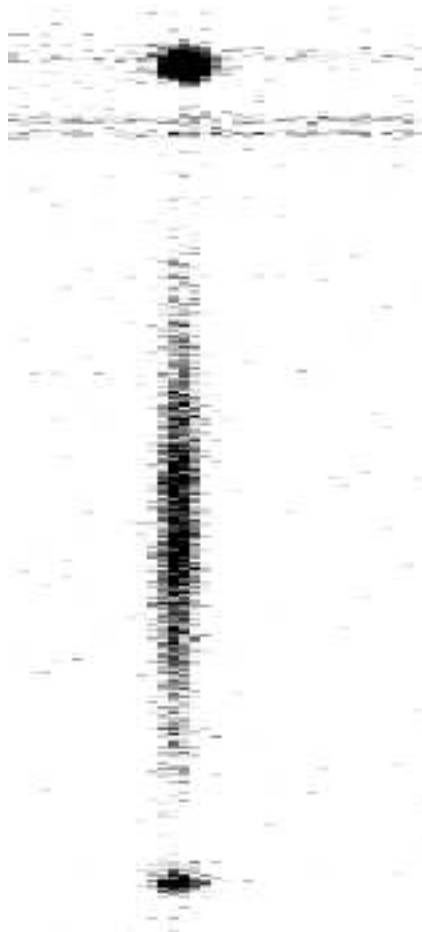


Figure 4.13: The upper point in this EMMI REMD spectrum of the C_{IV} line is HeI_{5876} , the other point is $[NII]_{5755}$. These two points were used to straighten the line for further investigations.

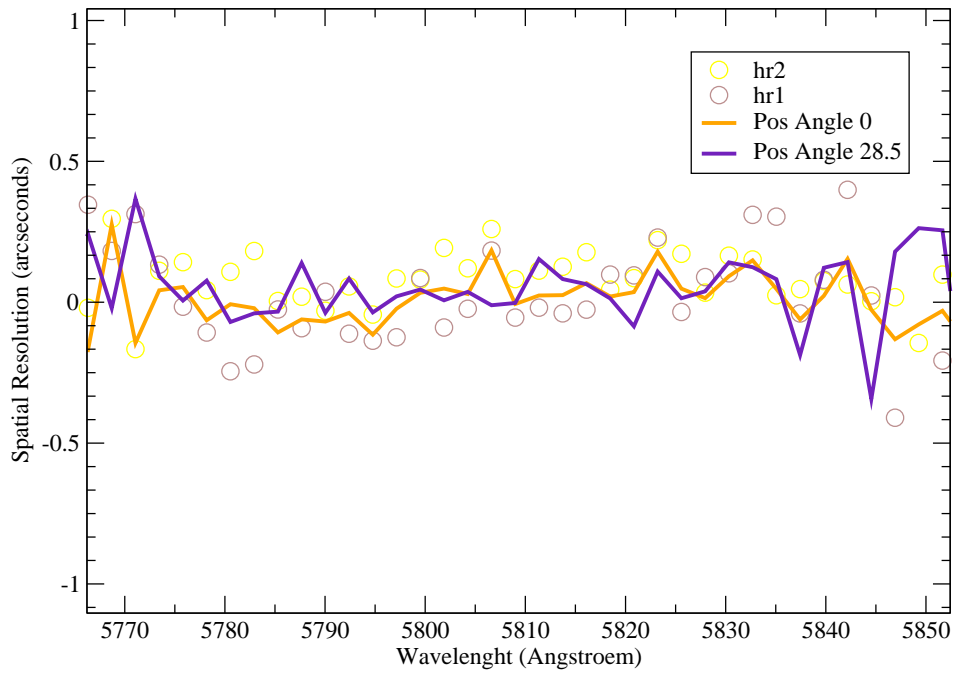


Figure 4.14: High resolution spectra of the C_{IV} line. It was tried to find the spatial resolution to derive different velocities. The data was taken with two different slit-positions, one from north to south (position angle 0) and the other one rotated by 28.5° to the north east. One might interpret that the mean line of position angle 28.5° is rather constant over the whole C_{IV} feature, whereas the mean line for position angle 0 shows a slight wave. But as seen on the y-axis this tendency is on a rather small scale. The data of the two images used for the mean line of position angle 0 is plotted to give an impression of the accuracy.

High resolution spectra were also taken around $HeII_{4685}$. A quick look didn't reveal more than described in section 4.4. Careful data reduction has to be applied to improve the signal to noise.

5. Conclusions and future Prospects

Although being one of the most interesting objects to study the behavior of the born-again phenomenon, V605 Aql had been completely neglected for more than six decades. Only in the 1980's did theorists claim that final helium flash objects should exist and the wrongly qualified nova came back into scientific view. However it was always outshined by its younger brother Sakurai's Object (V4334 Sgr), which became the proto-typical final flash object. Sakurai's object is still frozen in its reborn AGB resp. post-AGB state, whereas V605 Aql is already in transition.

The parameters used to calculate stellar evolution become crucial when we consider such subtleties as born-again objects. Hence the physical properties of born-again in all stages provide a hard constraint on valid evolution theories.

In section 3.6 we conclude based on recombination time-scales that the time between the end of the UV radiation of the central star (= the time of the late helium flash) and the nova burst of V605 in the 1920's is at around one hundred years. Modelling the surrounding old PN A58 with CLOUDY, we obtain that the central star had a mass of $0.6 M_{\odot}$ and a temperature of 120 000 Kelvin before the final helium flash (see section 3.7). The time since leaving the post-AGB was set to 8200 years. The abundances for these photoionizing models were derived from the presented spectra and the most crucial parameter - the distance - was extracted from radio observations (see section 3.2).

Comparing our findings with the results of the double-loop theory by [Lawlor & MacDonald (2003)] we see some severe discrepancies. Whilst the properties in point A (see figure 1.4 in section 1.2) correspond well to the properties of the central star as derived with CLOUDY, the transition time between point A and E is irreconcilable with our value of one hundred years. In the points D and F the luminosities diverge from the preferred values of CLOUDY, but above all the temperature is too low at 50 000 and 80 000 Kelvin. The date of the nova burst can be identified either with point H or E, the luminosity is strongly dependent on the applied distance, and photometries of the light-curve indicated that V605 Aql has begun to form its dust-shell still in its rising. Besides the long time-scales the low temperature is the main argument to exclude the double-loop theory by [Lawlor & MacDonald (2003)] for V605 Aql. Also if they applied another convective parameter, the temperature didn't increase. However the theory by [Herwig (2001)] fulfills our requirements very well. His predictions for a very late thermal pulse with $0.6 M_{\odot}$ include transition-times from 10 to 200 years. His calculations had to be continued, to see whether we get a new hydrogen poor PN like A30 and A78 or RCrB stars, as a link between the born again scenario and RCrB has been often suggested.

Due their high carbon abundance the hydrogen poor objects can also be used for better dust-shell modelling and to test theories for the building of the winds in shorter timescales. Thus, the C_{IV} Wolf Rayet wind line is of special interest. The very fact of its existence tells us that V605 Aql has reached again a temperature above 50 000 Kelvin. Moreover, this line provides us also with information about the geometry. The non blueshifted broad C_{IV} lines give a hint of a thin but optically thick dusty shell surrounding a wide optically thin hot bubble around the central source. The absence of strong blue continuum by stray-light stemming from clumps

illuminated by the in line of sight hidden central source, excludes the possibility of an open geometry. Other wind lines like $O_{IV}5291$, as seen in the hydrogen poor PN A30, can not be found. This absence leads to the conclusion that the core of V605 Aql has been eroded down to the pure carbon core of the star during the 1919 event.

The dusty shell of V605 Aql is expanding at a velocity of about 125 km s^{-1} , confirming the result of [Pollacco *et al* (1992)]. It is non spherical, as shown in section 4.2 and seen on the HST images (see section 4.1). However, the required complex, non spherical dust models are not yet available. The visual light that can be seen in the spectra comes not from the main body of this shell but from one of its outest regions. I made a first attempt to derive different velocities for the individual parts of V605 Aql (see section 4.7). These preliminary results have to be verified.

We have to take into account that only 0.6% of the total luminosity of V605 Aql is emitted at wavelengths below $3.5 \mu\text{m}$. Known dust models rather concentrate on the infrared part of the spectrum, hence the calibration in the visual is difficult.

The lower mass of born-again objects reduces the gravitational binding, and the higher metallicity enhances the dust formation mechanisms. The whole transition from the AGB to the final white dwarf is performed at 'fast forward' speed. The stronger hydrogen under-abundance of V605 Aql in the presented spectra than in the statements by [Guerrero & Manachado (1996)](see section 4.3) might be already due to a temporal evolution.

The research in the field of the born-again scenario is far away from being at its end.

Bibliography

- [Abell (1966)] Abell, G. O. - *Properties of Some Old Planetary Nebulae*, ApJ, 144, 259, 1966
- [Armsdorfer *et al* (2002)] Armsdorfer, B., Kimeswenger, S., & Rauch, T. - *Effects of CSPN Models on PN Shell Modeling*, Revista Mexicana de Astronomia y Astrofisica Conference Series, 12, 180, 2002
- [Armsdorfer & Kimeswenger (2001)] Armsdorfer, B. & Kimeswenger, S. - *Central Star Models and Planetary Nebulae Shell Modeling*, Astronomische Gesellschaft Meeting Abstracts, 18, 906, 2001
- [Asplund *et al* (1997)] Asplund, M., Gustafsson, B., Kameswara Rao, N., & Lambert, D. L. - *A stellar endgame - the born-again Sakurai's object*, A&A, 332, 651, 1997
- [Asplund *et al* (1998)] Asplund, M., Gustafsson, B., Lambert, D. L., & Kameswara Rao, N. - *Abundance similarities between the RCrB star V854Cen and the born-again Sakurai's object*, A&A, 321, L17, 1998
- [Blöcker (1995)] Blöcker, T. - *Stellar evolution of low- and intermediate-mass stars. II. Post-AGB evolution.*, A&A, 299, 755, 1995
- [Blöcker (2001)] Blöcker, T. - *Evolution on the AGB and beyond: on the formation of H-deficient post-AGB stars*, Ap&SS, 275, 1, 2001
- [Borkowski *et al* (1994)] Borkowski, K. J., Harrington, J. P., Blair, W. P., & Bregman, J. D. - *The dust in the hydrogen-poor ejecta of Abell 30*, ApJ, 435, 722, 1994
- [Cahn & Kaler (1971)] Cahn, J. H., & Kaler, J. B. - *The Distances and Distribution of Planetary Nebulae*, ApJS, 22, 319, 1971
- [Cahn *et al* (1992)] Cahn, J. H., Kaler, J. B., & Stanghellini, L. - *A catalogue of absolute fluxes and distances of planetary nebulae*, A&AS, 94, 399, 1992
- [Clayton & de Marco (1997)] Clayton, G. C., & de Marco, O. - *The Evolution of the Final Helium Shell Flash Star V605 Aquilae From 1917 to 1997*, AJ, 114, 2697, 1997
- [Condon & Kaplan (1998)] Condon, J. J. & Kaplan, D. L. - *Planetary Nebulae in the NRAO VLA Sky Survey*, ApJS, 117, 361, 1998
- [Cuisinier *et al* (2002)] Cuisinier, F., Köppen, J., Acker, A., & Maciel, W. J. - *The Galactic Bulge: the Stellar and Planetary Nebula Populations*, Revista Mexicana de Astronomia y Astrofisica Conference Series, 12, 136, 2002
- [Ferland (1996)] Ferland, G. - *a Brief Introduction to Cloudy 90.05*, Univ. Kentucky, Department of Physics and Astronomy, Internal Report, 1996
- [Ford (1971)] Ford, H. C. - *V605 Aquilae: a Nova-Like Variable in an Old Planetary Nebula*, ApJ, 170, 547, 1971
- [Guerrero & Manchado (1996)] Guerrero, M. A., & Manchado, A. - *The Chemical Abundances of the Hydrogen-poor Planetary Nebulae A30 and A58*, ApJ, 472, 711, 1996
- [Harrison (1996)] Harrison, T. E. - *A Near-Infrared Survey of Old Novae-II. CK Vulpeculae and V605 Aquilae*, PASP, 108, 1112, 1996

- [Herwig (2001)] Herwig, F. - *The Evolutionary Timescale of Sakurai's Object: A Test of Convection Theory?*, ApJ, 554, L71, 2001
- [Hinkle *et al* (2001)] Hinkle, K. H., Joyce, R. R., Ridgway, S. T., Close, L., Lebzelter, T., Hron, J., Andre, K., & Sperl, M. - *Imaging the Ejecta from the Final Flash Star V605 Aql*, AAS, 199, 135, 2001
- [Hinkle *et al* (2002)] Hinkle, K., Joyce, R., Ridgway, S., Close, L., Lebzelter, T., Hron, J., & Andre, K. - *Imaging the Ejecta from the Final Flash Star V605 Aql* ASP Conf. Ser. 279: Exotic Stars as Challenges to Evolution, 187, 2002
- [Iben & Mac Donald (1994)] Iben, I. Jr. & MacDonald, J. - *The Born Again AGB Phenomenon*, Proceedings of the 9th European Workshop on White Dwarfs Held at Kiel, Germany, 29 August - 1 September 1994. Lecture Notes in Physics, Vol. 443, ed. D. Koester, & K. Werner, Springer-Verlag, Berlin Heidelberg New York, p.48, 1995
- [Kerber *et al* (1999)] Kerber, F., Köppen, J., Roth, M., & Trager, S. C. - *The hidden past of Sakurai's object. Stellar properties before the final helium flash*, A&A, 344, L79, 1999
- [Kimeswenger *et al* (1998)] Kimeswenger, S., Kerber, F., & Weinberger, R. - , MNRAS, 296, 614, 1998
- [Kimeswenger *et al* (2000)] Kimeswenger, S., Koller, J., & Schmeja, S. - *New identification of the near infrared source in the "born-again" planetary nebula A58 (=V605 Aql)*, A&A, 360, 699, 2000
- [Kimeswenger & Koller (2002)] Kimeswenger, S. & Koller, J. - *Modeling the Dust Shell of V4334 Sgr*, Ap&SS, 279, 149, 2002
- [Koller (2000)] Koller, J. - *Stochastic Heating of Small Dust Particles*, Innsbruck, Leopold Franzens Universität, 2000
- [Koller & Kimeswenger (2001)] Koller, J. & Kimeswenger, S. - *Modeling the IR spectrum of the dust shell around the [WC] star: V605 AQL*, Ap&SS, 275, 121, 2001
- [Kwok *et al* (1978)] Kwok, S., Purton, C. R., & Fitzgerald, P. M. - *On the origin of planetary nebulae*, ApJ219L.125K, 1978
- [Lawlor & MacDonald (2003)] Lawlor, T. M., & MacDonald, J. - *Sakurai's Object, V605 Aquilae, and FG Sagittae: An Evolutionary Sequence Revealed*, AJ, 583, 913, 2003
- [Maciel (1984)] Maciel, W. J. - *A catalogue of distances of planetary nebulae*, A&A, 55, 253, 1984
- [Nürnberg *et al* (2001)] Nürnberg, D., Durand, S., Köppen, J., Stanke, T., Sterzik, M., & Els, S. - *PN G291.4-00.3: A new type I planetary nebula*, A&A, 377, 241, 2001
- [Osterbrock (1974)] Osterbrock, Donald E. - *Astrophysics of gaseous nebulae*, W. H. Freeman and Co., San Francisco, ISBN 0-935702-22-9, 1974
- [Pollacco *et al* (1992)] Pollacco, D. L., Lawson, W. A., Clegg, R. E. S., & Hill, P. W. - *A hydrogen-deficient flow in the centre of the planetary nebula A58*, MNRAS, 257, 33p, 1992

- [Pollacco(1999)] Pollacco, D. L. - *The planetary nebula surrounding the final thermal pulse object V4334 Sagittarii*, MNRAS, 304, 127, 1999
- [Pottasch et al (1986)] Pottasch, S. R., Mampaso, A., Manchado, A., & Menzies, J. - *Hydrogen deficient planetary nebulae - Preliminary results*, ASSL Vol. 128: IAU Colloq. 87: Hydrogen Deficient Stars and Related Objects, 359, 1986
- [Rauch (1997)] Rauch, T. - *Implication of light metals (Li-Ca) on NLTE model atmospheres of compact hot stars.*, A&A, 320, 237, 1997
- [Rauch (2003)] Rauch, T. - *A grid of synthetic ionizing spectra for very hot compact stars from NLTE model atmospheres*, A&A, 403, 709, 2003
- [Schmeja & Kimeswenger (2002)] Schmeja, S. & Kimeswenger, S. - *A Catalogue of IJK Photometry of PNe with DENIS*, Revista Mexicana de Astronomia y Astrofisica Conference Series, 12, 176, 2002
- [Schneider & Buckley (1996)] Schneider, S. E. & Buckley, D. - *The Distances of Planetary Nebulae and the Galactic Bulge*, ApJ, 459, 606, 1996
- [Seitter (1987)] Seitter, W. C. - *V 605 Aquilae - A star and a nebula with no hydrogen*, Messenger, 50, 14, 1987
- [Strasbourg-ESO Catalogue of Galactic Planetary Nebulae (1992)] Acker A., Ochenbein F., Stenholm B., Tylenda R., Marcout J., & Schohn C. - *Strasbourg-ESO Catalogue of Galactic Planetary Nebulae*, European Southern Observatory, Garching, ISBN 3-923524-41-2, 1992
- [van Hoof & van de Steene (1999)] van Hoof, P. A. M. & van de Steene, G. C. - *Photoionization modelling of planetary nebulae - II. Galactic bulge nebulae, a comparison with literature results*, MNRAS, 308, 623, 1999
- [van de Steene (1995)] van de Steene, G. C. M. - *Obscured planetary nebulae*, Groningen: Rijksuniversiteit, —c1995, 1995
- [van de Steene & Zijlstra (1995)] van de Steene, G. C. & Zijlstra, A. A. - *On an alternative statistical distance scale for planetary nebulae*, A&A, 293, 541, 1995
- [Van der Veen et al (1989)] van der Veen, W. E. C. J., Habing, H. J., & Geballe, T. R. - *Objects in transition from the AGB to the planetary nebula stage - New visual and infrared observations*, A&A, 226, 108, 1989
- [Weinberger & Kerber (1997)] Weinberger, R., & Kerber, F. - *Planetary Nebulae: Understanding the Physical and Chemical Evolution of Dying Stars*, Science, Vol.276, 1997
- [Werner et al (1997)] Werner, K., Dreizler, S., Rauch, T., & Heber, U. - *Spectral Analyses of PG 1159 Stars with Line-Blanketed Non-Lte Model Atmospheres*, The Third Conference on Faint Blue Stars, 227, 1997

List of Tables

3.1	Recombination time-scale for atomic states at $T_e = 10.000$ K for electron densities n_e of 100 and 200 $\text{e}^{-}\text{cm}^{-3}$. The terms 'r' and 'd' refer to the radiative and dielectronic components in the total recombination coefficient 't'.	32
3.2	Dereddened line fluxes for the PN A58 relative to $\text{H}\beta$	33
3.3	Parameters of the best fit model.	35
4.1	Measured blueshifts with the aid of grism 6	46

List of Figures

1.1	Galactic Distribution of PNe	5
1.2	Born Again in HR diagram	6
1.3	Inner Region of A30	8
1.4	Double-Loop Scenario	9
1.5	Spectrum of V605 Aql by [Seitter (1987)]	10
2.1	Bias Structure	13
2.2	Spread of Bias Sessions	14
2.3	Multiplicational Factor	15
2.4	Correlation between $\Delta B1$ and $\Delta B3$	15
2.5	Problem with grism 2	16
2.6	Showing the scattered Light	18
2.7	Specifying the different Proportions of scattered Light for each Grism	19
2.8	Flat Reduction for Spectra	19
2.9	Defined Areas	20
2.10	Proof that the Offset between Amplifier 1 and 3 is stable	21
2.11	Wavelength Calibration	22
2.12	Successful Rebinning	23
2.13	Rows with hot Pixels in them	24
2.14	Response-Curves of the Grisms	25
3.1	Narrowband Images of PN A58	26
3.2	Used Slit-Positions	27
3.3	Correction of the interstellar Extinction	30
3.4	Best Fit Model	34
3.5	Position of the CSPN in the HRD	35
3.6	Temperature Variation in the CLOUDY Model	36
3.7	Other Variations in the Model	37

<i>LIST OF FIGURES</i>	57
4.1 Used Slit-Positions on V605 Aql	38
4.2 [NII] and [OIII] HST-Images of V605 Aql	39
4.3 Spectrum of H α	41
4.4 Spectrum by [Pollacco <i>et al</i> (1992)]	42
4.5 Hydrogen Under-Abundance in V605 Aql	42
4.6 Overview spectrum of V605 Aql	43
4.7 OII ₇₃₃₀₊₇₃₃₁ in V605 Aql	43
4.8 V605 Aql Spectral Lines around HeII ₄₆₈₅	44
4.9 Identified Spectral Lines around HeII ₄₆₈₅	45
4.10 Feature around 7751 Å	45
4.11 The C _{IV} Lines in all Slit-Positions	47
4.12 Best Fit to the The C _{IV} Lines	47
4.13 EMMI REMD Spectrum of the C _{IV} Line	48
4.14 High Resolution Spectra of the C _{IV} Line	49

A. Midas Batches

A.1. Defragmenting the Images

```

@@ inemmi ONTT.2002-08-03T21:23:47.347.fits b1001
@@ inemmi ONTT.2002-08-03T21:24:04.444.fits b1002
@@ inemmi ONTT.2002-08-03T21:24:21.701.fits b1003
@@ inemmi ONTT.2002-08-03T21:24:39.409.fits b1004
@@ inemmi ONTT.2002-08-03T21:24:56.711.fits b1005
@@ inemmi ONTT.2002-08-03T21:25:12.708.fits b1006
@@ inemmi ONTT.2002-08-03T21:25:28.509.fits b1007
@@ inemmi ONTT.2002-08-03T21:25:44.622.fits b1008
@@ inemmi ONTT.2002-08-03T21:26:00.691.fits b1009

@@ inemmi ONTT.2002-08-03T22:24:10.576.fits b2001
@@ inemmi ONTT.2002-08-03T22:24:28.974.fits b2002
@@ inemmi ONTT.2002-08-03T22:24:45.152.fits b2003
@@ inemmi ONTT.2002-08-03T22:25:01.709.fits b2004
@@ inemmi ONTT.2002-08-03T22:25:17.594.fits b2005
@@ inemmi ONTT.2002-08-03T22:25:33.513.fits b2006
@@ inemmi ONTT.2002-08-03T22:25:48.434.fits b2007
@@ inemmi ONTT.2002-08-03T22:26:04.908.fits b2008
@@ inemmi ONTT.2002-08-03T22:26:21.559.fits b2009

@@ inemmi ONTT.2002-08-04T18:53:24.125.fits b3001
@@ inemmi ONTT.2002-08-04T18:53:54.313.fits b3002
@@ inemmi ONTT.2002-08-04T18:54:24.944.fits b3003
@@ inemmi ONTT.2002-08-04T18:54:55.496.fits b3004
@@ inemmi ONTT.2002-08-04T18:55:23.205.fits b3005

! BINX, BINY !=2 :
! @@ inemmi ONTT.2002-08-04T19:04:14.777.fits b4001
! @@ inemmi ONTT.2002-08-04T19:04:42.871.fits b4002
! @@ inemmi ONTT.2002-08-04T19:05:13.879.fits b4003
! @@ inemmi ONTT.2002-08-04T19:05:41.514.fits b4004
! @@ inemmi ONTT.2002-08-04T19:06:09.200.fits b4005

! Bias Session without logs:
@@ inemmi ONTT.2002-08-04T22:18:56.623.fits b4001
@@ inemmi ONTT.2002-08-04T22:19:12.860.fits b4002
@@ inemmi ONTT.2002-08-04T22:19:31.563.fits b4003
@@ inemmi ONTT.2002-08-04T22:19:47.977.fits b4004
@@ inemmi ONTT.2002-08-04T22:20:06.210.fits b4005
@@ inemmi ONTT.2002-08-04T22:20:23.715.fits b4006
@@ inemmi ONTT.2002-08-04T22:20:41.943.fits b4007
@@ inemmi ONTT.2002-08-04T22:20:59.348.fits b4008
@@ inemmi ONTT.2002-08-04T22:21:18.230.fits b4009

@@ inemmi ONTT.2002-08-05T19:00:16.673.fits b5001
@@ inemmi ONTT.2002-08-05T19:00:37.233.fits b5002
@@ inemmi ONTT.2002-08-05T19:00:57.656.fits b5003
@@ inemmi ONTT.2002-08-05T19:01:18.216.fits b5004
@@ inemmi ONTT.2002-08-05T19:01:36.517.fits b5005
@@ inemmi ONTT.2002-08-05T19:01:54.700.fits b5006
@@ inemmi ONTT.2002-08-05T19:02:13.797.fits b5007
@@ inemmi ONTT.2002-08-05T19:02:32.711.fits b5008
@@ inemmi ONTT.2002-08-05T19:02:51.226.fits b5009

@@ inemmi ONTT.2002-08-05T21:22:44.036.fits b6001
@@ inemmi ONTT.2002-08-05T21:23:02.266.fits b6002
@@ inemmi ONTT.2002-08-05T21:23:21.309.fits b6003
@@ inemmi ONTT.2002-08-05T21:23:39.782.fits b6004
@@ inemmi ONTT.2002-08-05T21:23:57.609.fits b6005
@@ inemmi ONTT.2002-08-05T21:24:16.400.fits b6006
@@ inemmi ONTT.2002-08-05T21:24:34.964.fits b6007
@@ inemmi ONTT.2002-08-05T21:24:53.427.fits b6008
@@ inemmi ONTT.2002-08-05T21:25:13.983.fits b6009

@@ inemmi ONTT.2002-08-05T22:54:14.954.fits b7001
@@ inemmi ONTT.2002-08-05T22:54:33.498.fits b7002
@@ inemmi ONTT.2002-08-05T22:54:51.794.fits b7003
@@ inemmi ONTT.2002-08-05T22:55:10.885.fits b7004
@@ inemmi ONTT.2002-08-05T22:55:29.777.fits b7005
@@ inemmi ONTT.2002-08-05T22:55:48.269.fits b7006
@@ inemmi ONTT.2002-08-05T22:56:11.141.fits b7007
@@ inemmi ONTT.2002-08-05T22:56:31.632.fits b7008

```

```
@@ inemmi ONTT.2002-08-05T22:56:51.617.fits b7009
```

A.2. Looking at the seven different Bias Sessions

```
! i Integer, Array with one element define/local i/I/1/1
define/local cut/R/1/2

cut(1) = 300.0 cut(2) = 325.0

define/local subim/R/1/4

subim(1) = 1050.0 subim(2) = 20.0 subim(3) = 1550.0 subim(4) =
2050.0

set/format i3

do i = 1 9 ! load b1{i}.bdf[@1050,@20:@1550,@2050] scale=-4
cuts={cut(1)},{cut(2)}
load b1{i}.bdf[@{subim(1)},{subim(2)}:{subim(3)},{subim(4)}] scale=-4 cuts={cut(1)},{cut(2)}
enddo

do i = 1 9
load b2{i}.bdf[@{subim(1)},{subim(2)}:{subim(3)},{subim(4)}] scale=-4 cuts={cut(1)},{cut(2)}
enddo

do i = 1 5
load b3{i}.bdf[@{subim(1)},{subim(2)}:{subim(3)},{subim(4)}] scale=-4 cuts={cut(1)},{cut(2)}
enddo

do i = 1 9
load b4{i}.bdf[@{subim(1)},{subim(2)}:{subim(3)},{subim(4)}] scale=-4 cuts={cut(1)},{cut(2)}
enddo

do i = 1 9
load b5{i}.bdf[@{subim(1)},{subim(2)}:{subim(3)},{subim(4)}] scale=-4 cuts={cut(1)},{cut(2)}
enddo

do i = 1 9
load b6{i}.bdf[@{subim(1)},{subim(2)}:{subim(3)},{subim(4)}] scale=-4 cuts={cut(1)},{cut(2)}
enddo

do i = 1 9
load b7{i}.bdf[@{subim(1)},{subim(2)}:{subim(3)},{subim(4)}] scale=-4 cuts={cut(1)},{cut(2)}
enddo
```

A.3. Standard Approach to compute a correct Bias

```
define/local i/I/1/1
define/local cut/R/1/2

cut(1) = -3.0 cut(2) = 3.0

define/local subim/R/1/4

subim(1) = 1050.0 subim(2) = 20.0 subim(3) = 1550.0 subim(4) =
2050.0

set/format i3

goto onlybla

CREATE/IMAG biassum = b1001.bdf

do i = 1 9 ! load
b1{i}.bdf[@{subim(1)},{subim(2)}:{subim(3)},{subim(4)}]
scale=-4 cuts={cut(1)},{cut(2)}
COMPUTE/IMAG biassum = biassum + b1{i}
enddo

! COMPUTE/IMAG b001mean = biassum/9.0 COMPUTE/IMAG tmp =
biassum/9.0 STAT/IMAG tmp
```

```

[#{@subim(1)},#{@subim(2)}:#{@subim(3)},#{@subim(4)}] ?? G

! after STAT/IMAG the MEDIAN Value should be in de outputr field
nr.8

COMPUT/IMAG b001mean = tmp - {outputr(8)} CREATE/IMAG biassum =
b1001.bdf

do i = 1 9 ! load
b2{i}.bdf[#{@subim(1)},#{@subim(2)}:#{@subim(3)},#{@subim(4)}]
scale=-4 cuts={cut(1)},{cut(2)}
  COMPUTE/IMAG biassum = biassum + b2{i}
enddo

COMPUTE/IMAG tmp = biassum/9.0 STAT/IMAG tmp
[#{@subim(1)},#{@subim(2)}:#{@subim(3)},#{@subim(4)}] ?? G ! after
STAT/IMAG the MEDIAN Value should be in de outputr field nr.8
COMPUT/IMAG b002mean = tmp - {outputr(8)}

CREATE/IMAG biassum = b1001.bdf

do i = 1 5 ! load
b3{i}.bdf[#{@subim(1)},#{@subim(2)}:#{@subim(3)},#{@subim(4)}]
scale=-4 cuts={cut(1)},{cut(2)}
  COMPUTE/IMAG biassum = biassum + b3{i}
enddo

COMPUTE/IMAG tmp = biassum/5.0 STAT/IMAG tmp
[#{@subim(1)},#{@subim(2)}:#{@subim(3)},#{@subim(4)}] ?? G ! after
STAT/IMAG the MEDIAN Value should be in de outputr field nr.8
COMPUT/IMAG b003mean = tmp - {outputr(8)}

CREATE/IMAG biassum = b1001.bdf

do i = 1 9 ! load
b4{i}.bdf[#{@subim(1)},#{@subim(2)}:#{@subim(3)},#{@subim(4)}]
scale=-4 cuts={cut(1)},{cut(2)}
  COMPUTE/IMAG biassum = biassum + b4{i}
enddo

COMPUTE/IMAG tmp = biassum/9.0 STAT/IMAG tmp
[#{@subim(1)},#{@subim(2)}:#{@subim(3)},#{@subim(4)}] ?? G ! after
STAT/IMAG the MEDIAN Value should be in de outputr field nr.8
COMPUT/IMAG b004mean = tmp - {outputr(8)}

CREATE/IMAG biassum = b1001.bdf

do i = 1 9 ! load
b5{i}.bdf[#{@subim(1)},#{@subim(2)}:#{@subim(3)},#{@subim(4)}]
scale=-4 cuts={cut(1)},{cut(2)}
  COMPUTE/IMAG biassum = biassum + b5{i}
enddo

COMPUTE/IMAG tmp = biassum/9.0 STAT/IMAG tmp
[#{@subim(1)},#{@subim(2)}:#{@subim(3)},#{@subim(4)}] ?? G ! after
STAT/IMAG the MEDIAN Value should be in de outputr field nr.8
COMPUT/IMAG b005mean = tmp - {outputr(8)}

CREATE/IMAG biassum = b1001.bdf

do i = 1 9 ! load
b6{i}.bdf[#{@subim(1)},#{@subim(2)}:#{@subim(3)},#{@subim(4)}]
scale=-4 cuts={cut(1)},{cut(2)}
  COMPUTE/IMAG biassum = biassum + b6{i}
enddo

COMPUTE/IMAG tmp = biassum/9.0 STAT/IMAG tmp
[#{@subim(1)},#{@subim(2)}:#{@subim(3)},#{@subim(4)}] ?? G ! after
STAT/IMAG the MEDIAN Value should be in de outputr field nr.8
COMPUT/IMAG b006mean = tmp - {outputr(8)}

CREATE/IMAG biassum = b1001.bdf

do i = 1 9 ! load
b7{i}.bdf[#{@subim(1)},#{@subim(2)}:#{@subim(3)},#{@subim(4)}]
scale=-4 cuts={cut(1)},{cut(2)}
  COMPUTE/IMAG biassum = biassum + b7{i}
enddo

```

```

COMPUTE/IMAG tmp = biassum/9.0 STAT/IMAG tmp
[#{subim(1)},#{subim(2)}:#{subim(3)},#{subim(4)}] ? ? G

! after STAT/IMAG the MEDIAN Value should be in de outputr field
nr.8

COMPUT/IMAG b007mean = tmp - {outputr(8)}

onlybla:

do i = 1 7
  load b{i}mean.bdf [#{subim(1)},#{subim(2)}:#{subim(3)},#{subim(4)}] scale=-4 cuts={cut(1)},{cut(2)}
enddo

```

A.4. Meanrow out of the different Bias Sessions

```

define/local i/I/1/1
set/format i3

do i = 1 7
  aver/row bmean{i}row = bmean{i}.bdf @100,@1900
enddo
set/gra lwidth=1

create/grap 9
!set/grap yaxis=295,310
set/grap yaxis=260,320

set/grap color=1
plot bmean001row.bdf @1000,@1500
set/gra color=2
over bmean002row.bdf @1000,@1500
set/gra color=3
over bmean003row.bdf @1000,@1500
set/gra color=4
over bmean004row.bdf @1000,@1500
set/gra color=5
over bmean005row.bdf @1000,@1500
set/gra color=6
over bmean006row.bdf @1000,@1500
set/gra color=7
over bmean007row.bdf @1000,@1500

com/ima meanrow = bmean001row + bmean002row + bmean003row + bmean004row
com/ima meanrow = (meanrow + bmean005row + bmean006row + bmean007row) / 7.0

set/gra color=4
set/gra lwidth=3

over meanrow.bdf @1000,@1500

!do i = 1 7
! comp/ima tmp = bmean{i}row.bdf - meanrow.bdf
! stat/ima tmp [@15:@503]
! stat/ima tmp [@1059:@1541]
! write/out "#####"
!enddo

```

A.5. Reassambling the Flatfield Images

```

!Flats first night:
@@ inemmi ONTT.2002-08-03T20:51:17.893.fits Flnight0001
@@ inemmi ONTT.2002-08-03T20:51:52.925.fits Flnight0002
@@ inemmi ONTT.2002-08-03T20:52:19.987.fits Flnight0003
@@ inemmi ONTT.2002-08-03T20:52:46.812.fits Flnight0004
@@ inemmi ONTT.2002-08-03T20:54:59.377.fits Flnight0005
@@ inemmi ONTT.2002-08-03T20:55:38.292.fits Flnight0006
@@ inemmi ONTT.2002-08-03T20:56:10.309.fits Flnight0007
@@ inemmi ONTT.2002-08-03T20:56:42.446.fits Flnight0008
@@ inemmi ONTT.2002-08-03T21:04:53.594.fits Flnight0009
@@ inemmi ONTT.2002-08-03T21:05:28.053.fits Flnight0010
@@ inemmi ONTT.2002-08-03T21:06:05.001.fits Flnight0011

```

```

@@ inemmi ONTT.2002-08-03T21:06:43.580.fits F1night0012
@@ inemmi ONTT.2002-08-03T21:08:51.308.fits F1night0013
@@ inemmi ONTT.2002-08-03T21:09:26.448.fits F1night0014
@@ inemmi ONTT.2002-08-03T21:09:51.512.fits F1night0015
@@ inemmi ONTT.2002-08-03T21:10:18.679.fits F1night0016
@@ inemmi ONTT.2002-08-03T21:11:39.536.fits F1night0017
@@ inemmi ONTT.2002-08-03T21:12:15.996.fits F1night0018
@@ inemmi ONTT.2002-08-03T21:12:45.684.fits F1night0019
@@ inemmi ONTT.2002-08-03T21:13:14.907.fits F1night0020
@@ inemmi ONTT.2002-08-03T21:20:55.504.fits F1night0021
@@ inemmi ONTT.2002-08-03T21:21:30.749.fits F1night0022
@@ inemmi ONTT.2002-08-03T21:21:59.292.fits F1night0023
@@ inemmi ONTT.2002-08-03T21:22:28.798.fits F1night0024

```

```

!there are no flats from the second night!
!used medianvalue for bias 3 night: 306
!flats third night

```

```

@@ inemmi ONTT.2002-08-05T20:04:40.436.fits F3night0001
@@ inemmi ONTT.2002-08-05T20:05:21.316.fits F3night0002
@@ inemmi ONTT.2002-08-05T20:07:45.679.fits F3night0003
@@ inemmi ONTT.2002-08-05T20:09:56.595.fits F3night0004
@@ inemmi ONTT.2002-08-05T20:10:35.779.fits F3night0005
@@ inemmi ONTT.2002-08-05T20:11:05.079.fits F3night0006
@@ inemmi ONTT.2002-08-05T20:11:34.962.fits F3night0007
@@ inemmi ONTT.2002-08-05T20:12:02.753.fits F3night0008
@@ inemmi ONTT.2002-08-05T20:12:29.724.fits F3night0009
@@ inemmi ONTT.2002-08-05T20:15:37.694.fits F3night0010
@@ inemmi ONTT.2002-08-05T20:16:14.879.fits F3night0011
@@ inemmi ONTT.2002-08-05T20:16:54.052.fits F3night0012
@@ inemmi ONTT.2002-08-05T20:17:32.174.fits F3night0013
@@ inemmi ONTT.2002-08-05T20:18:11.451.fits F3night0014
@@ inemmi ONTT.2002-08-05T20:18:49.554.fits F3night0015
@@ inemmi ONTT.2002-08-05T20:23:33.133.fits F3night0016
@@ inemmi ONTT.2002-08-05T20:24:10.371.fits F3night0017
@@ inemmi ONTT.2002-08-05T20:24:36.055.fits F3night0018
@@ inemmi ONTT.2002-08-05T20:25:04.551.fits F3night0019
@@ inemmi ONTT.2002-08-05T20:25:32.524.fits F3night0020
@@ inemmi ONTT.2002-08-05T20:25:58.390.fits F3night0021
@@ inemmi ONTT.2002-08-05T20:28:32.990.fits F3night0022
@@ inemmi ONTT.2002-08-05T20:30:07.449.fits F3night0023
@@ inemmi ONTT.2002-08-05T20:30:47.620.fits F3night0024
@@ inemmi ONTT.2002-08-05T20:31:22.456.fits F3night0025
@@ inemmi ONTT.2002-08-05T20:31:56.239.fits F3night0026
@@ inemmi ONTT.2002-08-05T20:32:33.956.fits F3night0027
@@ inemmi ONTT.2002-08-05T20:33:06.571.fits F3night0028
@@ inemmi ONTT.2002-08-05T20:34:19.028.fits F3night0029
@@ inemmi ONTT.2002-08-05T20:35:00.879.fits F3night0030
@@ inemmi ONTT.2002-08-05T20:35:40.598.fits F3night0031
@@ inemmi ONTT.2002-08-05T20:36:19.709.fits F3night0032
@@ inemmi ONTT.2002-08-05T20:36:59.928.fits F3night0033
@@ inemmi ONTT.2002-08-05T20:37:38.586.fits F3night0034
@@ inemmi ONTT.2002-08-05T20:40:46.071.fits F3night0035
@@ inemmi ONTT.2002-08-05T20:43:23.506.fits F3night0036
@@ inemmi ONTT.2002-08-05T20:44:00.978.fits F3night0037
@@ inemmi ONTT.2002-08-05T20:44:25.773.fits F3night0038
@@ inemmi ONTT.2002-08-05T20:44:51.052.fits F3night0039
@@ inemmi ONTT.2002-08-05T20:45:17.910.fits F3night0040
@@ inemmi ONTT.2002-08-05T20:45:43.196.fits F3night0041

```

A.6. Subtracting the Reference Bias from the Flats

```

define/local i/I/1/1
set/format i4

do i = 1 24
  COMPUT/IMAG F1bnight{i} = F1night{i} - refbias
enddo

do i = 1 41
  COMPUT/IMAG F3bnight{i} = F3night{i} - refbias
enddo

```

A.7. Splitting the Flats for the different Grisms

```

define/local i/I/1/1

set/format i4

do i = 1 24
  READ/DESC F1bnight{i} ESO.INS.GRIS1.NAME,ESO.DET.WIN1.DKTM
enddo

do i = 1 41
  READ/DESC F3bnight{i} ESO.INS.GRIS1.NAME,ESO.DET.WIN1.DKTM
enddo

```

A.8. Proof of the Scattering in the upper left Corner

```

set/gra yaxis=0,200
set/gra color=1
set/gra bin=on

plot F1bnight0001.bdf @1900 <,@150
over F1bnight0002.bdf @1900 <,@150

```

A.9. Influence of scattered Light on each Grism

```

define/param P1 ? N
!2 = grism 2, 3 = grism 6, 1 = grism 3

define/local i/I/1/1
define/local k/I/1/1
define/local subimbias/R/1/4
define/local grism/I/1/1
define/local exptime/D/1/1
define/local subimup/R/1/4

!I1:
subimbias(1) = 10.0
subimbias(2) = 1984.0
subimbias(3) = 70.0
subimbias(4) = 2049.0

!up:
subimup(1) = 1070.0
subimup(2) = 2003.0
subimup(3) = 1540.0
subimup(4) = 2012.0

set/format F20.16
set/format i4

CREATE/TABLE testgrism.tbl
CREATE/COL testgrism :TIME ? D24.18 R*8
CREATE/COL testgrism :NAME ? ? C*20
CREATE/COL testgrism :MEDI1
CREATE/COL testgrism :MEDUP

k = 1
do i = 1 24

  COPY/DKEY F1bnight{i}.bdf ESO.INS.GRIS1.NO grism
  if grism .eq. {P1} then
    write/out yezzz
    COPY/DKEY F1bnight{i}.bdf ESO.DET.WIN1.DKTM exptime
    WRITE/TAB testgrism :TIME @k {exptime}
    WRITE/TAB testgrism :NAME @k F1bnight{i}.bdf
    STAT/IMAG F1bnight{i}.bdf [@[subimup(1)],[@subimup(2)]:@[subimup(3)],[@subimup(4)]] ? ? G
    WRITE/TAB testgrism :MEDUP @k {OUTPUTR(8)}
    STAT/IMAG F1bnight{i}.bdf [@[subimbias(1)],[@subimbias(2)]:@[subimbias(3)],[@subimbias(4)]] ? ? G
    WRITE/TAB testgrism :MEDI1 @k {OUTPUTR(8)}
  endif
enddo

```

```

        k = k + 1
    endif
enddo

do i = 1 41

    COPY/DKEY F3bnight{i}.bdf ESO.INS.GRIS1.NO grism
    if grism .eq. {P1} then
        write/out yezzz
        COPY/DKEY F3bnight{i}.bdf ESO.DET.WIN1.DKTM exptime
        WRITE/TAB testgrism :TIME @{k} {exptime}
        WRITE/TAB testgrism :NAME @{k} F3bnight{i}.bdf
        STAT/IMAG F3bnight{i}.bdf [@{subimup(1)},@{subimup(2)}:@{subimup(3)},@{subimup(4)}] ? ? G
        WRITE/TAB testgrism :MEDUP @{k} {OUTPUTR(8)}
        STAT/IMAG F3bnight{i}.bdf [@{subimbias(1)},@{subimbias(2)}:@{subimbias(3)},@{subimbias(4)}] ? ? G
        WRITE/TAB testgrism :MEDI1 @{k} {OUTPUTR(8)}
        k = k + 1
    endif
enddo

READ/TAB testgrism
ASSIGN/PRINT FILE testgrism.txt
PRINT/TAB testgrism.tbl ? ? ? 100.0

! tail -n 'wc -l testgrism.txt | awk '{print $1-3}' testgrism.txt | head -n 'wc -l testgrism.txt | awk
'{print $1-4}' > testgrism.dat

```

A.10. Testing if ΔB is really zero

```

define/param P1 ? N
!2 = grism 2, 3 = grism 6, 1 = grism 3

define/local i/I/1/1
define/local k/I/1/1
define/local subimbias/R/1/4
define/local grism/I/1/1
define/local exptime/D/1/1
define/local subimup/R/1/4

!I1:
subimbias(1) = 10.0
subimbias(2) = 1984.0
subimbias(3) = 70.0
subimbias(4) = 2049.0

!up:
subimup(1) = 1070.0
subimup(2) = 2003.0
subimup(3) = 1540.0
subimup(4) = 2012.0

set/format F20.16
set/format i4

CREATE/TABLE testdeltab.tbl
CREATE/COL testdeltab :TIME ? D24.18 R*8
CREATE/COL testdeltab :NAME ? ? C*20
CREATE/COL testdeltab :MEDI1
CREATE/COL testdeltab :MEDUP
CREATE/COL testdeltab :DELTA_B

k = 1
do i = 1 24

    COPY/DKEY F1bnight{i}.bdf ESO.INS.GRIS1.NO grism
    if grism .eq. {P1} then
        write/out yezzz
        COPY/DKEY F1bnight{i}.bdf ESO.DET.WIN1.DKTM exptime
        WRITE/TAB testdeltab :TIME @{k} {exptime}
        WRITE/TAB testdeltab :NAME @{k} F1bnight{i}.bdf
        STAT/IMAG F1bnight{i}.bdf [@{subimup(1)},@{subimup(2)}:@{subimup(3)},@{subimup(4)}] ? ? G
        WRITE/TAB testdeltab :MEDUP @{k} {OUTPUTR(8)}
        STAT/IMAG F1bnight{i}.bdf [@{subimbias(1)},@{subimbias(2)}:@{subimbias(3)},@{subimbias(4)}] ? ? G
        WRITE/TAB testdeltab :MEDI1 @{k} {OUTPUTR(8)}
        k = k + 1
    endif
enddo

```

A.11. STATISTICALLY WEIGHTING THE FLATS FOR EACH GRISM AND SLIT65

```
endif
enddo

do i = 1 41

  COPY/DKEY F3bnight{i}.bdf ESO.INS.GRIS1.NO grism
  if grism .eq. {P1} then
    write/out yezzz
    COPY/DKEY F3bnight{i}.bdf ESO.DET.WIN1.DKTM exptime
    WRITE/TAB testdeltab :TIME @{k} {exptime}
    WRITE/TAB testdeltab :NAME @{k} F3bnight{i}.bdf
    STAT/IMAG F3bnight{i}.bdf [@[subimup(1)],[@subimup(2)]:@[subimup(3)],[@subimup(4)]] ? ? G
    WRITE/TAB testdeltab :MEDUP @{k} {OUTPUTR(8)}
    STAT/IMAG F3bnight{i}.bdf [@[subimbias(1)],[@subimbias(2)]:@[subimbias(3)],[@subimbias(4)]] ? ? G
    WRITE/TAB testdeltab :MEDI1 @{k} {OUTPUTR(8)}
    k = k + 1

  endif
enddo

!grism2:
if {P1} .eq. 2 then
!  COMPUT/TABL testdeltab.tbl :DELTA_B = :MEDI1 - (:MEDUP / 849.083 )
  COMPUT/TABL testdeltab.tbl :DELTA_B = :MEDI1 - (:MEDUP / 690.874 )

endif

!grism3:
if {P1} .eq. 1 then
  COMPUT/TABL testdeltab.tbl :DELTA_B = :MEDI1 - (:MEDUP / 241.562 )
  COMPUT/TABL testdeltab.tbl :DELTA_B = :MEDI1 - (:MEDUP / 232.391 )
endif

!grism6:
if {P1} .eq. 3 then
  COMPUT/TABL testdeltab.tbl :DELTA_B = :MEDI1 - (:MEDUP / 1036.7 )
  COMPUT/TABL testdeltab.tbl :DELTA_B = :MEDI1 - (:MEDUP / 897.653 )
endif

endif

READ/TAB testdeltab
ASSIGN/PRINT FILE testdeltab.txt
PRINT/TAB testdeltab.tbl ? ? ? 100.0

! tail -n 'wc -l testdeltab.txt | awk '{print $1-3}'' testdeltab.txt | head -n 'wc -l
  testdeltab.txt | awk '{print $1-4}'' > testdeltab.dat
```

A.11. Statistically weighting the Flats for each Grism and Slit

```
define/param P1 ? N
!2 = grism 2, 3 = grism 6, 1 = grism 3
define/param P2 ? N
!2= slit 1, 4= slit5

define/local i/I/1/1
define/local k/I/1/1
define/local grism/I/1/1
define/local slit/I/1/1
define/local sum/R/1/1 0
define/local subim/R/1/4

!Amp 3 ohne unteren Teil:
subim(1) = 1050.0
subim(2) = 860.0
subim(3) = 1550.0
subim(4) = 2050.0

CREATE/IMAG flatsum = F1bnight0001
!WRITE/DESC flatsum START/D/1/2 1.0,1.0
!WRITE/DESC flatsum STEP/D/1/2 2.0,2.0

set/format i4

do i = 1 24
```

```

COPY/DKEY F1bnight{i}.bdf ESO.INS.GRIS1.NO grism
COPY/DKEY F1bnight{i}.bdf ESO.INS.SLIT2.NO slit
if grism .eq. {P1} .AND. slit .eq. {P2} then
  write/out yezzz
  STAT/IMA F1bnight{i}.bdf [#{subim(1)},#{subim(2)}:#{subim(3)},#{subim(4)}]

  !Flats gewichten:
  sum = sum + {outputr(8)}**0.5
  COMPUTE/IMAG tmp = F1bnight{i} / {outputr(8)}**0.5

  COMPUTE/IMAG flatsum = flatsum + tmp

endif
enddo

do i = 1 41

COPY/DKEY F3bnight{i}.bdf ESO.INS.GRIS1.NO grism
COPY/DKEY F3bnight{i}.bdf ESO.INS.SLIT2.NO slit
if grism .eq. {P1} .AND. slit .eq. {P2} then

  write/out yezzz
  STAT/IMA F3bnight{i}.bdf [#{subim(1)},#{subim(2)}:#{subim(3)},#{subim(4)}]

  !Flats gewichten:
  sum = sum + {outputr(8)}**0.5
  COMPUTE/IMAG tmp = F3bnight{i} / {outputr(8)}**0.5

  COMPUTE/IMAG flatsum = flatsum + tmp

endif
enddo

COMPUTE/IMAG flatg1ngr = flatsum / {sum}
load flatg1ngr.bdf [#{subim(1)},#{subim(2)}:#{subim(3)},#{subim(4)}] scale=-4 cuts=0,5
STAT/IMA flatg1ngr.bdf [#{subim(1)},#{subim(2)}:#{subim(3)},#{subim(4)}]

```

A.12. Wavelength Calibration for Grism 2

```

define/local calib/c/1/60 {P1}
define/param P1 ? I "calib image:"

INITIA/DISP p5=RGBQ
set/cont long

EXTRAC/IMAG lampex = {calib}[@1050,@1:1500,@2055]
ROTATE/ lampex lampexr.bdf
WRITE/DESC lampexr.bdf START/D/1/2 1.0,1.0
WRITE/DESC lampexr.bdf STEP/D/1/2 1.0,1.0
CUTS/IMAG lampexr.bdf 0,30000

!fuer grism 6:
!COMPUTE/IMAG lampexr_he2 = lampexr

REPLACE/IMAG lampexr lampexrr <,0=100

!fuer grism 2:
filter/smo lampexrr.bdf mask1 2,0,0.01 ? [0970,<:0974,>]
cre/ima mask2 = mask1
extra/ima mask3 = mask1 [0950,<:1000,>]
replace/ima mask3 mask4 <,3000=0
insert/ima mask4 mask2
replace/ima mask2 mask5 1,>=1
comp/ima mask6 = lampexrr.bdf * mask5
replace/ima lampexr.bdf lampexr_he.bdf mask6/1,32768.0=lampexr.bdf*(-1.0)
replace/ima lampexr_he.bdf lampexr_he2.bdf mask6/1,32768.0=lampexr_he.bdf+65536.0

SET/LONG TWODOPT=YES
SET/LONG WLCNITER=10,50
set/long DCX=3,2
set/long TOL=-5.0
SET/LONG LINCAT=myhear.tbl
!SET/LONG YSTART=10
GRAPH/LONG 1150,350
SEARCH/LONG lampexr_he2.bdf 100 10 7 3 GAUSSIAN
IDENTI/LONG
CALIBR/LONG -5.0 3,2 IDENT

```

```

CALIBR/TWICE
REBIN/LONG lampexr.bdf lamprebin.bdf
load lamprebin.bdf scale=-4,1

SAVE/LONG {calib}gr2save

plot/calib

```

A.13. Correct Bias Reduction for the Spectra

```

define/local i/I/1/1
define/local subimbias/R/1/4

subimbias(1) = 10.0
subimbias(2) = 1984.0
subimbias(3) = 70.0
subimbias(4) = 2049.0

set/format i3

do i = 1 30
  COMPUT/IMAG tmp = objb{i} - refbias
  ! COMPUT/IMAG objb{i} = objb{i} - refbias

  STAT/IMAG tmp.bdf [@(subimbias(1)),@(subimbias(2)):(subimbias(3)),@(subimbias(4))] ? ? G

  COMPUT/IMAG objb{i} = tmp - (2.9369 * {OUTPUTR(8)})
enddo

```

A.14. Reducing the Flatfield in the Spectra

```

define/local grism/I/1/1
define/local slit/I/1/1
define/local i/I/1/1
!define/local exptime/D/1/1

set/format i3

do i = 1 30

  COPY/DKEY objb{i}.bdf ESO.INS.GRIS1.NO grism
  COPY/DKEY objb{i}.bdf ESO.INS.SLIT2.NO slit

  !2 = grism 2, 3 = grism 6, 1 = grism 3
  !2= slit 1, 4= slit5

  ! COPY/DKEY objb{i}.bdf ESO.DET.WIN1.DIT1 exptime

  if grism .eq. 2 .AND. slit .eq. 2 then
    ! COMPUT/IMAG objbn{i} = objb{i} / ( {exptime} * fbngr2s11.bdf )
    !besser erst nach cospics auf 1 normieren!
    ! COMPUT/IMAG objbf{i} = objb{i} / ( fbngr2s11.bdf )
    !und gleich ausschneiden
    COMPUT/IMAG tmp = objb{i} / ( fbngr2s11.bdf )

  endif

  if grism .eq. 2 .AND. slit .eq. 4 then
    COMPUT/IMAG tmp = objb{i} / ( fbngr2s15.bdf )
  endif

  if grism .eq. 1 .AND. slit .eq. 2 then
    COMPUT/IMAG tmp = objb{i} / ( fbngr3s11.bdf )
  endif

  if grism .eq. 1 .AND. slit .eq. 4 then
    COMPUT/IMAG tmp = objb{i} / ( fbngr3s15.bdf )
  endif

  if grism .eq. 3 .AND. slit .eq. 2 then
    COMPUT/IMAG tmp = objb{i} / ( fbngr6s11.bdf )
  endif
endif

```

```

if grism .eq. 3 .AND. slit .eq. 4 then
  COMPUT/IMAG tmp = objb{i} / ( fbng6sl5.bdf )
endif

!gleich ausschneiden!
  EXTRAC/IMAG tmp = tmp[@1050,@1:1500,@2055]
  ROTATE/ tmp objbfexr{i}.bdf
  WRITE/DESC objbfexr{i}.bdf START/D/1/2 1.0,1.0
  WRITE/DESC objbfexr{i}.bdf STEP/D/1/2 1.0,1.0
!binning auch gleich umsetzen!

enddo

```

A.15. Rebinning all Spectra and Reducing the Cosmics

```

FILTER/COSM objbfexr001.bdf objexrc.bdf 20,0.7,6,4,1.5 comask
@@ ../lamps/rebinme.prg objexrc.bdf rebin001 ../lamps/lamp004gr6save.tbl

FILTER/COSM objbfexr002.bdf objexrc.bdf 20,0.7,6,4,1.5 comask
@@ ../lamps/rebinme.prg objexrc.bdf rebin002 ../lamps/lamp004gr6save.tbl

FILTER/COSM objbfexr003.bdf objexrc.bdf 20,0.7,6,4,1.5 comask
@@ ../lamps/rebinme.prg objexrc.bdf rebin003 ../lamps/lamp004gr6save.tbl

FILTER/COSM objbfexr004.bdf objexrc.bdf 20,0.7,6,4,1.5 comask
@@ ../lamps/rebinme.prg objexrc.bdf rebin004 ../lamps/lamp003gr3save.tbl

FILTER/COSM objbfexr005.bdf objexrc.bdf 20,0.7,6,4,1.5 comask
@@ ../lamps/rebinme.prg objexrc.bdf rebin005 ../lamps/lamp004gr6save.tbl

FILTER/COSM objbfexr006.bdf objexrc.bdf 20,0.7,6,4,1.5 comask
@@ ../lamps/rebinme.prg objexrc.bdf rebin006 ../lamps/lamp004gr6save.tbl

FILTER/COSM objbfexr007.bdf objexrc.bdf 20,0.7,6,4,1.5 comask
@@ ../lamps/rebinme.prg objexrc.bdf rebin007 ../lamps/lamp003gr3save.tbl

FILTER/COSM objbfexr008.bdf objexrc.bdf 20,0.7,6,4,1.5 comask
@@ ../lamps/rebinme.prg objexrc.bdf rebin008 ../lamps/lamp003gr3save.tbl

FILTER/COSM objbfexr009.bdf objexrc.bdf 20,0.7,6,4,1.5 comask
@@ ../lamps/rebinme.prg objexrc.bdf rebin009 ../lamps/lamp003gr3save.tbl

FILTER/COSM objbfexr010.bdf objexrc.bdf 20,0.7,6,4,1.5 comask
@@ ../lamps/rebinme.prg objexrc.bdf rebin010 ../lamps/lamp003gr3save.tbl

FILTER/COSM objbfexr011.bdf objexrc.bdf 20,0.7,6,4,1.5 comask
@@ ../lamps/rebinme.prg objexrc.bdf rebin011 ../lamps/lamp003gr3save.tbl

FILTER/COSM objbfexr012.bdf objexrc.bdf 20,0.7,6,4,1.5 comask
@@ ../lamps/rebinme.prg objexrc.bdf rebin012 ../lamps/lamp004gr6save.tbl

FILTER/COSM objbfexr013.bdf objexrc.bdf 20,0.7,6,4,1.5 comask
@@ ../lamps/rebinme.prg objexrc.bdf rebin013 ../lamps/lamp004gr6save.tbl

FILTER/COSM objbfexr014.bdf objexrc.bdf 20,0.7,6,4,1.5 comask
@@ ../lamps/rebinme.prg objexrc.bdf rebin014 ../lamps/lamp010gr2save.tbl

FILTER/COSM objbfexr015.bdf objexrc.bdf 20,0.7,6,4,1.5 comask
@@ ../lamps/rebinme.prg objexrc.bdf rebin015 ../lamps/lamp010gr2save.tbl

FILTER/COSM objbfexr016.bdf objexrc.bdf 20,0.7,6,4,1.5 comask
@@ ../lamps/rebinme.prg objexrc.bdf rebin016 ../lamps/lamp010gr2save.tbl

FILTER/COSM objbfexr017.bdf objexrc.bdf 20,0.7,6,4,1.5 comask
@@ ../lamps/rebinme.prg objexrc.bdf rebin017 ../lamps/lamp010gr2save.tbl

FILTER/COSM objbfexr018.bdf objexrc.bdf 20,0.7,6,4,1.5 comask
@@ ../lamps/rebinme.prg objexrc.bdf rebin018 ../lamps/lamp010gr2save.tbl

FILTER/COSM objbfexr019.bdf objexrc.bdf 20,0.7,6,4,1.5 comask
@@ ../lamps/rebinme.prg objexrc.bdf rebin019 ../lamps/lamp010gr2save.tbl

FILTER/COSM objbfexr020.bdf objexrc.bdf 20,0.7,6,4,1.5 comask
@@ ../lamps/rebinme.prg objexrc.bdf rebin020 ../lamps/lamp010gr2save.tbl

```

A.16. FINDING GOOD STANDARD-STARS TO CORRECT THE EXTINCTION⁶⁹

```
FILTER/COSM objbfexr021.bdf objexrc.bdf 20,0.7,6,4,1.5 comask
@@ ../lamps/rebinme.prg objexrc.bdf rebin021 ../lamps/lamp003gr3save.tbl

FILTER/COSM objbfexr022.bdf objexrc.bdf 20,0.7,6,4,1.5 comask
@@ ../lamps/rebinme.prg objexrc.bdf rebin022 ../lamps/lamp004gr6save.tbl

FILTER/COSM objbfexr023.bdf objexrc.bdf 20,0.7,6,4,1.5 comask
@@ ../lamps/rebinme.prg objexrc.bdf rebin023 ../lamps/lamp003gr3save.tbl

FILTER/COSM objbfexr024.bdf objexrc.bdf 20,0.7,6,4,1.5 comask
@@ ../lamps/rebinme.prg objexrc.bdf rebin024 ../lamps/lamp003gr3save.tbl

FILTER/COSM objbfexr025.bdf objexrc.bdf 20,0.7,6,4,1.5 comask
@@ ../lamps/rebinme.prg objexrc.bdf rebin025 ../lamps/lamp010gr2save.tbl

FILTER/COSM objbfexr026.bdf objexrc.bdf 20,0.7,6,4,1.5 comask
@@ ../lamps/rebinme.prg objexrc.bdf rebin026 ../lamps/lamp010gr2save.tbl

FILTER/COSM objbfexr027.bdf objexrc.bdf 20,0.7,6,4,1.5 comask
@@ ../lamps/rebinme.prg objexrc.bdf rebin027 ../lamps/lamp003gr3save.tbl

FILTER/COSM objbfexr028.bdf objexrc.bdf 20,0.7,6,4,1.5 comask
@@ ../lamps/rebinme.prg objexrc.bdf rebin028 ../lamps/lamp003gr3save.tbl

FILTER/COSM objbfexr029.bdf objexrc.bdf 20,0.7,6,4,1.5 comask
@@ ../lamps/rebinme.prg objexrc.bdf rebin029 ../lamps/lamp004gr6save.tbl

FILTER/COSM objbfexr030.bdf objexrc.bdf 20,0.7,6,4,1.5 comask
@@ ../lamps/rebinme.prg objexrc.bdf rebin030 ../lamps/lamp004gr6save.tbl
```

A.16. Finding good Standard-Stars to correct the Extinction

```
define/local image/c/1/60 {P1}
define/local graph/c/1/60 {P2}
define/local slitcenter/i/1/1 {P3}
define/local sumup/i/1/1 {P4}
define/local scale/r/1/1 {P5}
define/local dummy1/i/1/1
define/local dummy2/i/1/1

define/param P1 ? I "image:"
define/param P2 ? I "name of graph:"
define/param P3 ? I "center of slit:"
define/param P4 ? I "sumup howmuch lines?"
define/param P5 ? N "scale parameter for the extinction ?"

define/local airbegin/D/1/1
define/local airend/D/1/1
define/local airmass/D/1/1
define/local otime/D/1/7

COPY/DKEY {image} ESO.TEL.AIRM.START airbegin
COPY/DKEY {image} ESO.TEL.AIRM.END airend

!Write/out "airbegin:" {airbegin}
!Write/out "airend:" {airend}

airmass = {airbegin} + {airend}
airmass = {airmass} / 2.0

Write/out "airmass:" {airmass}

!nightsky abziehen:
!vergleich oben unten:
set/gra color=1

dummy1 = {slitcenter} + 20
dummy2 = {slitcenter} + 45

AVERAG/ROW tmp1 = {image} @{dummy1},{dummy2}
dummy1 = {slitcenter} - 20
dummy2 = {slitcenter} - 45
AVERAG/ROW tmp2 = {image} @{dummy2},{dummy1}
```

```

COMPUT/IMAG tmp = tmp2 - tmp1
set/gra yaxis=-5,5
plot tmp
$sleep 2

!nightsky mitteln:
COMPUT/IMAG tmp = tmp1 + tmp2
COMPUT/IMAG tmp = tmp / 2.0
plot tmp
$sleep 2

!unkorrigiertes spektrum:
dummy1 = {slitcenter} - (({sumup} - 1)/ 2.0)
dummy2 = {slitcenter} + (({sumup} - 1)/ 2.0)

Write/out "von:" {dummy1}
Write/out "bis:" {dummy2}

AVERAG/ROW tmp{graph} = {image} @{dummy1},{dummy2} sum
set/gra yaxis=0,1500
plot tmp{graph}
set/gra color=2
over tmp
!nightsky korrigiertes spektrum:
COMPUT/IMAG corr{graph} = tmp{graph} - ({sumup}.0 * tmp)
set/gra color=3
over corr{graph}
$sleep 4

COMPUT/IMAG corr{graph} = corr{graph} / {sumup}.0

CONVER/TABL extcurve = atmoexan.tbl #1 #2 corr{graph} SPLINE 3.0,2

!ohne nightsky korrektur:
!COMPUT/IMAG {graph} = tmp{graph} * 10^{(airmass} * extcurve.bdf / 2.5)
!mit nightsky korrektur
COMPUT/IMAG {graph} = corr{graph} * exp({airmass} * extcurve.bdf) * {scale}

plot {graph}
$sleep 4

!-----

!auf 1 sekunde normieren, zum vergleich!
COPY/DKEY {image} 0_TIME otime
COMPUT/IMAG amn{graph} = {graph} / {otime(7)}

set/gra yaxis=0,0.1
set/gra color=1
plot amn{graph}

```

A.17. Correction Functions for the Quantum Efficiency

```

@@ look_g93.prg rebin022.bdf test22 343 14 1
CONVER/TABL truespec22.bdf = /midas/calib/data/spec/flux/lt6248.tbl #1 #2 amntest22.bdf SPLINE
COMPUT/IMAG correctfun22 = (truespec22.bdf / amntest22.bdf )

@@ look_g93.prg rebin020.bdf test20 343 14 1
CONVER/TABL truespec20.bdf = /midas/calib/data/spec/flux/lt6248.tbl #1 #2 amntest20.bdf SPLINE
COMPUT/IMAG correctfun20 = (truespec20.bdf / amntest20.bdf )

@@ look_g93.prg rebin021.bdf test21 343 14 1
CONVER/TABL truespec21.bdf = /midas/calib/data/spec/flux/lt6248.tbl #1 #2 amntest21.bdf SPLINE
COMPUT/IMAG correctfun21 = (truespec21.bdf / amntest21.bdf )

set/cont long

CONTIN/SPEC correctfun20.bdf correctfun21.bdf ? ALL 1 2
!v
!<
!3750
!v
!8930

```

```

!>
!n

CONTIN/SPEC correctfun21.bdf correctfungr3.bdf ? ALL 1 2
!v
!<
!3800
!v
!8900
!>
!n

CONTIN/SPEC correctfun22.bdf correctfungr6.bdf ? ALL 1 2
!v
!7150
!7350
!v
!7580
!7740
!v
!8690
!>
!n

set/gra yaxis=0,2000
set/gra color=1
plot correctfungr2
set/gra color=2
over correctfungr3.bdf
set/gra color=3
over correctfungr6.bdf

```

A.18. Airmass Correction

```

define/local image/c/1/60 {P1}
define/local amn/c/1/60 {P2}

define/param P1 ? I "image (rebinned):"
define/param P2 ? I "normalized image with airmass correction"

define/local airbegin/D/1/1
define/local airend/D/1/1
define/local airmass/D/1/1
define/local otime/D/1/7

COPY/DKEY {image} ESO.TEL.AIRM.START airbegin
COPY/DKEY {image} ESO.TEL.AIRM.END airend

!Write/out "airbegin:" {airbegin}
!Write/out "airend:" {airend}

airmass = {airbegin} + {airend}
airmass = {airmass} / 2.0

Write/out "airmass:" {airmass}

! 1 zeile rausschneiden
extrac/ima tmp = {image} [<,1:>,1]

CONVER/TABL extcurve = atmoexan.tbl #1 #2 tmp SPLINE 3.0,2
!das ganzes bild:
Grow/imag extbild = extcurve.bdf 1.0,1.0,451

COMPUT/IMAG {amn} = {image} * exp({airmass} * extbild.bdf )

COPY/DKEY {image} O_TIME otime
COMPUT/IMAG {amn} = {amn} / {otime(7)}

```

A.19. Correcting the Quantum Efficiency in the Spectra

```

@@ makeamn.prg rebin003.bdf tmp3
@@ makeamn.prg rebin004.bdf tmp4
@@ makeamn.prg rebin014.bdf tmp14
@@ makeamn.prg rebin015.bdf tmp15
@@ makeamn.prg rebin016.bdf tmp16
@@ makeamn.prg rebin017.bdf tmp17
@@ makeamn.prg rebin018.bdf tmp18
@@ makeamn.prg rebin019.bdf tmp19
@@ makeamn.prg rebin023.bdf tmp23
@@ makeamn.prg rebin024.bdf tmp24

GROW/imag tmpcorr = correctfungr6.bdf 1,1,451 ? L

!gr 6:
COMPUT/IMAG qamn3 = tmp3 * tmpcorr

GROW/imag tmpcorr = correctfungr3.bdf 1,1,451 ? L

!gr 3:

COMPUT/IMAG qamn4 = tmp4 * tmpcorr
COMPUT/IMAG qamn23 = tmp23 * tmpcorr
COMPUT/IMAG qamn24 = tmp24 * tmpcorr

GROW/imag tmpcorr = correctfungr2.bdf 1,1,451 ? L

!gr2:
COMPUT/IMAG qamn14 = tmp14 * tmpcorr
COMPUT/IMAG qamn15 = tmp15 * tmpcorr
COMPUT/IMAG qamn16 = tmp16 * tmpcorr
COMPUT/IMAG qamn17 = tmp17 * tmpcorr

COMPUT/IMAG qamn18 = tmp18 * tmpcorr
COMPUT/IMAG qamn19 = tmp19 * tmpcorr

```

A.20. Splitting the Skyflats in the different Filters

```

define/local i/I/1/1
define/local k/I/1/1 0
define/local filter/C/1/20
define/local sum/R/1/1 0
define/local subim/R/1/4

!Amp 3 ohne unteren Teil:
subim(1) = 1050.0
subim(2) = 860.0
subim(3) = 1550.0
subim(4) = 2050.0

CREATE/IMAG flatsum = sky001
!WRITE/DESC flatsum START/D/1/2 1.0,1.0
!WRITE/DESC flatsum STEP/D/1/2 2.0,2.0

set/format i3

do i = 1 82

    COPY/DKEY skyb{i}.bdf ESO.INS.FILT2.NAME filter

!   write/out {i}
!   READ/KEY filter

!       if filter(1:4) .eq. "Free" then
!           if filter(1:6) .eq. "Hb#770" then
!           if filter(1:7) .eq. "NII#653" then
!           if filter(1:7) .eq. "HbC#771" then
!           if filter(1:5) .eq. "V#606" then
!           if filter(1:5) .eq. "r#773" then
!           if filter(1:6) .eq. "Ha#654" then
!           if filter(1:6) .eq. "Bb#605" then
!           if filter(1:5) .eq. "i#774" then
!           if filter(1:8) .eq. "OIII#589" then

```

```

        write/out yezzz
        k = k + 1

        STAT/IMA skyb{i}.bdf [#{subim(1)},#{subim(2)}:#{subim(3)},#{subim(4)}]
        COMPUTE/IMAG tmp{k} = skyb{i} / {outputr(8)}
    endif
enddo

do i = 1 {k}
    COMPUTE/IMAG tmp = 10000.0 * tmp{i}
    OUTDISK/SFITS tmp tmp{i}.fits B ?
enddo

$median_test flatsum.fits tmp0??fits

COMPUTE/IMAG flatimage2 = flatsum.fits / 10000.0
load flatimage2.bdf[#{subim(1)},#{subim(2)}:#{subim(3)},#{subim(4)}] scale=-4 cuts=0.5,1.5
STAT/IMA flatimage2.bdf [#{subim(1)},#{subim(2)}:#{subim(3)},#{subim(4)}]
WRITE/DESC flatimage2 STEP/D/1/2 2.0,2.0

! wegen so wenige bilder fast besser ohne median, zwecks rauschunterdrueckung!

do i = 1 82

    COPY/DKEY skyb{i}.bdf ESO.INS.FILT2.NAME filter
    ! READ/KEY filter

    !         if filter(1:4) .eq. "Free" then
    !         if filter(1:6) .eq. "Hb#770" then
    !         if filter(1:7) .eq. "NII#653" then
    !         if filter(1:7) .eq. "HbC#771" then
    !         if filter(1:5) .eq. "V#606" then
    !         if filter(1:5) .eq. "r#773" then
    !         if filter(1:6) .eq. "Ha#654" then
    !         if filter(1:6) .eq. "Bb#605" then
    !         if filter(1:5) .eq. "i#774" then
    !         if filter(1:8) .eq. "OIII#589" then

        write/out yezzz

        STAT/IMA skyb{i}.bdf [#{subim(1)},#{subim(2)}:#{subim(3)},#{subim(4)}]

        !Flats gewichten:
        sum = sum + {outputr(8)}**0.5
        COMPUTE/IMAG tmp = skyb{i} / {outputr(8)}**0.5

        COMPUTE/IMAG flatsum = flatsum + tmp
    endif
enddo

COMPUTE/IMAG flatimage = flatsum / {sum}
load flatimage.bdf[#{subim(1)},#{subim(2)}:#{subim(3)},#{subim(4)}] scale=-4 cuts=0.5,1.5
STAT/IMA flatimage.bdf [#{subim(1)},#{subim(2)}:#{subim(3)},#{subim(4)}]

!optische kontrolle kein stern:
do i = 1 {k}

    write/out k: {i}
    COMPUTE/IMAG tmp = tmp{i}.bdf / flatimage.bdf
    load tmp scale=-4 cuts=0.95,1-05

enddo

write/out "mit median: "

do i = 1 {k}

    write/out k: {i}
    COMPUTE/IMAG tmp = tmp{i}.bdf / flatimage2.bdf
    load tmp scale=-4 cuts=0.95,1-05

enddo

$ rm -rf tmp0*

COMPUT/IMAG tmp = flatimage.bdf / flatimage2.bdf
!load tmp scale=-4 cuts=0.95,1.05

!$cp flatimage.bdf OIII589flat.bdf

```

A.21. Correct Bias Reduction for the Images

```

define/local i/I/1/1
define/local subimbias/R/1/4

subimbias(1) = 10.0
subimbias(2) = 1984.0
subimbias(3) = 70.0
subimbias(4) = 2049.0

set/format i3

do i = 1 46
  COMPUT/IMAG tmp = image{i} - refbias

  STAT/IMAG tmp.bdf [#{subimbias(1)},#{subimbias(2)}:#{subimbias(3)},#{subimbias(4)}] ? ? G

  COMPUT/IMAG imgb{i} = tmp - (2.9369 * {OUTPUTR(8)})
enddo

```

A.22. Correcting hot Pixels and Flatfield of the Images

```

define/local i/I/1/1
define/local filter/C/1/20

set/format i3

do i = 1 46

COPY/DKEY imgb{i}.bdf ESO.INS.FILT2.NAME filter

COPY/II imgb{i} imgbh
WRITE/DESC imgbh.bdf START/D/1/2 1.0,1.0
WRITE/DESC imgbh.bdf STEP/D/1/2 2.0,2.0

extra/ima leftlineunten = imgb{i} [01468,0459:01468,>]
extra/ima rightlineunten = imgb{i} [01471,0459:01471,>]

extra/ima leftlineoben = imgb{i} [01108,01586:01108,>]
extra/ima rightlineoben = imgb{i} [01110,01586:01110,>]

COMPUT/IMAG tmp = leftlineoben + rightlineoben
COMPUT/IMAG lineoben = tmp / 2.0

COMPUT/IMAG tmp = leftlineunten + rightlineunten
COMPUT/IMAG lineunten = tmp / 2.0

WRITE/DESC lineoben.bdf START/D/1/1 1.0
WRITE/DESC lineunten.bdf START/D/1/1 1.0

ROTATE/CLOCK imgbh tmp1
WRITE/DESC tmp1.bdf START/D/1/2 1.0,1.0
WRITE/DESC tmp1.bdf STEP/D/1/2 2.0,2.0

!insert/ima lineoben tmp1 01586,01109
!2076 - 1109 +1
insert/ima lineoben tmp1 01586,0968

!insert/ima lineunten tmp1 0459,01469
!insert/ima lineunten tmp1 0459,01470
!2076 - 1470 +1

insert/ima lineunten tmp1 0459,0608
insert/ima lineunten tmp1 0459,0607
ROTATE/COUNTER tmp1 imgbh
WRITE/DESC imgbh.bdf START/D/1/2 1.0,1.0
WRITE/DESC imgbh.bdf STEP/D/1/2 2.0,2.0

!load imgbh scale=-4

if filter(1:6) .eq. "Hb#770" then
  COMPUT/IMAG imgbf{i} = imgbh / ( hb770flat.bdf )
endif

```

```

if filter(1:7) .eq. "NII#653" then
  COMPUT/IMAG imgbf{i} = imgbh / ( NII653flat.bdf )
endif
if filter(1:7) .eq. "HbC#771" then
  COMPUT/IMAG imgbf{i} = imgbh / ( hbC771flat.bdf )
endif
if filter(1:5) .eq. "V#606" then
  COMPUT/IMAG imgbf{i} = imgbh / ( V606flat.bdf )
endif
if filter(1:5) .eq. "r#773" then
  COMPUT/IMAG imgbf{i} = imgbh / ( r773flat.bdf )
endif
if filter(1:6) .eq. "Ha#654" then
  COMPUT/IMAG imgbf{i} = imgbh / ( halphaflat.bdf )
endif
if filter(1:6) .eq. "Bb#605" then
  COMPUT/IMAG imgbf{i} = imgbh / ( Bb605flat.bdf )
endif
if filter(1:5) .eq. "i#774" then
  COMPUT/IMAG imgbf{i} = imgbh / ( i774flat.bdf )
endif
if filter(1:8) .eq. "OIII#589" then
  COMPUT/IMAG imgbf{i} = imgbh / ( OIII589flat.bdf )
endif

enddo

```

A.23. Proof that the Rebinning was successful

```

@@ rebinme lamp003 tmp lamp003gr3save
  EXTRAC/IMAG tmp = tmp[@1050,@1:~1500,@2055]
  ROTATE/ tmp lamp003rebin.bdf
  WRITE/DESC lamp003rebin.bdf START/D/1/2 1.0,1.0
  WRITE/DESC lamp003rebin.bdf STEP/D/1/2 1.0,1.0

EXTRAC/IMAG objex = lamp003[@1050,@1:~1500,@2055]
ROTATE/ objex objexr.bdf
WRITE/DESC objexr.bdf START/D/1/2 1.0,1.0
WRITE/DESC objexr.bdf STEP/D/1/2 1.0,1.0
CUTS/IMAG objexr.bdf 0,2000

AVERAG/ROW row1lamprebined = lamp003rebin [@420,@430]
AVERAG/ROW row2lamprebined = lamp003rebin [@220,@230]
AVERAG/ROW row3lamprebined = lamp003rebin [@20,@30]
AVERAG/ROW row1lampbefore = objexr [@420,@430]
AVERAG/ROW row2lampbefore = objexr [@220,@230]
AVERAG/ROW row3lampbefore = objexr [@20,@30]

!@@ rebinme ../all/a0260.bdf tmp lamp003gr3save
!EXTRAC/IMAG tmp = tmp[@1050,@1:~1500,@2055]
! ROTATE/ tmp a0260rebin.bdf
! WRITE/DESC a0260rebin.bdf START/D/1/2 1.0,1.0
! WRITE/DESC a0260rebin.bdf STEP/D/1/2 1.0,1.0

EXTRAC/IMAG objex = ../all/a0260.bdf[@1050,@1:~1500,@2055]
ROTATE/ objex objexr.bdf
WRITE/DESC objexr.bdf START/D/1/2 1.0,1.0
WRITE/DESC objexr.bdf STEP/D/1/2 1.0,1.0
CUTS/IMAG objexr.bdf 0,2000

FILTER/COSM objexr.bdf objexrc.bdf 100,2.4,3.5,4,1.37 comask

REBIN/LONG objexrc.bdf a0260rebin
load a0260rebin scale=-4,1

AVERAG/ROW row3objbefore = objexrc.bdf [@20,@30]
AVERAG/ROW row2objbefore = objexrc.bdf [@220,@230]
AVERAG/ROW row1objbefore = objexrc.bdf [@420,@430]
AVERAG/ROW row1objrebined = a0260rebin.bdf [@420,@430]
AVERAG/ROW row2objrebined = a0260rebin.bdf [@220,@230]
AVERAG/ROW row3objrebined = a0260rebin.bdf [@20,@30]

set/gra bin=on

CREATE/GRA 1

set/gra color=1

```

```

plot row1lampbefore.bdf
set/gra color=2
over row2lampbefore.bdf
set/gra color=3
over row3lampbefore.bdf

CREATE/GRA 2

set/gra color=1
plot row1lamprebind.bdf
set/gra color=2
over row2lamprebind.bdf
set/gra color=3
over row3lamprebind.bdf

CREATE/GRA 3

set/gra color=1
plot row1objbefore.bdf
set/gra color=2
over row2objbefore.bdf
set/gra color=3
over row3objbefore.bdf

CREATE/GRA 4

set/gra color=1
plot row1objrebind.bdf
set/gra color=2
over row2objrebind.bdf
set/gra color=3
over row3objrebind.bdf

```

A.24. Creation of Compound Spectra for each Grism

```

define/param P1 ? N "start wavelength:"
define/param P2 ? N "end wavelength:"

goto skip

!sky
average/row tmp1 = qamn14 @52,@83 sum
average/row tmp2 = qamn14 @99,@122 sum
average/row tmp3 = qamn14 @192,@205 sum
average/row tmp4 = qamn14 @220,@232 sum
average/row tmp5 = qamn14 @409,@421 sum
COMPUTE/IMAG tmpsky = (tmp1 + tmp2 + tmp3 + tmp4 + tmp5) / 96
grow/imag tmp = tmpsky
Compute/imag qamns14 = qamn14 - tmp
load qamns14.bdf scale=-4,1 cuts=0,3

average/row tmp1 = qamn24 @52,@83 sum
average/row tmp2 = qamn24 @99,@122 sum
average/row tmp3 = qamn24 @192,@205 sum
average/row tmp4 = qamn24 @220,@232 sum
average/row tmp5 = qamn24 @409,@421 sum
COMPUTE/IMAG tmpsky = (tmp1 + tmp2 + tmp3 + tmp4 + tmp5) / 96
grow/imag tmp = tmpsky
Compute/imag qamns24 = qamn24 - tmp
load qamns24.bdf scale=-4,1 cuts=0,3

average/row tmp1 = qamn3 @6,@16 sum
average/row tmp2 = qamn3 @49,@73 sum
average/row tmp3 = qamn3 @170,@188 sum
average/row tmp4 = qamn3 @209,@227 sum
average/row tmp5 = qamn3 @434,@450 sum
COMPUTE/IMAG tmpsky = (tmp1 + tmp2 + tmp3 + tmp4 + tmp5) / 91
grow/imag tmp = tmpsky
Compute/imag qamns3 = qamn3 - tmp
load qamns3.bdf scale=-4,1 cuts=0,3

average/row tmp1 = qamn4 @6,@16 sum
average/row tmp2 = qamn4 @49,@73 sum
average/row tmp3 = qamn4 @170,@188 sum
average/row tmp4 = qamn4 @209,@227 sum

```

```

average/row tmp5 = qamn4 @434,@450 sum
COMPUTE/IMAG tmpsky = (tmp1 + tmp2 + tmp3 + tmp4 + tmp5) / 91
grow/imag tmp = tmpsky
Compute/imag qamns4 = qamn4 - tmp
load qamns4.bdf scale=-4,1 cuts=0,3

```

```

average/row tmp1 = qamn16 @7,@27 sum
average/row tmp2 = qamn16 @102,@117 sum
average/row tmp3 = qamn16 @146,@156 sum
average/row tmp4 = qamn16 @174,@205 sum
COMPUTE/IMAG tmpsky = (tmp1 + tmp2 + tmp3 + tmp4) / 80
grow/imag tmp = tmpsky
Compute/imag qamns16 = qamn16 - tmp
load qamns16.bdf scale=-4,1 cuts=0,3

```

```

average/row tmp1 = qamn23 @36,@52 sum
average/row tmp2 = qamn23 @78,@105 sum
average/row tmp3 = qamn23 @135,@144 sum
average/row tmp4 = qamn23 @222,@238 sum
average/row tmp5 = qamn23 @404,@419 sum
COMPUTE/IMAG tmpsky = (tmp1 + tmp2 + tmp3 + tmp4 + tmp5) / 88
grow/imag tmp = tmpsky
Compute/imag qamns23 = qamn23 - tmp
load qamns23.bdf scale=-4,1 cuts=0,3

```

```

average/row tmp1 = qamn15 @36,@54 sum
average/row tmp2 = qamn15 @166,@216 sum
average/row tmp3 = qamn15 @124,@133 sum
average/row tmp4 = qamn15 @421,@445 sum
COMPUTE/IMAG tmpsky = (tmp1 + tmp2 + tmp3 + tmp4) / 105
grow/imag tmp = tmpsky
Compute/imag qamns15 = qamn15 - tmp
load qamns15.bdf scale=-4,1 cuts=0,3

```

!-----

!jetzt moeglichst nah mit pn an v605, aber nichts wegnehmen:

skip:

```

!grism2
average/row tmp = qamns14 @352,@358
COMPUTE/IMAG defaultpn2 = tmp

average/row tmp = qamns15 @333,@338
COMPUTE/IMAG defaultpn2 = tmp + defaultpn2

average/row tmp1 = qamns16 @329,@336 sum
average/row tmp2 = qamns16 @353,@357 sum
COMPUTE/IMAG tmp = (tmp1 + tmp2) / 13

COMPUTE/IMAG defaultpn2 = tmp + defaultpn2

average/row tmp1 = qamns14 @340,@343
average/row tmp2 = qamns15 @341,@345
average/row tmp3 = qamns16 @340,@345
COMPUTE/IMAG tmp = tmp1 + tmp2 + tmp3
COMPUTE/IMAG defaultv605gr2 = tmp - defaultpn2

```

```

create/gra 2
set/gra bin=on
set/gra color=1
plot defaultv605gr2 ? {P1},{P2}
set/gra color=4
over defaultpn2

```

```

!grism 3
average/row tmp1 = qamns24 @327,@333
average/row tmp2 = qamns24 @251,@358
COMPUTE/IMAG tmp = (tmp1 + tmp2) / 15
COMPUTE/IMAG defaultpn3 = tmp

```

```

average/row tmp = qamns4 @353,@362
COMPUTE/IMAG defaultpn3 = defaultpn3 + tmp

```

```

average/row tmp = qamns23 @350,@359
COMPUTE/IMAG defaultpn3 = defaultpn3 + tmp

```

```

average/row tmp1 = qamns4 @339,@343
average/row tmp2 = qamns24 @339,@344

```

```

average/row tmp3 = qamns23 @340,@344
COMPUTE/IMAG tmp = tmp1 + tmp2 + tmp3

COMPUTE/IMAG defaultv605gr3 = tmp - defaultpn3

create/gra 3
set/gra bin=on
set/gra color=1
plot defaultv605gr3 ? {P1},{P2}
set/gra color=4
over defaultpn3

!goto end

!grism 6
average/row tmp = qamns3 @351,@360
COMPUTE/IMAG defaultpn6 = tmp
average/row tmp = qamns3 @339,@342
COMPUTE/IMAG defaultv605gr6 = tmp - defaultpn6

create/gra 6
set/gra bin=on
set/gra color=1
if {P1} .GE. 5800 THEN
  plot defaultv605gr6 ? {P1},{P2}
else
  write/out "readjusted scale for grism 6"
  plot defaultv605gr6 ? 5800,8000
endif
set/gra color=4
over defaultpn6

end:

```

A.25. Correction of the Interstellar Extinction

```

define/param P1 ? N "E(B-V):"
define/param P2 ? N "start wavelength"
define/param P3 ? N "end wavelength"

set/context long
COMPUT/image tmp1 = defaultpn3
COMPUT/image tmp1 = tmp1 - defaultpn3 + 1.0
EXTINC/SPEC tmp1 intextgr3 {P1} /midas/calib/data/spec/exti/instexan.tbl

COMPUT/image tmp1 = defaultpn6
COMPUT/image tmp1 = tmp1 - defaultpn6 + 1.0
EXTINC/SPEC tmp1 intextgr6 {P1} /midas/calib/data/spec/exti/instexan.tbl

COMPUT/image tmp1 = defaultpn2
COMPUT/image tmp1 = tmp1 - defaultpn2 + 1.0
EXTINC/SPEC tmp1 intextgr2 {P1} /midas/calib/data/spec/exti/instexan.tbl

!set/gra yaxis=auto
set/gra color=1
plot intextgr2
set/gra color=3
over intextgr3
set/gra color=6
over intextgr6

@@ defaultspecs.prg 6000 8000

COMPUTE/IMAG defaultpn2 = defaultpn2 * intextgr2
COMPUTE/IMAG defaultpn3 = defaultpn3 * intextgr3
COMPUTE/IMAG defaultpn6 = defaultpn6 * intextgr6
!ausmessen HBETA da auf 100 normieren.... fuer cloudy

!jetzt ausgabe intextkorrigiertes PN spektrum:
goto forward

create/gra 1
set/gra yaxis=auto
set/gra color=1
plot defaultpn2.bdf ? 6000,7000
set/gra color=4
over defaultpn3

```

```

set/gra color=6
over defaultpn6

COMPUTE/IMAG defaultpn2 = defaultpn2 * 12.2
COMPUTE/IMAG defaultpn3 = defaultpn3 * 20.7
COMPUTE/IMAG defaultpn6 = defaultpn6 * 15.9

!goto forward

create/gra 5
!set/gra yaxis=-5,15
set/gra yaxis=auto
set/gra color=1
plot defaultpn2.bdf ? {P2},{P3}
set/gra color=4
over defaultpn3
set/gra color=6
if {P1} .GE. 5800 THEN
  over defaultpn6
else
  write/out "grism 6 non overplotted"
endif

forward:

COMPUTE/IMAG defaultv605gr6 = defaultv605gr6 * intextgr6
COMPUTE/IMAG defaultv605gr2 = defaultv605gr2 * intextgr2
!v605 fuer grism 3 neu berechnen wegen fehler in bild23 (oIII), bild24(NII)

average/row tmp1 = qamns24 @327,@333
average/row tmp2 = qamns24 @251,@358
COMPUTE/IMAG tmp = (tmp1 + tmp2) / 15
COMPUTE/IMAG defaultpn3oiii = tmp

average/row tmp = qamns4 @353,@362
COMPUTE/IMAG defaultpn3oiii = defaultpn3oiii + tmp
COMPUTE/IMAG defaultpn3nii = tmp

average/row tmp = qamns23 @350,@359
COMPUTE/IMAG defaultpn3nii = defaultpn3nii + tmp

average/row tmp1 = qamns4 @339,@343
average/row tmp2 = qamns24 @339,@344
average/row tmp3 = qamns23 @340,@344

!bild fuer bestimmung oiii:
COMPUTE/IMAG tmp = tmp1 + tmp2
COMPUTE/IMAG defaultv605gr3oiii = tmp - defaultpn3oiii
!bild fuer bestimmung nii:
COMPUTE/IMAG tmp = tmp1 + tmp3
COMPUTE/IMAG defaultv605gr3nii = tmp - defaultpn3nii

!mit fehler in oiii und n2
COMPUTE/IMAG defaultv605gr3 = defaultv605gr3 * intextgr3
COMPUTE/IMAG defaultv605gr3oiii = defaultv605gr3oiii * intextgr3
COMPUTE/IMAG defaultv605gr3nii = defaultv605gr3nii * intextgr3

create/gra 8
!set/gra yaxis=-1,11
set/gra yaxis=auto
set/gra color=1
plot defaultv605gr2.bdf ? {P2},{P3}
set/gra color=4
!over defaultv605gr3
over defaultv605gr3oiii
!over defaultv605gr3nii
set/gra color=6
if {P2} .GE. 5700 THEN
  over defaultv605gr6
else
  write/out "grism 6 non overplotted"
endif

assign/gra g,2
set/gra yaxis=auto
set/gra color=1
plot defaultv605gr2.bdf ? {P2},{P3}
set/gra color=2
over defaultpn2

assign/gra g,3

```

```

set/gra yaxis=auto
set/gra color=1
!plot defaultv605gr3.bdf ? {P2},{P3}
plot defaultv605gr3oiii.bdf ? {P2},{P3}
!plot defaultv605gr3nii.bdf ? {P2},{P3}
set/gra color=2
!over defaultpn3
over defaultpn3oiii
!over defaultpn3nii
set/gra color=1
over defaultv605gr3oiii.bdf

assign/gra g,6
set/gra yaxis=auto
set/gra color=1
if {P2} .GE. 5700 THEN
    plot defaultv605gr6.bdf ? {P2},{P3}
else
    plot defaultv605gr6.bdf ? 5700,6800
endif
set/gra color=2
over defaultpn6

!center/gauss gcursor

COPY/IT defaultv605gr2 tabv605gr2 world_coord

ASSIGN/PRINT FILE tabv605gr2.txt
PRINT/TAB tabv605gr2.tbl
$$ tail -n 'wc -l tabv605gr2.txt | awk '{print $1-3}'' tabv605gr2.txt | head -n 'wc -l
    tabv605gr2.txt | awk '{print $1-4}'' > tabv605gr2.dat

COPY/IT defaultv605gr6 tabv605gr6 world_coord

ASSIGN/PRINT FILE tabv605gr6.txt
PRINT/TAB tabv605gr6.tbl
$$ tail -n 'wc -l tabv605gr6.txt | awk '{print $1-3}'' tabv605gr6.txt | head -n 'wc -l
    tabv605gr6.txt | awk '{print $1-4}'' > tabv605gr6.dat

!COPY/IT defaultv605gr3 tabv605gr3 world_coord
COPY/IT defaultv605gr3oiii tabv605gr3 world_coord

ASSIGN/PRINT FILE tabv605gr3.txt
PRINT/TAB tabv605gr3.tbl
$$ tail -n 'wc -l tabv605gr3.txt | awk '{print $1-3}'' tabv605gr3.txt | head -n 'wc -l
    tabv605gr3.txt | awk '{print $1-4}'' > tabv605gr3.dat

COPY/IT defaultpn3oiii tabpngr3 world_coord

ASSIGN/PRINT FILE tabpngr3.txt
PRINT/TAB tabpngr3.tbl
$$ tail -n 'wc -l tabpngr3.txt | awk '{print $1-3}'' tabpngr3.txt | head -n 'wc -l
    tabpngr3.txt | awk '{print $1-4}'' > tabpngr3.dat

```

A.26. Determining an Angel-Dependency

```

define/param P1 ? N "start wavelength:"
define/param P2 ? N "end wavelength:"

!grism 6
average/row tmppn = qamns3 @351,@360
average/row tmp = qamns3 @339,@342
COMPUTE/IMAG tmpv = tmp - tmppn

COMPUTE/IMAG tmpv = tmpv * intextgr6
COMPUTE/IMAG tmppn = tmppn * intextgr6

COMPUTE/IMAG tmpv3 = tmpv

create/gra 1
set/gra bin=on
set/gra color=1

if {P1} .GE. 5700 THEN
    plot tmpv ? {P1},{P2}
! plot tmppn ? {P1},{P2}

```

```

else
  write/out "readjusted scale for grism 6"
  plot tmpv ? 5800,8000
  ! plot tmppn ? 5800,8000
endif
set/gra color=4
over tmppn
!over tmpv

!grism 3
average/row tmppn = qamns4 @353,@362
average/row tmp = qamns4 @339,@343
COMPUTE/IMAG tmpv = tmp - tmppn
COMPUTE/IMAG tmpv = tmpv * intextgr3
COMPUTE/IMAG tmppn = tmppn * intextgr3
COMPUTE/IMAG tmpv4 = tmpv

create/gra 2
set/gra bin=on
set/gra color=1
plot tmpv ? {P1},{P2}
set/gra color=4
over tmppn
!plot tmppn ? {P1},{P2}
!set/gra color=4
!over tmpv

!grism 3
average/row tmppn = qamns23 @350,@359
average/row tmp = qamns23 @340,@344
COMPUTE/IMAG tmpv = tmp - tmppn
COMPUTE/IMAG tmpv = tmpv * intextgr3
COMPUTE/IMAG tmppn = tmppn * intextgr3
COMPUTE/IMAG tmpv23 = tmpv

create/gra 3
set/gra bin=on
set/gra color=1
plot tmpv ? {P1},{P2}
set/gra color=4
over tmppn

!grism 2
average/row tmp1 = qamns16 @329,@336 sum
average/row tmp2 = qamns16 @353,@357 sum
COMPUTE/IMAG tmppn = (tmp1 + tmp2) / 13
average/row tmp = qamns16 @340,@345
COMPUTE/IMAG tmpv = tmp - tmppn
COMPUTE/IMAG tmpv = tmpv * intextgr2
COMPUTE/IMAG tmppn = tmppn * intextgr2
COMPUTE/IMAG tmpv16 = tmpv

create/gra 4
set/gra bin=on
set/gra color=1
plot tmpv ? {P1},{P2}
set/gra color=4
over tmppn

!grism 2
average/row tmppn = qamns15 @333,@338
average/row tmp = qamns15 @341,@345
COMPUTE/IMAG tmpv = tmp - tmppn
COMPUTE/IMAG tmpv = tmpv * intextgr2
COMPUTE/IMAG tmppn = tmppn * intextgr2
COMPUTE/IMAG tmpv15 = tmpv

create/gra 5
set/gra bin=on
set/gra color=1
plot tmpv ? {P1},{P2}
set/gra color=4
over tmppn

! grism 2
average/row tmppn = qamns14 @352,@358
average/row tmp = qamns14 @340,@343
COMPUTE/IMAG tmpv = tmp - tmppn
COMPUTE/IMAG tmpv = tmpv * intextgr2
COMPUTE/IMAG tmppn = tmppn * intextgr2
COMPUTE/IMAG tmpv14 = tmpv

```

```

create/gra 6
set/gra bin=on
set/gra color=1
plot tmpv ? {P1},{P2}
set/gra color=4
over tmppn

!grism 3
average/row tmp1 = qamns24 @327,@333
average/row tmp2 = qamns24 @251,@358
COMPUTE/IMAG tmppn = (tmp1 + tmp2) / 15
average/row tmp = qamns24 @339,@344
COMPUTE/IMAG tmpv = tmp - tmppn
COMPUTE/IMAG tmpv = tmpv * intextgr3
COMPUTE/IMAG tmppn = tmppn * intextgr3
COMPUTE/IMAG tmpv24 = tmpv

create/gra 7
set/gra bin=on
set/gra color=1
plot tmpv ? {P1},{P2}
set/gra color=4
over tmppn

COMPUTE/IMAG tmp = tmpv24 + tmpv4

create/gra 8
set/gra color=1
plot tmp ? {P1},{P2}
!-----

COMPUTE/IMAG tmp24 = tmpv24 / 4.432
COMPUTE/IMAG tmp14 = tmpv14 / 1.479
COMPUTE/IMAG tmp15 = tmpv15 / 1.471
COMPUTE/IMAG tmp16 = tmpv16 / 2.06
COMPUTE/IMAG tmp23 = tmpv23 / 1.323
COMPUTE/IMAG tmp4 = tmpv4 / 3.6

COPY/IT tmp4 tab4 world_coord
COPY/IT tmp24 tab24 world_coord
COPY/IT tmp14 tab14 world_coord
COPY/IT tmp15 tab15 world_coord
COPY/IT tmp16 tab16 world_coord
COPY/IT tmp23 tab23 world_coord

ASSIGN/PRINT FILE tab23.txt
PRINT/TAB tab23.tbl
$$ tail -n 'wc -l tab23.txt | awk '{print $1-3}'' tab23.txt | head -n 'wc -l tab23.txt
| awk '{print $1-4}'' > tab23.dat

ASSIGN/PRINT FILE tab24.txt
PRINT/TAB tab24.tbl
$$ tail -n 'wc -l tab24.txt | awk '{print $1-3}'' tab24.txt | head -n 'wc -l tab24.txt
| awk '{print $1-4}'' > tab24.dat

ASSIGN/PRINT FILE tab14.txt
PRINT/TAB tab14.tbl
$$ tail -n 'wc -l tab14.txt | awk '{print $1-3}'' tab14.txt | head -n 'wc -l tab14.txt
| awk '{print $1-4}'' > tab14.dat

ASSIGN/PRINT FILE tab15.txt
PRINT/TAB tab15.tbl
$$ tail -n 'wc -l tab15.txt | awk '{print $1-3}'' tab15.txt | head -n 'wc -l tab15.txt
| awk '{print $1-4}'' > tab15.dat

ASSIGN/PRINT FILE tab16.txt
PRINT/TAB tab16.tbl
$$ tail -n 'wc -l tab16.txt | awk '{print $1-3}'' tab16.txt | head -n 'wc -l tab16.txt
| awk '{print $1-4}'' > tab16.dat

ASSIGN/PRINT FILE tab4.txt
PRINT/TAB tab4.tbl
$$ tail -n 'wc -l tab4.txt | awk '{print $1-3}'' tab4.txt | head -n 'wc -l tab4.txt
| awk '{print $1-4}'' > tab4.dat

!$rm -rf tmp*

```

A.27. [SII] Clump Density at the outer Rim of A58

```

goto skip

average/row tmp1 = qamn3 @6,@16 sum
average/row tmp2 = qamn3 @49,@73 sum
average/row tmp3 = qamn3 @170,@188 sum
average/row tmp4 = qamn3 @209,@227 sum
average/row tmp5 = qamn3 @434,@450 sum
COMPUTE/IMAG tmpsky = (tmp1 + tmp2 + tmp3 + tmp4 + tmp5) / 91
grow/imag tmp = tmpsky
Compute/imag qamns3 = qamn3 - tmp
load qamns3.bdf scale=-4,1 cuts=0,1

average/row tmp1 = qamn4 @6,@16 sum
average/row tmp2 = qamn4 @49,@73 sum
average/row tmp3 = qamn4 @170,@188 sum
average/row tmp4 = qamn4 @209,@227 sum
average/row tmp5 = qamn4 @434,@450 sum
COMPUTE/IMAG tmpsky = (tmp1 + tmp2 + tmp3 + tmp4 + tmp5) / 91
grow/imag tmp = tmpsky
Compute/imag qamns4 = qamn4 - tmp
load qamns4.bdf scale=-4,1 cuts=0,1

average/row tmp1 = qamn23 @36,@52 sum
average/row tmp2 = qamn23 @78,@105 sum
average/row tmp3 = qamn23 @135,@144 sum
average/row tmp4 = qamn23 @222,@238 sum
average/row tmp5 = qamn23 @404,@419 sum
COMPUTE/IMAG tmpsky = (tmp1 + tmp2 + tmp3 + tmp4 + tmp5) / 88
grow/imag tmp = tmpsky
Compute/imag qamns23 = qamn23 - tmp
load qamns23.bdf scale=-4,1 cuts=0,1

average/row tmp1 = qamn17 @5,@14 sum
average/row tmp2 = qamn17 @155,@167 sum
average/row tmp3 = qamn17 @185,@218 sum
average/row tmp4 = qamn17 @239,@263 sum

COMPUTE/IMAG tmpsky = (tmp1 + tmp2 + tmp3 + tmp4) / 82
grow/imag tmp = tmpsky
Compute/imag qamns17 = qamn17 - tmp
load qamns17.bdf scale=-4,1 cuts=0,1

!sterne abziehen:

average/col tmp1 = qamns3 6630,6670
average/col tmp2 = qamns3 6750,6790
COMPUTE/IMAG tmp = (tmp1 + tmp2) / 2.0

grow/imag tmp1 = tmp 5729.9799804688,1.4774999618530,2018 ? C
!grow/imag tmp1 = tmp
!grow/imag tmp1 = tmp ? ? C
Compute/imag qamns13 = qamns3 - tmp1
load qamns13.bdf scale=1,4 cuts=0,1 center=6720,300

average/col tmp1 = qamns23 6630,6670
average/col tmp2 = qamns23 6750,6790
COMPUTE/IMAG tmp = (tmp1 + tmp2) / 2.0

grow/imag tmp1 = tmp 3353.0200195312,2.8621399402618,2003 ? C
!grow/imag tmp1 = tmp
!grow/imag tmp1 = tmp ? ? C
Compute/imag qamns123 = qamns23 - tmp1
load qamns123.bdf scale=1,4 cuts=0,1 center=6720,300

average/col tmp1 = qamns4 6630,6670
average/col tmp2 = qamns4 6750,6790
COMPUTE/IMAG tmp = (tmp1 + tmp2) / 2.0

grow/imag tmp1 = tmp 3353.0200195312,2.8621399402618,2003 ? C
!grow/imag tmp1 = tmp
!grow/imag tmp1 = tmp ? ? C
Compute/imag qamns14 = qamns4 - tmp1
load qamns14.bdf scale=1,4 cuts=0,1 center=6720,300

average/col tmp1 = qamns17 6630,6670
average/col tmp2 = qamns17 6750,6790
COMPUTE/IMAG tmp = (tmp1 + tmp2) / 2.0

```

```
grow/imag tmp1 = tmp 2785,3.5358700752258,1980 ? C
!grow/imag tmp1 = tmp 3.5358700752258
!grow/imag tmp1 = tmp ? ? C
Compute/imag qamns117 = qamns17 - tmp1
load qamns117.bdf scale=1,4 cuts=0,1 center=6720,300
```

```
!-----
average/row tmp3 = qamns13 @291,@293 sum
average/row tmp4 = qamns14 @291,@293 sum
average/row tmp23 = qamns123 @291,@293 sum
average/row tmp17 = qamns117 @306,@309 sum
```

```
skip:
```

```
create/gra 7
set/gra bin=on
set/gra yaxis=-0.1,14
set/gra color=1
set/gra lwidth=1
plot tmp23 ? 6650,6800
set/gra color=2
over tmp17
set/gra color=3
over tmp3
set/gra color=4
over tmp4
```

A.28. The Gauss-Fit of the C_{IV} Feature

```
set/gra lwidth=4
set/gra ltype=1

!plot A58_KNOT ? 5700,5900

!
! FWHM der normalen Linien 7.9 bis 8.5, geht noch bissi besser: 7.3
!
cre/ima tmp_1 1,200 5700.0,1.0 GAUSS 5754.6,3.1
find/minmax tmp_1
comp/ima A58_CIV_MOD = tmp_1 / {outputr(2)} * 4.05

cre/ima tmp_2 1,200 5700.0,1.0 GAUSS 5875.7,3.1
find/minmax tmp_2
comp/ima A58_CIV_MOD = A58_CIV_MOD + tmp_2 / {outputr(2)} * 9.5

!
! C IV
!
cre/ima tmp_3 1,200 5700.0,1.0 GAUSS 5801.3,3.1
find/minmax tmp_3
comp/ima A58_CIV_MOD = A58_CIV_MOD + tmp_3 / {outputr(2)} * 0.7
comp/ima A58_CIV_C1 = tmp_3 / {outputr(2)} * 0.7

cre/ima tmp_4 1,200 5700.0,1.0 GAUSS 5812.0,3.1
find/minmax tmp_4
comp/ima A58_CIV_MOD = A58_CIV_MOD + tmp_4 / {outputr(2)} * 0.3
comp/ima A58_CIV_C2 = tmp_4 / {outputr(2)} * 0.3

cre/ima tmp_5 1,200 5700.0,1.0 GAUSS 5803.7,22
!cre/ima tmp_5 1,200 5700.0,1.0 GAUSS 5801.3,22
find/minmax tmp_5
comp/ima A58_CIV_MOD = A58_CIV_MOD + tmp_5 / {outputr(2)} * 4
comp/ima A58_CIV_C3 = tmp_5 / {outputr(2)} * 4

cre/ima tmp_6 1,200 5700.0,1.0 GAUSS 5814.4,22
!cre/ima tmp_6 1,200 5700.0,1.0 GAUSS 5812.0,22
find/minmax tmp_6
comp/ima A58_CIV_MOD = A58_CIV_MOD + tmp_6 / {outputr(2)} * 3.2
comp/ima A58_CIV_C4 = tmp_6 / {outputr(2)} * 3.2

set/gra color=2
plot A58_CIV_MOD

set/gra lwidth=3
set/gra color=4
set/gra ltype=5
```

```

over A58_CIV_C1
over A58_CIV_C2
over A58_CIV_C3
over A58_CIV_C4

! an kontinuum anpassen
comp/ima A58_CIV_MOD = A58_CIV_MOD + 0.5
comp/ima A58_CIV_C4 = A58_CIV_C4 + 0.5
comp/ima A58_CIV_C3 = A58_CIV_C3 + 0.5
comp/ima A58_CIV_C2 = A58_CIV_C2 + 0.5
comp/ima A58_CIV_C1 = A58_CIV_C1 + 0.5

COPY/IT A58_CIV_MOD tabgauss world_coord

ASSIGN/PRINT FILE tabgauss.txt
PRINT/TAB tabgauss.tbl
$$ tail -n 'wc -l tabgauss.txt | awk '{print $1-3}'' tabgauss.txt | head -n 'wc -l
  tabgauss.txt | awk '{print $1-4}'' > tabgauss.dat

!COPY/IT A58_CIV_C4 tabgausspart world_coord
!COPY/IT A58_CIV_C3 tabgausspart world_coord
!COPY/IT A58_CIV_C2 tabgausspart world_coord
COPY/IT A58_CIV_C1 tabgausspart world_coord

ASSIGN/PRINT FILE tabgausspart.txt
PRINT/TAB tabgausspart.tbl
$$ tail -n 'wc -l tabgausspart.txt | awk '{print $1-3}'' tabgausspart.txt | head -n 'wc -l
  tabgausspart.txt | awk '{print $1-4}'' > tabgausspart.dat

```

A.29. The C_{IV} Feature in High Resolution

```

!goto skip

FILTER/COSM E21T031434 tmp 260,1.5,5,1.5,3 comask
EXTRACT/IMAG hr1 = tmp [2579,1800:2657,2497]
write/des hr1 START/D/1/2 1.0,1.0
load hr1 scale=5,2 cuts=250,350
$sleep 1
rebin/linear hr1 hr1r 2,12
load hr1r scale=5,12 cuts=250,350

FILTER/COSM E21T035337 tmp 260,1.5,5,1.5,3 comask
EXTRACT/IMAG hr2 = tmp [2587,1800:2665,2497]
write/des hr2 START/D/1/2 1.0,1.0
load hr2 scale=5,2 cuts=250,350
$sleep 1
rebin/linear hr2 hr2r 2,12
load hr2r scale=5,12 cuts=250,350

FILTER/COSM E23T012910 tmp 260,1.5,5,1.5,3 comask
EXTRACT/IMAG hr3 = tmp [2477,1800:2555,2497]
write/des hr3 START/D/1/2 1.0,1.0
load hr3 scale=5,2 cuts=250,350
$sleep 1
rebin/linear hr3 hr3r 2,12
load hr3r scale=5,12 cuts=250,350

FILTER/COSM E23T021018 tmp 260,1.5,5,1.5,3 comask
EXTRACT/IMAG hr4 = tmp [2476,1800:2554,2497]
write/des hr4 START/D/1/2 1.0,1.0
load hr4 scale=5,2 cuts=250,350
$sleep 1
rebin/linear hr4 hr4r 2,12
load hr4r scale=5,12 cuts=250,350

FILTER/COSM E24T030751 tmp 260,1.5,5,1.5,3 comask
EXTRACT/IMAG hr5 = tmp [2603,1800:2681,2497]
write/des hr5 START/D/1/2 1.0,1.0
load hr5 scale=5,2 cuts=250,350
$sleep 1
rebin/linear hr5 hr5r 2,12
load hr5r scale=5,12 cuts=250,350

FILTER/COSM E25T011319 tmp 260,1.5,5,1.5,3 comask
EXTRACT/IMAG hr6 = tmp [2582,1800:2660,2497]
write/des hr6 START/D/1/2 1.0,1.0
load hr6 scale=5,2 cuts=250,350

```

```

$sleep 1
rebin/linear hr6 hr6r 2,12
load hr6r scale=5,12 cuts=250,350

!skip:
aver/col t1 = hr1 @2,@11 SUM
aver/col t2 = hr1 @22,@31 SUM
aver/col t3 = hr1 @12,@21 SUM
comp/ima hr1s = t3 - (t1+t2) / 2.0
aver/col t1 = hr2 @2,@11 SUM
aver/col t2 = hr2 @22,@31 SUM
aver/col t3 = hr2 @12,@21 SUM
comp/ima hr2s = t3 - (t1+t2) / 2.0
aver/col t1 = hr3 @2,@11 SUM
aver/col t2 = hr3 @22,@31 SUM
aver/col t3 = hr3 @12,@21 SUM
comp/ima hr3s = t3 - (t1+t2) / 2.0
aver/col t1 = hr4 @2,@11 SUM
aver/col t2 = hr4 @22,@31 SUM
aver/col t3 = hr4 @12,@21 SUM
comp/ima hr4s = t3 - (t1+t2) / 2.0
aver/col t1 = hr5 @2,@11 SUM
aver/col t2 = hr5 @22,@31 SUM
aver/col t3 = hr5 @12,@21 SUM
comp/ima hr5s = t3 - (t1+t2) / 2.0
aver/col t1 = hr6 @2,@11 SUM
aver/col t2 = hr6 @22,@31 SUM
aver/col t3 = hr6 @12,@21 SUM
comp/ima hr6s = t3 - (t1+t2) / 2.0

!filter/med E21T031434ss E21T031434ssf 1

skip:
set/gra lwidth=3
create/gra 4
!set/gra color=1
set/gra color=0
plot hr1s
set/gra color=2
!over hr2s
set/gra color=3
over hr3s
set/gra color=4
over hr4s
set/gra color=5
over hr5s
set/gra color=6
!over hr6s

goto end

filter/med hr1s hr1m
filter/med hr2s hr2m
filter/med hr3s hr3m
filter/med hr4s hr4m
filter/med hr5s hr5m
filter/med hr6s hr6m

create/gra 5
!set/gra color=1
set/gra color=0
plot hr1m
set/gra color=2
!over hr2m
set/gra color=3
over hr3m
set/gra color=4
over hr4m
set/gra color=5
over hr5m
set/gra color=6
!over hr6m

end:

```

A.30. Spatial Resolution and different Velocities

```

define/local I/I/1/1
define/local store1/D/1/1
define/local store2/D/1/1
define/local store3/D/1/1
define/local store4/D/1/1

!goto computing

creat/tab centerit2 1 58
cre/col centerit2 :HR0
cre/col centerit2 :HR285

COMPUTE/IMAGE HR0 = hr1 + hr2
rebin/linear HR0 HR0r 2,12
load HR0r scale=5,12 cuts=500,600

COMPUTE/IMAGE HR285 = hr3 + hr4 + hr5
rebin/linear HR285 HR285r 2,12
load HR285r scale=5,12 cuts=850,900

do I = 1 58

    extra/ima row = HR0r [<,@{i}:>,@{i}]
    center/gauss row
        write/tab centerit2 :HR0 @{i} {outputr(5)}

    extra/ima row = HR285r [<,@{i}:>,@{i}]
    center/gauss row
        write/tab centerit2 :HR285 @{i} {outputr(5)}
enddo

goto fixedvalue

!auslesen zeilen und berechnung steigung:
store1 = m$value(centerit2,HR0,54)
store2 = m$value(centerit2,HR0,55)
store3 = m$value(centerit2,HR0,56)
store4 = m$value(centerit2,HR0,4)
store1 = {store1} + {store2} + {store3}
store1 = {store1} / 3.0
store1 = ({store1} - {store4} ) / 51.0
write/out HR0: {store1}

!offset dazugeben (kein muss nur schoener)
COMPUTE/TABLE centerit2.tbl :HROG = {store1} * SEQ + 31.6

store1 = m$value(centerit2,HR285,54)
store2 = m$value(centerit2,HR285,55)
store3 = m$value(centerit2,HR285,56)
store4 = m$value(centerit2,HR285,4)

store1 = {store1} + {store2} + {store3}
store1 = {store1} / 3.0
store1 = ({store1} - {store4} ) / 51.0
write/out HR285: {store1}

!offset dazugeben (kein muss nur schoener)
COMPUTE/TABLE centerit2.tbl :HR285G = {store1} * SEQ + 31.6

fixedvalue:
!optically best fit through NII and HeI
COMPUTE/TABLE centerit2.tbl :GERADE = 0.028 * SEQ + 31.0

!differences:

COMPUTE/TABLE centerit2.tbl :HROG = :HRO - :GERADE
COMPUTE/TABLE centerit2.tbl :HR285G = :HR285 - :GERADE - 0.5

READ/TAB centerit2
ASSIGN/PRINT FILE centerit2.txt
PRINT/TAB centerit2 ? ? ? 200

$$ tail -n 'wc -l centerit2.txt | awk '{print $1-3}'' centerit2.txt | head -n 'wc -l
centerit2.txt | awk '{print $1-4}'' > centerit2.dat

```

B. Acknowledgements

Primarily I want to thank my energetic supervisor Stefan Kimeswenger, who gave me the idea for this thesis and who was always by my side, whenever I needed motivation or advice. He seemed to know the answers to all questions, and not only answered them, but communicated a deeper understanding for coherences.

Many thanks go also to em. Prof. Jörg Pfeleiderer who aroused my interest in astrophysics and taught me that curiosity is not only human, but also a fundamental basis for being a real scientist.

Actually I have to thank all members of the Institute of Astrophysics for the warm and cooperative atmosphere which is always present, and the cookies every Thursday.

Then I hope that all my friends are willing to accept my apologies for all the card games I didn't play or all the coffees I didn't drink with them while sitting in front of my computer or reading a paper. Additionally they had to endure my bad moods, whenever I was dealing with an unsolvable problem. Please say you like me still a little bit!

The same is directed towards my family, specially to my brother and my mother, who saw me most of the time either eating, sleeping or reading. I know without the both of you I wouldn't even had the possibility of a higher education.

Special thanks go to Markus for all his love, moral support, his perfect proof-reading and his stupid 'when will you finish?' questions.

Thanks to all of you.